



Magnetic properties, phase transitions and critical behavior of quasi-two dimensional systems : studies on several layered copper compounds
by Ping Zhou

A thesis submitted in partial fulfillment of the requirements for the degree of Doctor of Philosophy in Physics
Montana State University
© Copyright by Ping Zhou (1991)

Abstract:

The reorientation of the sublattice magnetizations from the antiferromagnetic (AF) to the spin-flop (SF) phase is studied by magnetization measurements on new anisotropic Heisenberg quasi-two dimensional antiferromagnets $[C_6H_5(CH_2)_nNH_3]_2CuBr_4$ with $n = 1, 2$ and 3 . The isothermal magnetic phase diagrams along the spin principal axes are obtained, and an analysis from the mean-field theory yields (for the $n = 1$) $J_1 = 25.49$ K/kB and $J_n = 25.45$ K/kB for the intralayer perpendicular and parallel exchange components, respectively. A weak antiferromagnetic interlayer interaction and a relatively strong uniaxial anisotropy with the easy axis within the layer are found. Evidence for a possible existence of an intermediate (IN) phase between the AF and SF phase and a comparison for the magnetic phase boundaries between the mean-field calculations and experimental data are presented. Spin-canting effect along the easy and intermediate axes is seen in the isotherms. It is suggested from the results of the isothermal measurements that a competition between the antisymmetric exchange and Zeeman energy above the SF critical field may lead to a "fan" phase which may persist up to a triple point along the intermediate axis while a competition between the inter- and intralayer exchange anisotropies leads to an intermediate phase which can persist up to a tetracritical point along the easy axis. Thermodynamic considerations near the phase boundaries are also discussed. Critical exponent γ and transition temperature T_c were determined by the measurements of a.c. initial susceptibility and critical isothermal magnetization. By employing the static scaling law to analyze the data of isothermal magnetizations near T_c , it was found that at a certain low field and low temperature regions the powder magnetizations are suppressed so that the scaling hypothesis no longer holds.

Zero-field a.c. susceptibility and isothermal magnetization of the quasi-2D systems (alkanediammonium copper tetrahalide series) $[NH_3(CH_2)_nNH_3]CuX_4$ where $n = 4, 5, 7$ and 10 with $X = Cl$ and Br are also reported. The 3D antiferromagnetic ordering at T_c for the Cl compounds is found. It is shown that the critical susceptibilities decay exponentially as the temperature increases ($T > T_c$). A power-law divergence in the Br compounds with $n = 7$ and 10 is seen. This behavior is characteristic of 3D ferromagnetic ordering at T_c . The critical exponent γ for the initial susceptibility ($T > T_c$) has been obtained for these Br compounds. It is found that there is a second (minor) peak below T_c in the Br compounds with $n = 5$ and 7 . The transition associated with this peak may be interpreted as a long range (spontaneous) ordering due to very small spin anisotropies, such as a spin canting effect between the layers. It is seen from the results of isothermal magnetization measurements for these Br compounds that the magnetization is suppressed as the field decreases as compared to the behavior of most 3D ferromagnets. The value of the critical exponent δ estimated from the isothermal data is considerably smaller than that given by the well-studied models. The apparent crossovers are seen in both the initial susceptibility and isothermal magnetization data in which a combination of the spatial- and spin-dimensionality crossovers may be present. To discuss the spin-dimensionality crossover in 2D systems, thermal and field perturbations away from the renormalization-group fixed point are considered in 2D conformal field theory. By applying the c-theorem, general expressions for the effective critical exponents ν , α and δ are obtained in terms of the central charge, the third moment of

energy and spin correlations, temperature and external field. These expressions may be described as critical behavior and crossover phenomena for the 2D systems away from the critical points.

**MAGNETIC PROPERTIES, PHASE TRANSITIONS AND CRITICAL BEHAVIOR
OF QUASI-TWO DIMENSIONAL SYSTEMS: STUDIES ON SEVERAL
LAYERED COPPER COMPOUNDS**

by

Ping Zhou

**A thesis submitted in partial fulfillment
of the requirements for the degree**

of

Doctor of Philosophy

in

Physics

**MONTANA STATE UNIVERSITY
Bozeman, Montana**

May 1991

D378
2599

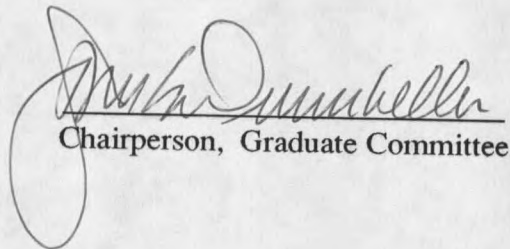
APPROVAL

of a thesis submitted by

Ping Zhou

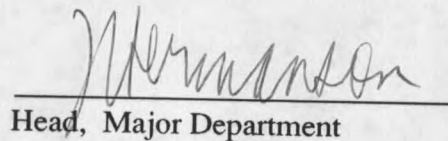
This thesis has been read by each member of the thesis committee and has been found to be satisfactory regarding content, English usage, format, citations, bibliographic style, and consistency, and is ready for submission to the college of Graduate Studies.

14 June 1991
Date


Chairperson, Graduate Committee

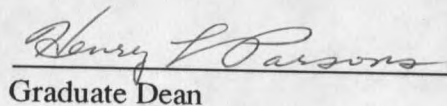
Approved for the Major Department

6-14-91
Date


Head, Major Department

Approved for the College of Graduate Studies

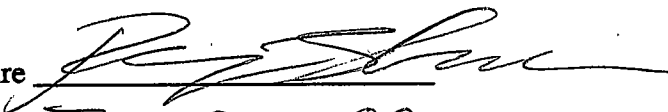
June 14, 1991
Date


Graduate Dean

STATEMENT OF PERMISSION TO USE

In presenting this thesis in partial fulfillment of the requirements for a doctoral degree at Montana State University, I agree that the Library shall make it available to borrowers under rules of the Library. I further agree that copying of this thesis is allowable only for scholarly purposes, consistent with "fair use" as prescribed in the U.S. Copyright Law. Requests for extensive copying or reproduction of this thesis should be referred to University Microfilms International, 300 North Zeeb Road, Ann Arbor, Michigan 48106, to whom I have granted "the exclusive right to reproduce and distribute copies of the dissertation in and from microfilm and the right to reproduce and distribute by abstract in any format."

Signature



Date

Jun 13, 1991

ACKNOWLEDGEMENTS

I would like to express my deep thanks to my advisor John E. Drumheller, who continuously supported and encouraged me during this project. My special thanks also go to George F. Tuthill, Hugo V. Schmidt, Gerald Rubenacker, Roger Willett, K. Ravindran, C. Zaspel, and my family for their useful help and encouragement. It is difficult for me to list all my friends, colleagues, staff and faculty in the department who assisted me to make this thesis possible. This acknowledgement should include them too.

This work was financially supported by National Science Foundation under grants DMR-8702933 and DMR-9011072.

TABLE OF CONTENTS

	Page
I. INTRODUCTION	1
References of Chapter I	5
II. A SHORT REVIEW OF THE BASIC THEORIES	7
Phase Transitions and Critical Point	7
Critical Phenomena and Critical Exponents	10
Mean Field Theory, Landau Theory and Thermodynamic Scaling ..	18
Basic Spin Models, Spatial Scaling and Renormalization	
Group Theory	21
A Possible Universal Critical Theory in Two Dimensional Systems -	
Conformal Field Theory	26
References of Chapter II	32
III. MEAN FIELD THEORY OF QUASI-TWO DIMENSIONAL, SPIN-1/2, ANISOTROPIC, HEISENBERG ANTIFERROMAGNETS	35
Introduction	35
Generalized Formalism of the Mean Field Approximation for a Spin Bilinear Interaction System	38
An Intermediate Phase in Antiferromagnets and a Supersolid Phase in The ⁴ He Film	50
Mean Field Results for Quasi-two Dimensional, Anisotropic, Heisenberg Systems at T = 0 K	53
Mean Field Calculation at Finite Temperatures	64
Spin Canting Effect in the Transitions of Quasi-two Dimensional Systems	76
References of Chapter III	90
IV. EXPERIMENTAL STUDIES OF MAGNETIC PROPERTIES, PHASE TRANSITIONS AND CRITICAL BEHAVIOR OF THE QUASI-TWO DIMENSIONAL SYSTEMS [C ₆ H ₅ (CH ₂) _n NH ₃] ₂ CuBr ₄ (n=1,2 and 3). . . .	94
Introduction	94
Experiments and Results	99
Magnetizations and Susceptibilities of an n = 1 Single Crystal. .	99
Magnetizations and Susceptibilities of n = 2, 3 Single Crystals. .	109
Magnetizations and Susceptibilities of Powdered Samples. . . .	116

TABLE OF CONTENTS-Continued

	Page
Data Analysis, Discussion and Conclusions	126
Magnetic Phase Diagrams.	126
Thermodynamic Considerations	140
Critical Behavior and Critical Exponents for Powdered Samples	154
References of Chapter IV	166
V. INITIAL SUSCEPTIBILITY AND ISOTHERMAL MAGNETIZATION OF $[\text{NH}_2(\text{CH}_2)_n\text{NH}_3]\text{CuX}$ ($n=4,5,7,10$) FOR $\text{X}=\text{Cl}_4$ AND Br_4	171
Introduction.	171
Experiments and Results.	175
Discussion.	211
References of Chapter V	225
VI. CONCLUSION AND SUGGESTION FOR FURTHER WORK	230
VII. BIBLIOGRAPHY	233

LIST OF TABLES

Table		Page
1.	Definition of the Magnetic Critical Exponents	12
2.	Inequalities of Exponents	12
3.	Critical Fields at $T = 0$ K for $n = 1$ and 2 Compounds	135
4.	Values of the Exchange Constants for $n = 1$ Crystal	135

LIST OF FIGURES

Figure	Page
1. Phase diagrams illustrating the magnet-fluid analogy: (a) (P, T) phase diagram for a fluid system; (b) (H, T) phase diagram for a ferromagnet.	9
2. Coexistence diagrams illustrating the magnet-fluid analogy: (a) for a fluid and (b) for ferromagnet.	14
3. Magnetization curves (isotherms) for a simple ferromagnet. $M_0(T)$ indicates the spontaneous magnetization.	16
4. Schematic phase diagram of a uniaxial antiferromagnet for the field applied along the easy axis. $H_{PS}^C(T)$ and $H_{PA}^C(T)$ phase lines represent the phase boundaries between the PM and the SF phases and between the PM and the AF phases, respectively. The first-order AF-SF transition line is indicated by $H_T^C(T)$. The stability limits of the AF and SF phases are illustrated as the dashed lines H_{AF}^C and H_{SF}^C	47
5. (a) and (b) illustrate the fluid-magnet analogy in the isotherms. The instability points B and C correspond to $H_{AF}^C(T)$ and $H_{SF}^C(T)$ shown in the phase diagrams (c) and (d).	49
6. Phase diagrams for (a) the magnetic system, the anisotropic Heisenberg model, and (b) the quantum lattice gas model.	52
7. (a) phase diagram of a quasi-two dimensional antiferromagnet with an intermediate phase (IN), and (b) phase diagram for the thin film of ^4He with the supersolid phase.	54
8. Magnetization of the two sublattice according to the five different phases.	62
9. Sequences of the different phase transitions for different combinations of exchange constants at $T = 0$ (taken from Ref. 26) where J_x and J_z are positive and J_x' is negative.	62

LIST OF FIGURES - continued

Figure	Page
10. Illustrating the different behavior of the magnetization at $T = 0$ corresponding to the consequences shown in fig. 9; (a) $Z'J_z' \pm Z(J_x - J_z) > 0$ (or $Z(J_x - J_z) > J' J_z' $), (b) $Z'J_z' \pm Z(J_x - J_z) < 0$ (or $Z(J_x - J_z) < Z' J_z' $), $Z'(J_z' - J_x') \pm Z(J_x - J_z) > 0$ and $Z(J_z - J_x) / Z'J_x' > 0$, (c) $J_z > J_x$ and $Z'(J_z' - J_x') \pm Z(J_x - J_z) > 0$ (d) $Z'(J_z' - J_x') \pm Z(J_x - J_z) < 0$.	63
11. Illustrating the magnetization behavior at finite temperatures for the different phases.	63
12. Magnetization of the two sublattice corresponds to the Hamiltonian (20) adding the Dzyaloshinsky-Moriya interaction. (a) AF phase for the $\vec{H} = 0$, (b) AF phase for $0 < H_x < H_{SA}^C$ (c) SF phase for the $H_x > H_{SA}^C$ and (d) QP phase for the $H_x > H_{QS}^C$.	79
13. Illustration of the layer structure in $[C_6H_5C_2H_4NH_3]_2CuBr_4$. The \hat{a} axis is coming out of the plane of the illustration.	98
14. Isothermal magnetization vs. internal field along the \hat{z} axis (c axis) for the $n = 1$ compound.	101
15. The results of rotational measurements (15° apart) of isothermal magnetization at $T = 4.5K$ with field parallel to the surface of the plate (ab plane) for the $n = 1$ single crystal.	103
16. Isothermal magnetization data at several different temperatures with the field along the x axis.	104
17. Isothermal magnetization data with the field along the y axis at several different temperatures.	107

LIST OF FIGURES - continued

Figure	Page
18. Isothermal magnetization with the field along the spin principle (x, y and z) axes for the n = 1 single crystal.	108
19. Low-field d.c. Susceptibility vs. temperature along the spin principle axes (n = 1).	110
20. Isothermal magnetization with the field along the spin principle axes for the n = 2 compound.	112
21. Isothermal magnetization with the field parallel to the surface of the plate (ab plane) for the n = 3 single crystal.	113
22. Isothermal magnetization data along the z (c) axis for the n = 3 compound.	114
23. D.C. susceptibility data along the spin principle axes for the n = 3 compound.	115
24. Isothermal magnetization vs. field at several different temperatures for the n = 1 powdered sample.	117
25. Magnetization vs. temperature at several different applied fields for the n = 1 powdered sample.	119
26. Magnetization susceptibility versus temperature for the n = 1 powdered sample. The solid line is the best fit result calculated by a high-temperature series expansion with $J/k_B = 25.0$ K and $ J' /k_B < 1.0$ K.	120
27. Zero-field a.c. susceptibility vs. temperature for the powdered samples . .	122
28. Numerically differential plots, $\Delta(\chi \cdot T)/\Delta T$ vs. T, taken from the zero-field a.c. susceptibility data (fig. 27). $T_c = 12.81 \pm 0.05$ K and $T_c = 12.85 \pm 0.05$ K are estimated corresponding to the peaks a) and b) for n = 1 and 2 sample respectively.	124

LIST OF FIGURES - continued

Figure	Page
29. Magnetic phase diagrams along the z axis for the n = 1, 2 and 3 compounds. The solid line shown in (a) is a calculated result of the PM-SF transition line from mean-field theory (eqs. 47 - 48) with the values of the exchange constants listed in table IV.	127
30. Magnetic phase diagrams along the hard axis (y axis). These data indicating the PM-SF phase boundaries for the n = 1, 2 and 3 compounds are estimated from the isotherms along the y axis (fig. 17).	130
31. Magnetic phase diagrams along the x axis. The dots shown in a) and b), which estimated from the isothermal data (fig. 16) according to fig.11(c) discussed in chapter III, represent the SF- or SF* -IN and IN-AF phase boundaries for n = 1 and 2 compounds. The SF* -IN phase transition line (SI*) given by a simultaneous solution of eqs.(43) and (45), the IN-AF (IA) phase transition line given by the simultaneous solutions of eqs. (37), (38) and (41), and the PM-SF (PS*) phase transition line given by the solution of eqs. (47) and (48) are shown as solid lines in a) with the values of exchange constants listed in table IV for n = 1 compound.	133
32. Numerically differential perpendicular susceptibility ($\Delta M/\Delta H$) vs. field (H) taken from the isothermal data at T = 4.27K and 10.53 K for n = 1 compound.	144
33. Perpendicular critical magnetization (M_c) vs. temperature (T) taken from the isotherm data (fig. 14).	146
34. Perpendicular critical magnetization (M_c) vs. field (H) taken from the isothermal data (fig. 14).	148
35. The numerical differential susceptibility ($\Delta M/\Delta H$) vs. field (H) in the x direction at T = 4.23 K for the n = 1 compound.	155
36. (a) the SF-AF phase boundary for the n = 1 compound. (b) Latent heat Q of the first-order SF-AF transition plotted against temperature.	156

LIST OF FIGURES - continued

Figure	Page
37. Initial a.c. Susceptibility plotted in terms of $\ln(\chi)$ vs. $\ln(T/T_c - 1)$ at $T > T_c$. Solid lines are fit for $n = 1$ and 2 compounds with $\gamma = 1.39$. . .	159
38. Isothermal magnetization in a field range $70 < H < 1400$ Oe plotted in terms of $\ln(M)$ vs. $\ln(H)$	160
39. Isothermal magnetization in a field range $700 < H < 4000$ Oe plotted in terms of $\ln(M)$ vs. $\ln(H)$	162
40. The Arrott-Noakes plots with [Equation: γ] = 1.39 and $\beta = 0.32$ in a field range $700 \text{ Oe} < H < 4000 \text{ Oe}$. The dashed lines indicate that the magnetization starts to be suppressed as field decreases so that scaling law no longer holds.	165
41. Zero-field a.c. Susceptibility vs. temperature.	177
42. Numerically differential zero-field susceptibility $\Delta(\chi \cdot T)/\Delta T$ vs. temperature.	182
43. Initial susceptibility plotted in terms of $\ln(\chi)$ vs. $\ln(T/T_c - 1)$ at $T > T_c$ for $n\text{DACuCl}$ with $n = 4, 5, 7, 10$ and 5DACuBr compounds. . .	186
44. Initial susceptibility plotted in terms of $\ln(\chi)$ vs. $(T/T_c - 1)^{1/2}$ for $n\text{DACuCl}$ with $n = 4, 5, 7, 10$ and 5DACuBr compounds. T_p indicates a temperature at which data start to deviate from the exponential decay.	191
45. Inverse zero-field susceptibility vs. temperature for 7DACuCl	194
46. Isotherms near the T_c plotted in terms of $\ln(M)$ vs $\ln(H)$ for 5DACuCl and 10DACuCl compounds.	198
47. Initial susceptibility plotted in terms of $\ln(\chi)$ vs. $\ln(T/T_c - 1)$ at $T > T_c$ for 7DACuBr and 10DACuBr compounds.	199

LIST OF FIGURES - continued

Figure	Page
48. Initial susceptibility plotted in terms of $\ln(\chi)$ vs. $\ln (T/T_c' - 1)$ at $T > T_c'$ for 5DACuBr and 7DACuBr compounds.	201
49. Isotherms of Br compounds near the T_c plotted in terms of $\ln(M)$ vs. $\ln(H)$; (a) and (b) for 5DACuBr, (c) and (d) for 7DACuBr, and (d) and (e) for 10DACuBr compounds.	207

ABSTRACT

The reorientation of the sublattice magnetizations from the antiferromagnetic (AF) to the spin-flop (SF) phase is studied by magnetization measurements on new anisotropic Heisenberg quasi-two dimensional antiferromagnets $[C_6H_5(CH_2)_nNH_3]_2CuBr_4$ with $n = 1, 2$ and 3 . The isothermal magnetic phase diagrams along the spin principal axes are obtained, and an analysis from the mean-field theory yields (for the $n = 1$) $J_{\perp} = 25.49 \text{ K}/k_B$ and $J_{\parallel} = 25.45 \text{ K}/k_B$ for the intralayer perpendicular and parallel exchange components, respectively. A weak antiferromagnetic interlayer interaction and a relatively strong uniaxial anisotropy with the easy axis within the layer are found. Evidence for a possible existence of an intermediate (IN) phase between the AF and SF phase and a comparison for the magnetic phase boundaries between the mean-field calculations and experimental data are presented. Spin-canting effect along the easy and intermediate axes is seen in the isotherms. It is suggested from the results of the isothermal measurements that a competition between the antisymmetric exchange and Zeeman energy above the SF critical field may lead to a "fan" phase which may persist up to a triple point along the intermediate axis while a competition between the inter- and intralayer exchange anisotropies leads to an intermediate phase which can persist up to a tetracritical point along the easy axis. Thermodynamic considerations near the phase boundaries are also discussed. Critical exponent γ and transition temperature T_c were determined by the measurements of a.c. initial susceptibility and critical isothermal magnetization. By employing the static scaling law to analyze the data of isothermal magnetizations near T_c , it was found that at a certain low field and low temperature regions the powder magnetizations are suppressed so that the scaling hypothesis no longer holds.

Zero-field a.c. susceptibility and isothermal magnetization of the quasi-2D systems (alkanediammonium copper tetrahalide series) $[NH_3(CH_2)_nNH_3]CuX_4$ where $n = 4, 5, 7$ and 10 with $X = Cl$ and Br are also reported. The 3D antiferromagnetic ordering at T_c for the Cl compounds is found. It is shown that the critical susceptibilities decay exponentially as the temperature increases ($T > T_c$). A power-law divergence in the Br compounds with $n = 7$ and 10 is seen. This behavior is characteristic of 3D ferromagnetic ordering at T_c . The critical exponent γ for the initial susceptibility ($T > T_c$) has been obtained for these Br compounds. It is found that there is a second (minor) peak below T_c in the Br compounds with $n = 5$ and 7 . The transition associated with this peak may be interpreted as a long range (spontaneous) ordering due to very small spin anisotropies, such as a spin canting effect between the layers. It is seen from the results of isothermal magnetization measurements for these Br compounds that the magnetization is suppressed as the field decreases as compared to the behavior of most 3D ferromagnets. The value of the critical exponent δ estimated from the isothermal data is considerably smaller than that given by the well-studied models. The apparent crossovers are seen in both the initial susceptibility and isothermal magnetization data in which a combination of the spatial- and spin-dimensionality crossovers may be present. To discuss the spin-dimensionality crossover in 2D systems, thermal and field perturbations away from the renormalization-group fixed point are considered in 2D conformal field theory. By applying the c-theorem, general expressions for the effective critical exponents ν , α and δ are obtained in terms of the central charge, the third moment of energy and spin correlations, temperature and external field. These expressions may be described as critical behavior and crossover phenomena for the 2D systems away from the critical points.

CHAPTER I

INTRODUCTION

It is well known that uniaxial antiferromagnets exhibit a bicritical point at a finite magnetic field \vec{H} parallel to the easy axis. Many of the theoretical predictions, particularly from mean-field theory, renormalization group approach and high-temperature series expansions, concerning the bicritical phase diagram have been confirmed by the experiments. In general, it is expected that weakly anisotropic uniaxial antiferromagnets in a magnetic field \vec{H} parallel to the easy axis should exhibit a multicritical point at some finite, nonzero value of \vec{H} . The existence of a bicritical or tetracritical point in the uniaxial antiferromagnets is usually determined by the fourth-order spin anisotropy in the Hamiltonian.^[1,2] Studies of phase transitions in magnetism have contributed to the understanding of many aspects of other physical systems through the analogy with spin models. A typical example is the study, within mean-field theory, of the supersolid phase in the quantum lattice gas model.^[3,4] The supersolid phase introduced in the early 70's is a state in which there coexists both diagonal (crystalline) long-range order and off-diagonal (superfluid) long-range order.^[3-8] This phase was first observed experimentally by Rudnick *et al.*^[9] and Goodstein *et al.*^[10] who showed that a thin film of ^4He undergoes a transition from the superfluid phase to the solid phase with no latent heat, implying that there is no first-order phase transition between the superfluid and crystalline states. This model can be represented by the standard boson Hamiltonian in second-quantized form. In this form the Hamiltonian is fully analogous to that of

anisotropic Heisenberg spin systems.^[3,4,8] We refer here to an anisotropic (biaxial) Heisenberg spin system with two types of exchange interactions, $J(J_x, J_y, J_z)$ and $J'(J'_x, J'_y, J'_z)$. There may exist an intermediate (IN) phase between the spin flop (SF) and antiferromagnetic (AF) phases due to a competition between the interlayer and intralayer exchange anisotropies, which would correspond to the supersolid phase in the quantum lattice gas.

However, the spin system corresponding to the quantum crystal has many aspects which are different from the usual uniaxial antiferromagnets mentioned at the beginning: (a) the system is of biaxial anisotropic form (anisotropic Heisenberg or XYZ-like); (b) the system contains two types of exchange interactions (J and J'); and (c) the spin Hamiltonian contains only linear (Zeeman) and quadratic (exchange) terms. Thus, an important question may remain unresolved: is it possible to confirm this intermediate phase experimentally in quasi-two dimensional spin-1/2 anisotropic Heisenberg antiferromagnets at a finite temperature? In this work, as a part of the main purpose of this thesis, we strongly suggest that an intermediate phase may exist in the quasi-two dimensional anisotropic Heisenberg systems with strongly ferromagnetic intralayer exchange and weakly antiferromagnetic interlayer exchange. It may be possible to verify this phase in a large variety of layer-type magnetic metallate compounds since a rich variety of nonmagnetic organic cations produce large and variable separation between the magnetic metallate layers. In this thesis, the reorientation of the sublattice magnetizations from the antiferromagnetic to the spin-flop phase is studied by magnetization measurements on new anisotropic Heisenberg quasi-two dimensional antiferromagnets $[C_6H_5(CH_2)NH_3]_2CuBr_4$ ($n = 1$ and 2). The isothermal magnetic phase diagrams along the spin principal axes are obtained. Evidence for a possible existence of an intermediate phase between the AF and SF phases and a comparison

of the magnetic phase boundaries between the mean-field calculations and experimental data are presented.

The other major part of this thesis contributes to the study of the critical behavior of quasi-2D systems. One of the most fundamental quantities which is used to characterize the nature of magnetic systems near a critical region is the spin-spin correlation function, $\langle S(r)S(0) \rangle$. It does not decay to zero as $r \rightarrow \infty$ once long range order exists. Thus, in the critical region ($H_c = 0$), the initial (or staggered) susceptibility of a ferromagnet (or antiferromagnet) is expected to diverge like $\chi \sim (T/T_c - 1)^{-\gamma}$ as $T \rightarrow T_c$ ($T > T_c$). Divergent initial susceptibility quite often indicates the onset of an instability with the system starting to order spontaneously. Studies of initial susceptibility may provide direct evidence of anomalies that a system naturally display without involving any field-induced transitions. In the two-dimensional (2D) systems, however, it has been rigorously proven that no long-range order can exist at any nonzero temperature for the ideal (Heisenberg) case^[11]. Recently, theoretical studies have shown that even at zero temperature the existence of a long range order in 2D systems may require a certain spin anisotropy.^[12-18] Therefore, whether or not there possibly exists a finite "critical" temperature indicated by an infinite initial susceptibility, but no long range order (no phase transitions), has been the subject of many theoretical and experimental studies. Based upon an analysis of the high-temperature susceptibility series (ratio method), Stanley and Kaplan^[19] suggested that the combination $M_s = 0$ and $\chi \rightarrow \infty$ is possible in 2D Heisenberg systems if the spin correlation function decreases slowly enough with spin separation r specifically like $r^{-\lambda}$ with $0 < \lambda < 2$. Subsequently, a finite critical temperature was conjectured to exist for the 2D XY and planar magnets too.^[20-22] Experimentally it has been found that the quasi-2D systems in fact exhibit a finite critical temperature related to a long range order.^[23,24] It has been suggested that the

experimentally observed long range order is due to a consequence of the presence of a small anisotropy, interlayer coupling or even of the finite size of the sample. Thus, it seems to be difficult to examine the conjecture of Stanley and Kaplan directly since even minute deviations from ideality will cause the behavior near the T_c to be no longer characteristic of the 2D Heisenberg case. The finite T_c and degree of divergence (γ) in the initial susceptibility as $T \rightarrow T_c$ may play the important role in indicating the existence of a phase transition for the various realistic systems.

Zero-field a.c. susceptibility and isothermal magnetization of the quasi-2D systems (alkanediammonium copper tetrahalide series) $[\text{NH}_3(\text{CH}_2)_n\text{NH}_3]\text{CuX}_4$ where $n = 4, 5, 7$ and 10 with $X = \text{Cl}$ and Br are reported in this work. The 3D antiferromagnetic ordering for the Cl compounds is found. It is shown that the critical susceptibilities decay exponentially as the temperature increases ($T > T_c$). A power-law divergence in the Br compounds with $n = 7$ and 10 is seen. This behavior is characteristic of 3D ferromagnetic ordering at T_c . The critical exponent γ for the initial susceptibility ($T > T_c$) has been obtained for these Br compounds. It is found that there is a second (minor) peak below T_c in the Br compounds with $n = 5$ and 7. The apparent crossovers are seen in both the initial susceptibility and the isothermal magnetization data in which a combination of the spatial- and spin-dimensionality crossovers is present.

In the next chapter, the basic theories will be shortly reviewed. The remainder of that chapter is devoted to an understanding of the basic ideas in this work. Mean-field theory of quasi-2D spin-1/2 anisotropic Heisenberg antiferromagnets will be presented in chapter III. A generalized form of the mean-field approximation for a bilinear spin interaction system is outlined. Following the work of Van Wier *et al.*,^[25] the complete solutions of the quasi-2D, anisotropic, Heisenberg antiferromagnets at $T=0$ are discussed and finite temperature phase diagrams are derived. Liu and Fisher's^[3] analysis of a

supersolid phase in the quantum lattice gas is directly applied to study of an intermediate phase in the quasi-2D spin-1/2 anisotropic Heisenberg systems. The effect of spin-canting at the transition between the spin-flop and the antiferromagnetic phases are also discussed. The necessary formulae for carrying out a numerical calculation are given. In the chapter IV, experimental studies on the magnetic properties, phase transitions, phase diagrams and critical behavior of the layer compounds $[C_6H_5(CH_2)_nNH_3]_2CuBr_4$ ($n = 1, 2$ and 3) will be fully reported. Initial susceptibility and isothermal magnetization studies on $[NH_3(CH_2)_nNH_3]CuX$ with $n = 4, 5, 7$ and 10 for $X = Cl_4$ and Br_4 are given in chapter V. Spin-dimensionality crossover is also discussed.

References of Chapter I

1. M.E. Fisher, AIP Conf. Proc 24, 273 (1975); A. Aharony and A.D. Bruce, Phys. Rev. Lett. 33 427 (1974).
2. A.D. Bruce and A. Aharony, Phys. Rev. B11, 478 (1975).
3. Kao-Shien Liu and M.E. Fisher, J. Low Temp. Phys. 10, 655 (1973).
4. H. Matsuda and T. Tsuneto, Progr. Theoret. Phys., Suppl. 46, 411 (1970).
5. G.V. Chester, Phys. Rev. A2, 256 (1970).
6. A.J. Leggett, Phys. Rev. Lett. 25, 1543 (1970).
7. R.A. Guyer, Phys. Rev. Lett. 26, 174 (1971).
8. W.J. Mullin, Phys. Rev. Lett. 26, 611 (1971).
9. R.S. Kagiwoda, J.S. Fraser, I. Rudnick and D. Bergman, Phys. Rev. Lett. 22, 338 (1969).
10. D.L. Goodstein and R.L. Elgin, Phys. Rev. Lett. 22, 383 (1969).
11. N. D. Mermin and H. Wagner, Phys. Rev. Letters 17, 1133 (1966).
12. H. Nishimori, K. Kubo, Y. Ozeki, Y. Tomita and T. Kishi, J. Stat. Phys. 55, 259 (1989).
13. M. Kikuchi and Y. Okabe, J. Phys. Soc. Jpn. 58, 679 (1989).
14. Y. Ozeki, H. Nishimori and Y. Tomita, J. Phys. Soc. Jpn. 58, 82 (1989).
15. T. Kishi and K. Kubo, J. Phys. Soc. Jpn. 58, 2547 (1989).

16. H. Nishimori and Y. Ozeki, *J. Phys. Soc. Jpn.* 58, 1027 (1989).
17. T. Kawabe, *J. Phys. Soc. Jpn.* 58, 348 (1989).
18. S. Nagasawa, *J. Phys. Soc.* 59, 300 (1990).
19. H. E. Stanley and T. A. Kaplan, *Phys. Rev. Letters* 17, 913 (1966); H. E. Stanley, *J. Appl. Phys.* 40, 1546 (1969).
20. H. E. Stanley, *Phys. Rev. Letters* 20, 589 (1969).
21. M. A. Moore, *Phys. Rev. Letters* 23, 861 (1969).
22. D. D. Betts, C. J. Elliott and R. V. Ditzian, *Can. J. Phys.* 49, 1327 (1971).
23. P. Bloembergen, *Physica* 79B, 467 (1975).
24. L. J. de Jongh and A. R. Miedema, *Adv. Phys.* 23 (1974).
25. O. P. Van Wier, T. Van Peski-Tinbergen and C. J. Gorter, *Physica* 25, 116 (1959).

CHAPTER II

A SHORT REVIEW OF BASIC THEORIES

Phase Transitions and Critical Point

It has always been fascinating that the same substance may exist in different "phases" or "states" which show transitions into each other. The theoretical and experimental study of phase transitions has a long and illustrious history spanning over a century to the present day. In fact, the difference between different phases of the same substance was felt to be more significant than the difference between different substances. The familiar examples of a phase transition are the condensation of a gas to a liquid for a simple fluid system under pressure and the change from a ferromagnetic to a paramagnetic state for a simple ferromagnet under an applied field. A functional relationship of the form $f(P, \rho, T) = 0$ or $f(H, M, T) = 0$ the so-called equation of state which relates the thermodynamic parameters - pressure (or field), density (or magnetization) and temperature certainly characterizes phases. The equation of state thus defines a surface in a three-dimensional space whose coordinates are P, ρ, T (or H, M, T); each point on this surface corresponds to an equilibrium state of the system. The different forms of equation of state are thought to be due to different phases.

The fundamental problem of statistical mechanics to compute equations of state consists in evaluating the partition function

$$Z(N, \Omega, \beta, J) = \sum_{\{C\}} e^{-H\{C, J\}}$$

for a system of N particles in a region Ω with volume V described by a microscopic Hamiltonian or interaction energy $H \{ C, J \}$ which depends on the configurations C of the particles and some set of interaction potentials or coupling parameters J . The canonical partition function $Z (N, \Omega, \beta, J)$ depends on the meaning of the symbolic sum over configurations $\sum_{\{C\}}$ referred to the type of system under consideration. If the microscopic description is quantum mechanical, H is an operator and the sum denotes a trace of the operator $\exp(-\beta H)$. For a classical system of particles the "sum" denotes an integral over coordinates and momenta of the particles. Models for magnetic systems usually consist of a set of spins occupying fixed points in space. Configurations are then specified by the values of the spins $\{ \vec{S}_1, \vec{S}_2, \dots, \vec{S}_N \}$, which may be quantum mechanical operators, vectors with some fixed length, or scalars. In the quantum case the sum over configurations becomes a trace and when the \vec{S}_i are vectors (classical) the sum becomes an integral. The standard method of proceeding to an infinite system is via what is known as the thermodynamic limit. That is, the volume V and the number of particles N both go to infinity with density $\rho = N/V$ remaining finite. For magnetic systems the volume V plays no direct role so it is only necessary to take the limit $N \rightarrow \infty$. The sum over configuration for the partition function may develop singularities on certain surfaces in parameter space.^[1] These singularities are usually called phase transitions. One may distinguish first and second (or higher) order transitions according to whether the entropy $S = \partial(\beta^{-1} \ln Z) / \partial T$ has a discontinuity at the transition or not.

Up to now the theoretical study of transition phenomena has faced some considerable difficulties. Complete and rigorous analysis seems to be seldom possible. First order transitions, such as those taking place at the liquid-gas coexistence line, have been described quite successfully by the phenomenological theory of Van der Waals. This theory is actually recovered in the Landau theory of phase transitions. Fig 1 (a) and (b)

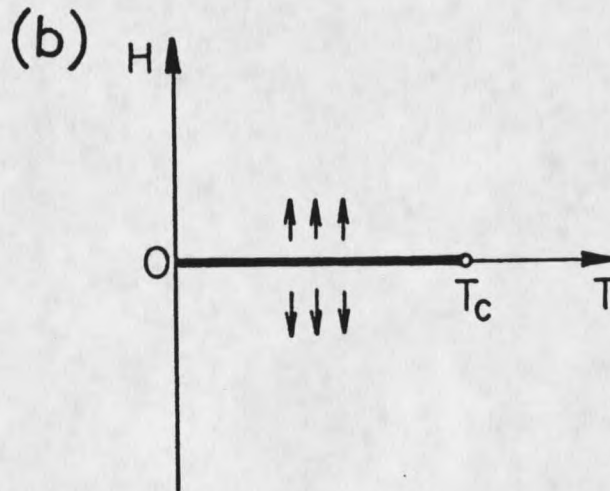
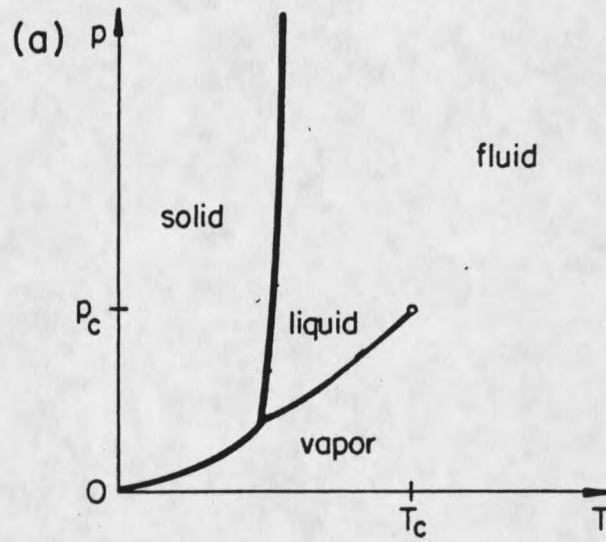


Fig. 1. Phase diagrams illustrating the magnet-fluid analogy: (a) (P, T) phase diagram for a fluid system; (b) (H, T) phase diagram for a ferromagnet.

illustrate the phase diagrams for fluid and ferromagnet systems, respectively. For the fluid there are three familiar phases--- the solid, liquid and gaseous phases. The solid and gaseous phases are in equilibrium along the sublimation curve, the solid and liquid phases are in equilibrium along the fusion curve, and the liquid and gaseous phases are in equilibrium along the vapor pressure curve. These curves, shown as solid lines where two phases coexist in Fig 1(a), are called phase boundaries. The vapor pressure curve terminates in a point at which the transition becomes second order. This point is called the critical point, (P_c, ρ_c, T_c) . Above this point, a liquid can change to a gas continuously without crossing the phase transition line. In the case of the magnet, there is a first order transition line separating the "up" and "down" ferromagnetic states; this line ends at the critical (Curie) point. Because of the symmetry under $H \rightarrow -H$, the phase transition line for magnet is entirely confined to the $H = 0$ or T -axis, as shown in Fig. 1 (b), in which the magnet breaks up into domains. The coexistence or "spontaneous magnetization " curve is symmetric about the T -axis while for the fluid this symmetry is absent.

Critical Phenomena and Critical Exponents

Critical phenomena refer to phase transition phenomena near the critical point. For a given physical system approaching the critical point, various thermodynamic quantities are found to diverge, or to present other singularities. The usual way to describe the transition around the critical point is in terms of the so-called "critical exponents" which characterize the singular behavior of response functions. Defining the reduced temperature $t = (T - T_c) / T_c$ and reduced field (or pressure) $h = H - H_c$ (or $h = P - P_c$), where T_c and H_c (or P_c) are critical values, the given response functions $f(t,h)$ will be $f(t,0) \propto t^{-\lambda_t}$ as $t \rightarrow 0$ or $f(0,h) \propto h^{-\lambda_h}$ as $h \rightarrow 0$ while λ_t and λ_h may correspond to various types

of behavior such as logarithmic divergence, cusp singularity or even analytic behavior with a jump discontinuity. Explicitly,

$$f(t, 0) = A t^{-\lambda_t} (1 + at^{\theta_t} + \dots)$$

$$f(0, h) = B h^{-\lambda_h} (1 + bh^{\theta_h} + \dots),$$

where λ_t and λ_h are called critical exponents and θ_t and θ_h are confluent "correction" exponents being positive and less than unity^[2]. The critical exponents characterizing the singular behavior (an asymptotically pure power law) then can be defined as

$$\lambda_t^+ = - \lim_{t \rightarrow 0^+} \frac{\ln f(t, h)}{\ln t} \Big|_{h=0},$$

$$\lambda_t^- = - \lim_{t \rightarrow 0^-} \frac{\ln f(t, h)}{\ln t} \Big|_{h=0},$$

$$\lambda_h^+ = - \lim_{h \rightarrow 0^+} \frac{\ln f(t, h)}{\ln h} \Big|_{t=0},$$

$$\lambda_h^- = - \lim_{h \rightarrow 0^-} \frac{\ln f(t, h)}{\ln h} \Big|_{t=0}.$$

One of the most striking features of critical phenomena is their large degree of universality. For a variety of physical systems, critical singularities of the basic response functions such as the specific heat C_H ($H=0$), spontaneous magnetization M_S ($H=0$), liquid-gas density difference $\rho_L - \rho_G$, initial susceptibility χ ($H=0$), isothermal compressibility K_T , critical isothermal magnetization M ($T=T_c$), pair correlation function G , and correlation length ξ , etc., are described by a set of exponents denoted by Greek letters. Table I lists the definitions of frequently encountered critical exponents for magnetic systems. Due to thermodynamic arguments, these exponents must necessarily satisfy a set of inequalities which are listed in table II.^[3]

Expo- nent	Definition	Conditions			Quantity
		ϵ	H	M	
α'	$C_H \sim (-\epsilon)^{-\alpha'}$	< 0	0	0	specific heat at constant magnetic field
α	$C_H \sim \epsilon^{-\alpha}$	> 0	0	0	
β	$M \sim (-\epsilon)^\beta$	< 0	0	$\neq 0$	zero-field magnetization
γ'	$\chi_T \sim (-\epsilon)^{-\gamma'}$	< 0	0	$\neq 0$	zero-field isothermal susceptibility
γ	$\chi_T \sim \epsilon^{-\gamma}$	> 0	0	0	
δ	$H \sim M ^\delta \text{sgn}(M)$	0	$\neq 0$	$\neq 0$	critical isotherm
ν'	$\xi \sim (-\epsilon)^{-\nu'}$	< 0	0	$\neq 0$	correlation length
ν	$\xi \sim \epsilon^{-\nu}$	> 0	0	0	
η	$\Gamma(r) \sim r ^{-(d-2+\eta)}$	0	0	0	pair correlation function (d = dimensionality)

Table I. Definition of the magnetic critical exponents.

Inequality
$\alpha' + 2\beta + \gamma' \geq 2$
$\alpha' + \beta(\delta + 1) \geq 2$
$(2 - \alpha')\xi + 1 \geq (1 - \alpha')\delta$
$\gamma'(\delta + 1) \geq (2 - \alpha')(\delta - 1)$
$\gamma' \geq \frac{\beta(\delta - 1)}{\delta + 1}$
$d(\delta - 1)/(\delta + 1) \geq 2 - \eta$
$d\gamma'/(2 - \alpha') \geq d\gamma'/(2\beta + \gamma') \geq 2 - \eta$
$(2 - \eta)\nu \geq \gamma$
$d\nu' \geq 2 - \alpha'$
$d\nu \geq 2 - \alpha$

Table II. Inequalities of exponents.

For most phase transitions, one can define an order parameter to distinguish the ordered phase. In the case of simple fluids (fig. 2(a)), the liquid-gas density difference $\rho_L - \rho_G$ is an order parameter along the coexistence curve because it is non-zero only in the ordered phase, $\rho_L - \rho_G \propto (-t)^\beta$ as $t \rightarrow 0^-$ at $P = P_c$ where the exponent β has been found to be about 1/3 for most simple fluids.^[3] For a simple ferromagnet (Fig 2(b)), the spontaneous magnetization ($H = 0$) should be an order parameter, $M_s \propto (-t)^\beta$ as $t \rightarrow 0^-$ and $H = 0$. The order parameter variation on the critical isotherm is generated by fixing the temperature precisely at T_c , varying the ordering field, h , and observing the change in M or $\Delta\rho$. Around the critical point for a magnet, the critical isothermal magnetization is $M(T = T_c) \propto H^{1/\delta}$ ($H \geq 0$). Naturally the critical isotherm near a fluid critical point has completely analogous behavior, $\Delta\rho \propto |P - P_c|^{1/\delta}$, ($T = T_c$).

In general, a properly chosen order parameter in any system should have the following properties: (1) it jumps discontinuously across the first order phase transition; (2) as criticality is approached, this jump gets smaller and smaller; (3) larger values of the order parameter imply that one is far away from criticality. Indeed, the order parameter has a tensorial character which may depend on the class of systems considered. It could be single-component (scalar) or n-component (vector or tensor). In many cases the Hamiltonian is invariant under certain transformations of spin operator $S(\vec{r})$ such as, depending on the spin dimensionality, i) reversal $S(\vec{r}) \rightarrow -S(\vec{r})$, ii) change of phase $S(\vec{r}) \rightarrow e^{i\phi} S(\vec{r})$ and iii) rotation $S(\vec{r}) \rightarrow U S(\vec{r})$. This holds for example^[2] with $n = 1$ for simple fluids, binary fluids, uniaxial ferromagnets, binary alloys, Ising systems, etc.; $n = 2$ for superfluid He^4 and $\text{He}^3 + \text{He}^4$ mixtures, XY systems; $n = 3$ for isotropic magnets, Heisenberg systems, etc., respectively. For large n , the $1/n$ expansion technique^[4] along with renormalization group and perturbation theory achieves its unique success in critical

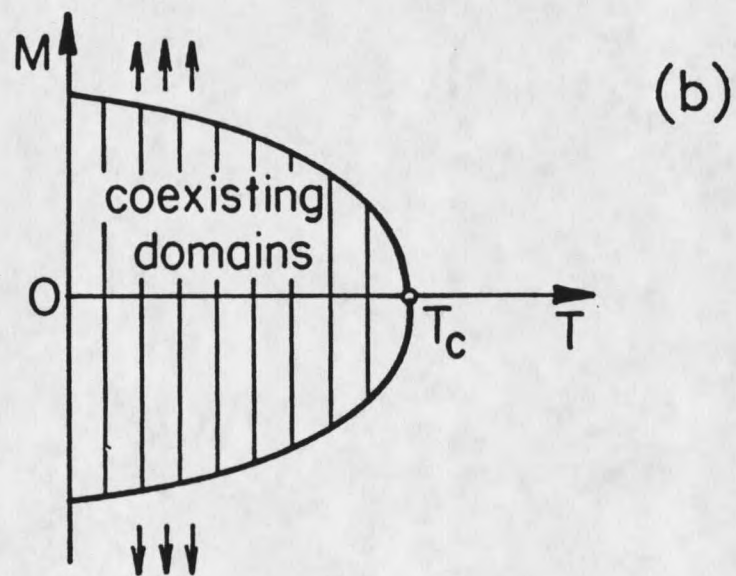
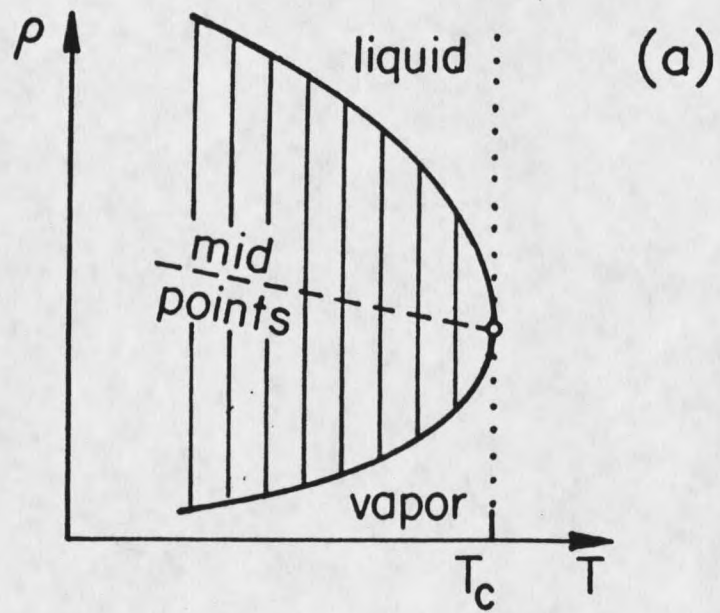


Fig. 2. Coexistence diagrams illustrating the magnet-fluid analogy: (a) for a fluid and (b) for ferromagnet.

theories. In the same spirit, the ϵ -expansion scheme^[5] presents the first example of practical successes of the renormalization group in critical field theory. This expansion is generated in terms of the parameter $\epsilon = 4 - d$, where d is the spatial dimensionality of the system.

The response of the order parameter to an external symmetry breaking field, H , is the susceptibility (or compressibility for a fluid) $\chi = \partial M / \partial H |_T$. Above T_c the spontaneous magnetization is identically zero (fig 2(b)), but magnetization can be induced by an applied field (fig. 3). The initial susceptibility is defined by $\chi_0(T) = \lim_{H \rightarrow 0^+} \left(\frac{\partial M}{\partial H} \right)_T$,

which measures the slope of the magnetization isotherm at zero field. It is clear from fig. 3 that χ_0 measures the ease of magnetizing a ferromagnet and hence is expected to become large and then diverge to infinity at the Curie point, $\chi_0 \propto t^{-\gamma}$. According to the fluctuation-dissipation theorem susceptibility is the sum over sites of a spin correlation function, $\chi = \sum_r G(r, h, t) = \sum_r \langle S(0)S(r) \rangle - \langle S(r) \rangle^2$. The infinity of χ_0 is achieved because at criticality the sum diverges: $G(r)$ is a power of the separation distance, $G(r, 0, 0) \propto 1/r^{2\alpha}$, for large r which is strictly bounded to be < 1 . It may be concluded that the characteristic infinities of thermodynamic response functions at critical point are reflections of correlations which extend over infinite distances in space. Away from criticality, correlations tend instead to fall off with exponential rapidity as $r \rightarrow \infty$, i.e. $\lim_{r \rightarrow \infty} G(r, h, t) = e^{(-r/\xi)} \times$ weaker function of r . The characteristic length, ξ , has the physical significance of being a range of correlations within the system. It diverges at the critical point, $\xi \propto t^{-\nu}$. However, the correlation length can be defined in many different ways,

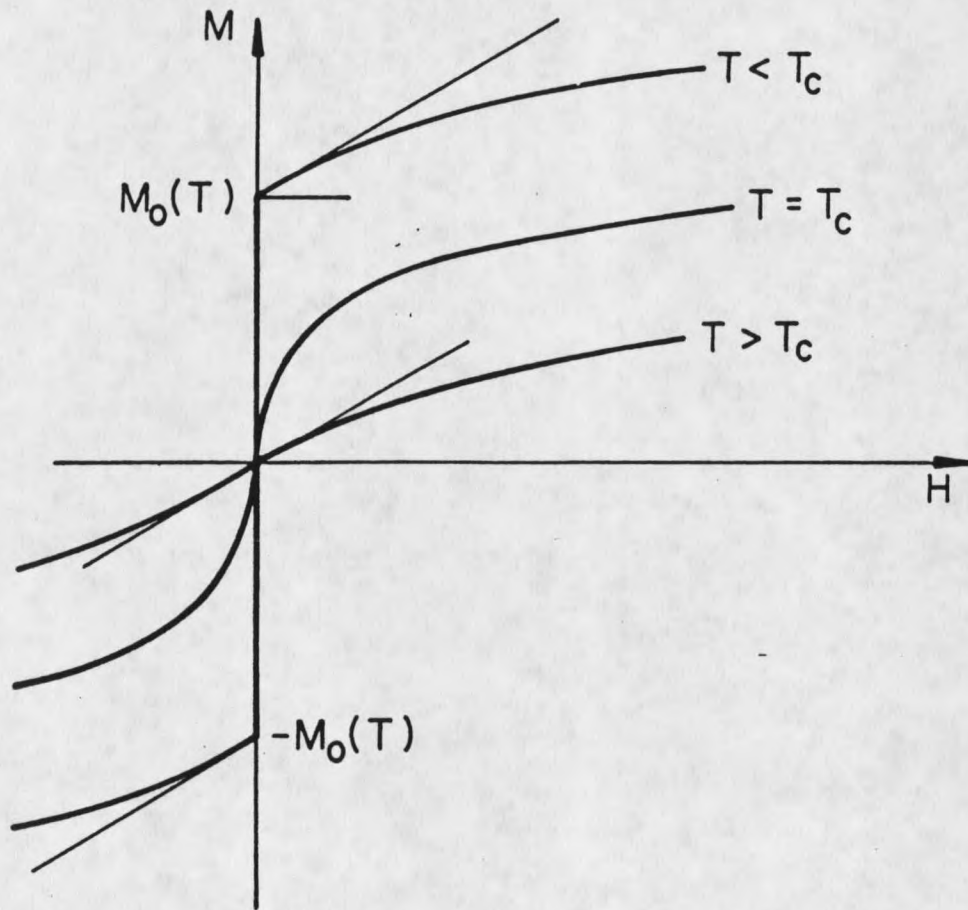


Fig. 3. Magnetization curves (isotherms) for a simple ferromagnet. $M_0(T)$ indicates the spontaneous magnetization.

$$\xi_s^2 = \frac{\int r^2 \langle S(r)S(0) \rangle d^d r}{\int \langle S(r)S(0) \rangle d^d r},$$

$$\xi_\epsilon^2 = \frac{\int r^2 \langle \epsilon(r)\epsilon(0) \rangle d^d r}{\int \langle \epsilon(r)\epsilon(0) \rangle}, \dots \text{etc.}$$

where $S(r)$ and $\epsilon(r)$ are local spin operator and energy density, respectively. At criticality all suitable definitions will give the same degree of divergence, the same exponent ν . Thus the fundamental source of all thermodynamic singularities at the critical point is the divergence in the correlation length. The physical source of correlation length divergence is related to fluctuations.^[2,3] For a given system, the equilibrium state may become more ordered as the temperature is lowered ($T < T_c$). Thus, the order parameter becomes larger. Once temperature is increasing to approach the critical point, the order parameter becomes smaller and smaller and fluctuations increase. The susceptibility is directly related to the spin fluctuations. As $T \rightarrow T_c$, the spin correlation function becomes very long range, which means the spin correlation length is much bigger than any microscopic scale of the system. In an analogy with the susceptibility, the specific heat at constant magnetic field can be expressed in terms of the energy fluctuations^[3] $C_H = (1/kT^2) (\langle E^2 \rangle - \langle E \rangle^2)$. For a fluid, similarly, the isothermal compressibility K_T directly relates the fluctuations in the total number of particles in the systems,^[3] $K_T = K_T^0 \langle (N - \langle N \rangle)^2 \rangle / N$, or $K_T = n^{-1} K_T^0 \int d^d r G(\vec{r})$ where $G(\vec{r})$ is the density-density correlation function $\langle \{n(\vec{r}) - \langle n(\vec{r}) \rangle\} \{n(0) - \langle n(0) \rangle\} \rangle$ and $K_T^0 = 1/nkT$. At the critical point, the divergence of K_T is equivalent to the long range of the density correlation function.

The nature of fluctuations over a long range near the critical point can be learned directly from scattering radiation (light, x-ray, neutrons, etc.) off the system of interest.

The scattering intensity is proportional to the fundamental quantity $G(\vec{k}) = \int d\vec{r} e^{i\vec{k}\cdot\vec{r}} G(\vec{r})$. In the scattering experiments the pair correlation can be measured by the fact that (1) the radiation couples to the order parameter; (2) the correlation range (real space) is of the same order as the wavelength of the radiation; and (3) the inverse correlation time (temporal correlation by inelastic scattering) is of the same order as the frequency of the radiation. For a fluid or fluid mixture the light scattering intensity is then determined by the density fluctuation in the medium. If the medium were perfectly uniform there would be no scattering at all. Once the critical point is approached enormously enhanced values of the light scattering are observed (critical opalescence) corresponding to long wavelength density fluctuations. For magnets, in neutron scattering experiments, the neutrons are scattered via the interaction between neutron and electron magnetic moments. Once the momentum transfer $k = P_f - P_0 \rightarrow 0$ (forward scattering or zero angle scattering),^[6] the scattering intensity determined by spin fluctuations behaves as $k^{(-2+\eta)}$ at $T = T_c$. The susceptibility is related to the zero k limit of $G(\vec{k})$, $\chi = T G(0)$.

Mean Field Theory, Landau Theory and Thermodynamic Scaling

In many-body problems, the mean-field approximation (or "molecular field") is one method of finding the best approximate one-body Hamiltonian. This approximation was first introduced by Weiss^[7] while studying the second order transition of ferromagnetic materials at the Curie point. Consider a spin Hamiltonian

$$H = -J \sum_{\langle ij \rangle} \vec{S}_i \cdot \vec{S}_j - \mu g H_z \sum_i S_{iz}$$

where the first sum extends over neighbor pairs only. Recognizing that the exact evaluation of the partition function is an intractable problem, the basic assumption of the mean field theory is that the sum over states of the system appearing in the Hamiltonian

can be broken into separate sums over states of individual magnetic moments. The influence of the interactions among the spins is described by an effective molecular field acting on each magnetic moment. This "molecular" field is assumed to be proportional to the magnetization, $\vec{H}_m = \langle \vec{S}_j \rangle = \lambda \cdot \langle S_z \rangle \vec{z}$. Thus $\vec{S}_i \cdot \vec{S}_j$ is replaced by $\lambda \langle S_z \rangle (S_{zi} + S_{zj}) - \lambda \langle S_z \rangle^2$. This replacement is a special case of the general approximation scheme for a product $\vec{S}_A \cdot \vec{S}_B = (\langle \vec{S}_A \rangle + \delta \vec{S}_A) \cdot (\langle \vec{S}_B \rangle + \delta \vec{S}_B)$ whereby one discards the term $\delta \vec{S}_A \cdot \delta \vec{S}_B$ so that $\vec{S}_A \cdot \vec{S}_B \rightarrow \langle \vec{S}_A \rangle \cdot \langle \vec{S}_B \rangle + \langle \vec{S}_A \rangle \cdot \delta \vec{S}_B + \langle \vec{S}_B \rangle \cdot \delta \vec{S}_A = \langle \vec{S}_A \rangle \cdot \vec{S}_B + \langle \vec{S}_B \rangle \cdot \vec{S}_A - \langle \vec{S}_A \rangle \cdot \langle \vec{S}_B \rangle$. Thus the Hamiltonian is replaced by $H = (1/2)N\lambda J \langle S_z \rangle^2 - (J\lambda \langle S_z \rangle + \mu g H_z) \cdot \sum_{i=1}^N S_{zi}$ where $(H_z + J \frac{\lambda}{\mu g} \langle S_z \rangle)$ is called the effective magnetic field. The "molecular" field then is determined by thermodynamic functions self-consistently. This theory, in one sense, is a great success. It does give first order phase transitions and gives also a qualitative indication of the types of singularities expected in the second order phase transition. However, in another sense, it is a complete failure in the critical region. Critical phenomena involve strong fluctuations (long-range correlations). Mean field theory is based upon the assumption of small fluctuations.

The Landau theory^[8] of phase transitions is built of two main ingredients. The first is the concept of the order parameter, giving a local macroscopic description of the state of the system. For a given thermodynamic system, as the temperature is lowered, the equilibrium state may become more ordered. As a critical point is reached, a symmetry of the high temperature phase is broken spontaneously. Thus the order parameter becomes nonzero. The second ingredient basically is the hypothesis that the Helmholtz free energy density is an analytic function of the order parameter, the temperature and any other variable, and that close to the criticality the order parameter remains small so that the

functional free energy can be expanded in powers of the order parameter. The precise coefficients of expansion depend crucially on the detailed symmetries of the disordered phase from which a second order, or continuous transition may or may not be allowed. The critical exponents predicted by both mean field and Landau theories are actually identical. Because the thermodynamic fluctuations are effectively neglected, the critical exponents given by both theories are wrong. These exponents turn out to be characteristic of the theories rather than of the physics even though mean-field theory is based on microscopic consideration. Landau theory presents unique values of exponents, independent of too many physically relevant quantities.

Since critical phenomena arise from long-range correlation, one may reasonably expect that some of the details of the microscopic interactions might be quite irrelevant to the critical behavior. Thus, it is usually asserted that the values of the critical exponents are independent of lattice structure. All critical problems may be simply classified by (1) the dimensionality of the systems; (2) the symmetry group of the order parameter; and (3) perhaps other criteria. The critical behavior, within each class, should be identical or may depend on a very few parameters. One of the original tasks to convert this universality statement into mathematical form is the scaling hypothesis. It states, in the critical region, that the singular part of the free energy, f , should be "invariant" (except for a scaling factor) under a scaling transformation. Therefore, f behaves as a generalized homogeneous function of its variables:^[3]

$$f(\lambda^{a_1} g_1, \lambda^{a_2} g_2, \dots, \lambda^{a_n} g_n) = \lambda f(g_1, g_2, \dots, g_n)$$

where g_1, g_2, \dots, g_n are the reduced temperature, reduced field ... other thermodynamic variables (conjugate local fields or scaling fields), and a_1, a_2, \dots, a_n are appropriate exponents (eigenvalues) related to the critical exponents defined previously. The fact

that exponents a_i cannot be specified corresponds to the fact that the homogeneous function or scaling hypothesis does not determine the value of the critical exponents. But, it does give rise to functional relations among the critical exponents and makes specific predications related to the form of the equation of state.^[3] The thermodynamic response functions can be obtained by differentiating f (once or twice) with respect to the fields g_i and $\lambda^{a_i} g_i$. By properly choosing λ , the leading singularities of the response functions then obey power laws which lead to various relations among the critical exponents. Some of these relations are listed in Table II while the inequalities are replaced by equalities. It is clear from the scaling assumption that there remain only two independent critical exponents. The scaling hypothesis is a basic assumption in modern critical theories. It is usually referred to as a law or principle. However, along with certain logic statements, it is sometimes called scaling theory.

Basic Spin Models, Spatial Scaling and Renormalization Group Theory

The spin Hamiltonian in the simple case usually would be

$$H = - \sum_{\langle ij \rangle} (J_x S_i^x \cdot S_j^x + J_y S_i^y \cdot S_j^y + J_z S_i^z \cdot S_j^z) - \vec{h} \cdot \sum_i \vec{S}_i$$

where the first term is the coupling between nearest neighbor spins and the second represents the interaction with the external magnetic field. If $J_x = J_y = J_z$, it is called the Heisenberg model (or XXX model) which is referred to as the isotropic case. By setting $J_z = 0$ and $J_x = J_y \neq 0$, it represents the planar model, the so-called XY model. For $J_z \neq 0$ and $J_x = J_y = 0$, one obtains the so-called Ising model. In general, if $J_x \neq J_y \neq J_z$ ($J_i \neq 0$) it is usually called an anisotropic Heisenberg or XYZ (or biaxial anisotropic) model. The XXZ model is the uniaxial anisotropy case, $J_x = J_y \neq J_z$. For the easy-axis case (Heisenberg-Ising like), $J_x = J_y < J_z$. For the easy-plane case (Heisenberg-XY like),

$J_x = J_y > J_z$. Positive J_i corresponds to "ferromagnetic" and negative J_i corresponds to "antiferromagnetic". Ising, XY and Heisenberg models, however, can be recovered by a more general model, n-vector model, which describes the spin as an n-component classical vector with fixed (normalized) length, $\vec{S}_i = (S_i^{(1)}, S_i^{(2)}, \dots, S_i^{(n)})$, $|\vec{S}_i| = 1$ (or \sqrt{N}). $n = 1, 2, 3$ and ∞ correspond to Ising, XY, Heisenberg and spherical models, respectively. The other discrete model is the so-called Potts model.^[9] The q-state Potts model assumes that the "spins" at lattices sites are variables which can be in any one of q states, $S_i = 1, 2, \dots, q$.

The continuous spin models can be obtained when each spin component in the n-vector models is allowed to range from $-\infty$ to $+\infty$ ($-\infty < S_i^{(n)} < +\infty$). Thus, in order to evaluate the integral for the partition function the spin distribution function or spin weighting function, $W(S_i)$, must be introduced. Otherwise, the partition function could diverge when all the spins become infinitely large. For the Ising case, $e^{-w(S_i)} = \delta(S_i + 1) + \delta(S_i - 1)$, the partition function then is

$$Z_N = \int_{-\infty}^{\infty} ds_1 \cdots \int_{-\infty}^{\infty} ds_N e^{-H/kT} \prod_{i=1}^N e^{-w(s_i)}$$

The simplest generalization that provides a genuinely continuous spin distribution is the Gaussian model, which is given by setting $w(S_i) = 1/2 |\vec{S}_i|^2$. The serious shortcoming of the Gaussian model is that it has no low temperature behavior. The reason for this is that the exponential decrease of the spin distribution function for large $|\vec{S}_i|$ is not rapid enough to keep the integrals convergent when T is too small. The LGW (Landau-Ginzburg-Wilson or so-called S^4) model overcomes this defect. In this model the spin weighting function is written as

$$e^{-w(\vec{S}_i)} = e^{-\frac{1}{2} |\vec{S}_i|^2 - u |\vec{S}_i|^4}$$

with $u > 0$. Up to now there are many other models in a variety of approximations. In the sense of symmetry group, the $O(n)$ model^[10] was originally defined as a system of n -dimensional spin vectors which interact in a rotational invariant way. If one lets n be a continuous variable and specifically chooses the interactions between the spins, the partition function can be expressed in terms of a loop gas.^[11] For particular lattice structures and range of n the loop model can be mapped onto the coulomb gas.^[12] Vertex, clock and non-linear σ models are other specific examples in the symmetry language.

Since critical properties of a system depend on long-range correlation or on the nature of long-wavelength fluctuations, critical phenomena are not characteristic of short distance details. The renormalization procedure (spatial rescaling) expresses this idea in a simple manner ----- scale-invariance. That is, since $\xi \rightarrow \infty$ at a critical point, the system behaves the same on all length scales, or scaling the unit of length leaves the correlation length the same. Kadanoff^[13] first introduced this idea in terms of "block spin" transformations in 2D Ising models. Near the critical point spins become highly correlated so the spins behave as large blocks which means that the degree of freedom of average block spins plays a main role, instead of the original individual spins. The idea of "block spin" transformation opened the modern era in the study of critical phenomena, later leading to the renormalization group (RG) theory.^[14] The renormalization group is defined as a set of symmetry transformations which essentially are a combination of the Kadanoff and scale transformations.

Let $\{ K \} = \{ K_1, K_2, \dots \}$ denote coupling parameters which depend on the physical parameters, temperature, external field, etc. for a given system. Under a RG transformation, R_b , the renormalized Hamiltonian should retain invariant form in terms of new coupling parameters $\{ K' \} = \{ K'_1, K'_2, \dots \}$ and block spins. That is, $H' = H'(K') = R_b[H]$ where b is spatial rescaling factor. In a d -dimensional system b is related to the

reductions in the number of degrees of freedom $N \rightarrow N' = N/b^d$ and in the lattice spacing $r \rightarrow r' = r/b$. The renormalized correlation length, $\xi' = \xi[H']$, then is given by $b\xi[H'] = \xi[H]$. One can show that in most cases the partition function is preserved under RG transformation, $Z_{N'}[H'] = Z_N[H]$, and free energy density obeys $f[H] = b^{-d} f[H']$. Thus a RG transformation fundamentally changes a given problem into a new one, but it still contains the same essential information as the original one. The renormalized coupling parameters turn out to be the functions of original coupling parameters, $K'_i = R_i(\{K\})$, which are usually called flow equations or recursion relations for the coupling constants.

If one denotes the recursion relation of coupling constants from n successive applications of a given RG transformation, $K^{(n+1)} = R(K^{(n)})$, a fixed point K^* of the map R is then defined by $K^* = R(K^*)$, while from assuming continuity of R , it follows that $K^{(n)}$ approaches a fixed point as $n \rightarrow \infty$. Implicitly, one has $T^* = R_T(T^*)$, which means that when the recursion relation is iterated the temperature T does not change if its initial value is set at $T = T^*$ i.e., it remains "fixed" at T^* . Subsequently, the flow equation for the correlation length must be $\xi(T^*) = b^n \xi(T^*)$. This equation has only two possible solutions, $\xi(T^*) = \infty$, which characterizes a critical point as we know, and $\xi(T^*) = 0$ which refers to a trivial fixed point. Therefore, the case of $\xi(T^*) = \infty$ is physically interesting. The cases where $\xi(T^*) = 0$ where spins are totally uncorrelated ($T^* \neq 0$) or where they are frozen in a ground state ($T^* = 0$ K) are not physically interesting here. The RG transformation itself acts on a space of Hamiltonians but can be characterized in momentum space too.^[14] It is important to stress that the fixed point is not the critical point of the original system unless that system itself happens to be the one with coupling constants K^* . To employ a RG transformation in a variety of models, it is usually essential to assume that the transformation is smooth^[2,15,16] in the sense that if $H \rightarrow H'$ and $H + \delta H \rightarrow H' + \delta H'$, and also when $\delta H \rightarrow 0$ one has $\delta H' \rightarrow 0$. This assumption means that

systems corresponding to the Hamiltonians at nearby points in the multidimensional parameter space (K - space) flow under renormalization to other points which also lie relatively close together. Consider an unrenormalized $H^{(0)}(t,h)$, near its ferromagnetic critical point, $t=0$ and $h=0$. At the critical point, $\xi = \infty$, it is characteristic of slow decay of the correlations. In general, the critical Hamiltonian $H_c^{(0)} = H^{(0)}(0,0)$ is not a fixed point. Under a RG transformation, a new critical Hamiltonian, $H'(t'=0, h'=0)$, can be recognized since $\xi_c \rightarrow \xi'_c = \frac{\xi_c}{b} = \frac{\infty}{b} = \infty$. Thus a line or trajectory of critical points is generated under successive RG transformations. The trajectory terminates at some fixed point H^* at which further renormalization produces no further motion. The set of all points in K -space flows into H^* . All points on this stable critical manifold, including the fixed point, correspond to systems at criticality. For different systems (starting in a quite different region of parameter space or different initial physical manifolds) and if the critical Hamiltonians under RG transformation flow to the same fixed point (same critical manifold), the critical behaviors of these systems are then described by the same class. The critical exponents are the same for all systems in the universality class defined by the critical manifold containing the fixed point.

Unlike scaling theory, RG theory actually gives a method for computing the exponents. Near a fixed point, a linear approximation can be made if n is very large, $R(K^{(n)}) = R(K^*) + T(K^{(n)} - K^*) = R(K^*) + T \delta K$ where T is the matrix with elements being

$$T_{\alpha\beta} = \left. \frac{\partial R_\alpha(K)}{\partial K_\beta} \right|_{K=K^*} = \left(\frac{\partial K'_\alpha}{\partial K_\beta} \right)^*$$

Thus, one has $K^{(n+1)} - K^* = T\delta K$ or $\delta K' = T\delta K$. To diagonalize T , a new complete set of eigenvectors $\{ \phi_i \}$ with eigenvalues $\{ \lambda_i \}$ should be introduced, $T\phi = \lambda\phi$. The scaling fields then can be constructed by $g'_i = \lambda_i g_i$ with $\lambda_i = b^{y_i}$. Near a fixed point, it is con-

venient to use the scaling fields $\{g_i\}$ as independent variables, instead of coupling constants $\{K_i\}$. The singular part of free energy and correlation length then take the forms $f(g_1, g_2, \dots) = b^{-dn} f(\lambda_1 g_1, \lambda_2 g_2, \dots)$ and $\xi(g_1, g_2, \dots) = b^n \xi(\lambda_1 g_1, \lambda_2 g_2, \dots)$, respectively. These forms are just generalized homogeneous functions (scaling assumption). At fixed point $K \rightarrow K^*$ ($\delta K \rightarrow 0$) as $n \rightarrow \infty$ hence $g_i \rightarrow 0$. For a given Hamiltonian, under a RG transformation, establishing the flow equations and choosing K as the origin ($K^* = K$) in the coupling-constants space, the exponents $\{y_i\}$ can be then obtained in principle by solving eigenvalues, $\{\lambda_i\}$, corresponding to the matrix T .

A Possible Universal Critical Theory in Two Dimensional Systems - Conformal Field Theory

Applications of conformal invariance in field theories have accumulated during the last few years.^[17] Particularly, it has been recognized that the principle of conformal invariance leads to a connection between interacting quantum field theories and statistical mechanics close to a critical point.^[18] A conformal transformation is, roughly, a generalization of a scale transformation in which the length-rescaling factor depends continuously on position, $b(\vec{r})$. Such transformation, $x^\mu = x'^\mu(x^\mu)$, may be visualized as local non-linear scale transformation with angles locally preserved, $dx^\mu dx_\mu = b(x^\mu)^{-2} dx'^\mu dx'_\mu$ (so-called local RG transformation). For the short-range interactions (locally), the conformal invariance is a combination of scale, translational and rotational invariance. In the field theories (both classical and quantum cases), conformal invariance yields a traceless stress-energy tensor, $T^\mu_\mu = 0$ (massless).^[19] For example, the vacuum Maxwell's equations are conformally invariant. The presence of a mass in field theories will always break the conformal invariance.

The applications of field theories in critical phenomena may be schematized

in the following manner: near the critical point, the system is characterized by two lengths, a lattice spacing a , and correlation length ξ . The introduction of characteristic length a is the origin of a cut-off k_Λ in momentum space of order $1/a$. Setting such limit in momentum space is for the purpose for removing the integral (or summation) divergences ---- renormalization. Critical behavior is involved only when the correlation length ξ is much larger than a ($\xi \gg a$), and one expects distances large compared to a in correlation functions. In this case, it is suggested that the discrete theory may be replaced by a continuous one described in terms of fields.^[20] Indeed, at a critical point one has the case of $m \propto \lambda^{-1} \propto \xi^{-1} = 0$ to which massless field theory is applied. Thus, conformal invariance is realized in nature at a critical point in field theory. It should be pointed out that, just as for scale invariance, there is no rigorous proof of conformal invariance in statistical mechanics at a critical point. It should be regarded as a principle.^[18]

In general, conformal transformations form a finite parameter family; in three dimensions it is a ten parameter family. However, in two dimensions the group of such transformations is an infinite-parameter family because any analytic mapping of the complex plane is conformal. In the complex plane, $z = x + i y$ and $\bar{z} = x - i y$, change of length elements with angles preserved is written as $dz' d\bar{z}' = b(z)^{-2} dz d\bar{z}$ where $b(z) = |f'(z)|^{-1}$ and $z' = f(z)$ is an analytic function. Möbius transformations, for example, are the sets of a subgroup in the conformal group, $z' = f(z) = (A z + B) / (C z + D)$ with $AB - BC \neq 0$, which generates rotations, translations, dilations and the inversion. The algebra corresponding to this group had been studied in the late 1960s by particle theorists in the context of dual string model^[21], where it is called the Virasoro algebra^[22]. Progress in connecting it with 2D conformal field theory has been made since the early 1970s^[23]. In 1984, Belavin, Polyakov and Zamolodchikov^[18] (BPZ theory) made an important advance to end a long hiatus in the development of the subject related to critical phe-

nomena. They proposed conformally invariant models of statistical mechanics. BPZ showed that to each "primary" scaling operator of a 2D system at critical point there corresponds a representation of Virasoro algebra. If a certain quantity called the Kac determinant^[24] in these representations with particular simple kind vanishes, then not only the critical exponents^[25], but all the multi-point correlation functions^[26] at critical point can be obtained. Because conformal field theory is so fruitful, remarkable progress has been made by field theorists in the last few years. We only briefly introduce here the spirit of this theory.

Consider the case where z' represents an infinitesimal transformation $z' = z + \varepsilon(z)$. In general coordinate, that is $x'^{\mu} = x^{\mu} + \alpha^{\mu}(x)$. The infinitesimal analytical function can be represented as an infinite Laurent series^[18] $\varepsilon(z) = \sum_{n=-\infty}^{\infty} \varepsilon_n z^{n+1}$. According to Lie groups, the algebra of differential operators $l_n = z^{n+1} \frac{d}{dz}$, with $n = 0, \pm 1, \pm 2, \dots$, leads to the commutation relations $[l_n, l_m] = (n - m) l_{n+m}$. In 2D, these transformations are conformal. Hence the stress tensor $T^{\mu\nu}$ must be symmetric and traceless^[19], $T_{\mu\nu} = T_{\nu\mu}$, $T_{\mu}^{\mu} = 0$. In the complex plane, through a metric tensor^[27],

$$g = \frac{1}{2} \begin{pmatrix} 0 & 1 \\ 1 & 0 \end{pmatrix},$$

the stress tensor is written as

$$T = \begin{pmatrix} T_{zz} & T_{z\bar{z}} \\ T_{\bar{z}z} & T_{\bar{z}\bar{z}} \end{pmatrix}$$

with $T_{z\bar{z}} = T_{\bar{z}z} = 0$ ($T_{\mu\nu} = T_{\nu\mu}$ and $T_{\mu}^{\mu} = 0$). The conservation of $T_{\mu\nu}$ ($\partial^{\mu} T_{\mu\nu} = 0$) leads to $\partial^z T_{zz} = \partial^{\bar{z}} T_{\bar{z}\bar{z}} = 0$ which also means T_{zz} and $T_{\bar{z}\bar{z}}$ are analytic functions of z and \bar{z} , respectively (that is, they coincide with the Cauchy-Riemann equation). Therefore in 2D the stress tensor has only two independent components $T(z) = T_{zz}$ and $\bar{T}(\bar{z}) = T_{\bar{z}\bar{z}}$.

BPZ introduced the operators $L_n, \bar{L}_n, n = 0, \pm 1, \pm 2, \dots$ as coefficients of the Laurent expansions

$$T(z) = \sum_{n=-\infty}^{\infty} \frac{L_n}{z^{n+2}}, \quad \bar{T}(\bar{z}) = \sum_{n=-\infty}^{\infty} \frac{\bar{L}_n}{\bar{z}^{n+2}}.$$

Using Lie algebra they have shown that the operators L_n satisfy the commutation relations^[18]:

$$[L_n, L_m] = (n - m) L_{n+m} + \frac{1}{12} c (n^3 - n) \delta_{n+m, 0}.$$

The \bar{L}_n obey the same algebra, and L_n and \bar{L}_n commute. This algebra is well known in the dual theory of the so-called Virasoro algebra^[22], where c is called the conformal anomaly or central charge of Virasoro algebra. Within this scheme, c is a single pure number which characterizes the realization of conformal invariance within a given system, (T, \bar{T}) . In the RG scheme the local scaling fields $g_i(\vec{r})$ are conjugates of the scaling densities or operators $\phi_i(\vec{r})$ in the Hamiltonian, $\sum_r g_i(\vec{r}) \phi_i(\vec{r})$. Since the RG transformation is local, the dilatation factor is a slowly varying function of \vec{r} , $g'(\vec{r}') = b(\vec{r})^{y_i} g_i(\vec{r})$. At fixed points, the Hamiltonian will remain invariant under these transformations, and as a consequence the correlation functions will transform covariantly^[28],

$$\langle \phi_1(\vec{r}_1) \phi_2(\vec{r}_2) \dots \rangle = b(\vec{r}_1)^{-x_1} b(\vec{r}_2)^{-x_2} \dots \langle \phi_1(\vec{r}'_1) \phi_2(\vec{r}'_2) \dots \rangle,$$

where scaling dimensions, x_i , of the operator ϕ_i are related to the eigenvalues y_i by $x_i = d - y_i$. The correlation functions under a conformal transformation $z' = w(z)$ in 2D then are generalized as^[18,28]

$$\langle \phi_1(z_1, \bar{z}_1) \phi_2(z_2, \bar{z}_2) \dots \rangle = \prod_j w'(z_j)^{\Delta_j} \overline{w'(z_j)^{\bar{\Delta}_j}} \langle \phi_1(w_1, \bar{w}_1) \phi_2(w_2, \bar{w}_2) \dots \rangle,$$

where the scaling dimensions are $x_j = \Delta_j + \bar{\Delta}_j$ and the "spins" S_j are $S_j = \Delta_j - \bar{\Delta}_j$. Here it should be noticed that $\Delta_j, \bar{\Delta}_j$ are real numbers, and $\bar{\Delta}_j$ is not the complex conjugate of Δ_j . The main ingredients in the BPZ analysis are the operator product expansion of $T(z)$ and the Ward identity^[18,28]. $L_n \phi_j$ can be defined as scaling operators. BPZ showed that if ϕ_j has scaling dimensions $(\Delta_j, \bar{\Delta}_j)$ then $L_n \phi_j$ has dimensions $(\Delta_j - n, \bar{\Delta}_j)$. Such operators, ϕ_j , are called primary by BPZ in the quantum field theory. They have made an operator interpretation of statistical mechanical models because of the transfer matrix construction which turns 2D statistical mechanical models into (1 + 1)-dimensional quantum field theories.

Let L_{-1}, L_0, L_{+1} and $\bar{L}_{-1}, \bar{L}_0, \bar{L}_{+1}$ be generator of the infinitesimal projective transformations ($n = 0, \pm 1$)

$$z \rightarrow z' = z + \varepsilon_{-1} + \varepsilon_0 z + \varepsilon_1 z^2, \quad \bar{z} \rightarrow \bar{z}' = \bar{z} + \bar{\varepsilon}_{-1} + \bar{\varepsilon}_0 \bar{z} + \bar{\varepsilon}_1 \bar{z}^2,$$

where ε and $\bar{\varepsilon}$ are infinitesimal parameters. The operators L (and \bar{L}) satisfy the commutation relations (from Virasoro algebra) $[L_0, L_{\pm}] = \pm L_{\pm}$ and $[L_1, L_{-1}] = 2L_0$. For $n = -1$, $z \rightarrow z + \varepsilon$. These are generated by L_{-1}, \bar{L}_{-1} and are just translations on the plane. For $n = 0$, $z \rightarrow (1 + \varepsilon)z$. If ε is real this is a dilation (i.e. a scale transformation) and this is generated by $L_0 + \bar{L}_0$. If ε is imaginary it is a rotation and is generated by $L_0 - \bar{L}_0$. Thus, the eigenvalues of $L_0 + \bar{L}_0$ must be number characteristic of scale invariance of the theory. That is $(L_0 + \bar{L}_0) | \phi_j \rangle = x_j | \phi_j \rangle$ where the scaling dimensions are $x_j = \Delta_j + \bar{\Delta}_j$. The rotation eigenvalues characterize the spatial " spin " of these field, $(L_0 - \bar{L}_0) | \phi_j \rangle = (\Delta_j - \bar{\Delta}_j) | \phi_j \rangle$, where $\Delta_j - \bar{\Delta}_j = \text{spin}$. The operator interpretation of the theory is made clear if one changes coordinates from z to the cylinder (σ, τ) where $z = e^{\tau + i\sigma}$. Dilation in z is translation in " time " τ so $L_0 + \bar{L}_0$ is the " Hamiltonian " ^[18]. The nature of the problem is very similar to that of angular momentum in quantum

mechanics (QM), that of the rotation group (or a simpler algebra). In QM case, there are three generators J_+ , J_- , J_z in which J_z is taken as diagonal and J_+ and J_- raise and lower it. The analogous representations in the Virasoro algebra are $J_z \rightarrow L_0$, $J_+ \rightarrow \{L_{-n}\}$, $J_- \rightarrow \{L_{+n}\}$, for $n > 0$. The requirement of unitarity in QM leads the eigenvalues of J_z to be integers or half-integer. Friedan, Qiu and Shenker^[25] (FQS) showed that in the Virasoro case unitarity severely restricts the positive eigenvalues ($\Delta > 0$) of L_0 . Thus, the Kac^[24] determinant must be zero^[25]

$$\det M_N = \prod_{pq \leq N} (\Delta - \Delta_{p,q}(c))^{p(N-pq)}$$

where p, q are positive integers,
$$\Delta_{p,q} = \frac{[(m+1)p - mq]^2 - 1}{4m(m+1)}$$

and the central charge c is parameterized by $c = 1 - [6/m(m+1)]$, with $m = 2, 3, 4, \dots$, ($c < 1$). The determinant vanishes on curves $\Delta = \Delta_{p,q}(c)$ in the (c, Δ) plane. Within this theory, a given universality class is characterized by the value of c . Once c is given, the possible values of critical exponents can be obtained. This approach is so general that it is not necessary to solve the microscopic model. Since only one number c must be specified, only one exponent need be identified, and then all the other exponents, plus the correlation functions, follow. In such a theory, the correlation functions and operator product expansion coefficients are calculable. This information is useful to identify the microscopic 2D models or, more generally, universality classes. Many different methods have been used to make these identifications during the last few years.^[28] Unitarity limits the allowed values of c ($c < 1$) and the scaling dimensions (Δ corresponding to critical exponents). In this case, the Ising ($c = 1/2$), tricritical Ising ($c = 7/10$), three-state Potts ($c = 4/5$), tricritical three state Potts ($c = 6/7$), and other $O(N)$ models are realized^[25]. For a complete catalogue of universality classes with $c \geq$

1, additional symmetries have to be invoked. In the special case $c = 1$, the Gaussian model is identified with a continuous internal symmetry group $G = U(1)$ by which the $q = 4$ Potts model, the XY model, eight-vertex model, the Ashkin-Teller model, Coulomb gas, and continuously varying exponents can be described^[28,29]. For $c > 0$, a new discrete set of central charges associated with a new Virasoro algebra was obtained from the Goddard-Kent-Olive construction^[30]. Although there are no identifiable specific models corresponding to $c > 1$ so far, the exact solutions of high-spin integrable generalization of the XXZ^[31,32] and XXX^[33] models may imply the existence of a class of $U(1)$ invariant models with $c > 1$ ^[34,35].

References of Chapter II

1. L. Onsager, Phys. Rev. 65, 117 (1947); C. N. Yang and T. D. Lee, Phys. Rev. 87, 404 (1952).
2. M. E. Fisher, Scaling, Universality and Renormalization Group Theory, Lecture Notes in Phys. 186, 1 (1983).
3. H. E. Stanley, Introduction to Phase Transitions and Critical Phenomena, Oxford Univ. Press (1971).
4. K. S. Ma, in Phase Transitions and Critical Phenomena, Domb and Green, eds., Academic Press, Vol.6, p. 250 (1976).
5. D. J. Wallace, in Phase Transitions and Critical Phenomena, Domb and Green, eds., Academic Press, Vol.6, p. 294 (1976).
6. Jens Als-Nielsen, in Phase Transitions and Critical Phenomena, Domb and Green, eds., Academic Press, Vol. 5A, p. 87 (1976).
7. P.J. Weiss, Phys. Radium, Paris 6, 667 (1907).
8. L. D. Landau and E. M. Lifschitz, Statistical Physics 2nd. ed. Pergamon Press, Oxford (1969).
9. R. B. Potts, Proc. Camb. Phil. Soc. 48, 106 (1952).
10. H. E. Stanley, in Phase Transitions and Critical Phenomena, Domb and Green, eds., Academic press, Vol. 3, p. 486 (1974).

11. E.M. Domany, B. Nienhuis and A. Schwimmer, Nucl. Phys. B190, 279 (1981).
12. B. Nienhuis, in Phase Transitions and Critical Phenomena, Domb and Lebowitz, eds., Academic Press, Vol. 11, p.1 (1987).
13. L. P. Kadanoff, Physics 2, 263 (1963).
14. K. G. Wilson, Phys. Rev. B4, 3174, 3184. (1971).
15. P. Pfeuty and G. Toulouse, Introduction to the Renormalization Group and Critical Phenomena, John Wiley & Sons, (1977).
16. C. D. Castro and G. Jona-Lasino, in Phase Transitions and Critical Phenomena, Domb and Green, eds., Academic Press, Vol. 6, p. 508 (1976).
17. A. O. Barut and H.-D. Doebner, (Edited), Conformal Group and Related Symmetries Physical Results and Mathematical Background, Lecture Notes in Phys. Vol. 261 (1986).
18. A. A. Belavin, A. M. Polyakov and A. B. Zamolodchikov, Nucl. Phys. B241, 333 (1984), and J. Stat. Phys. 34, 763 (1984).
19. N. D. Birrell and P. C. W. Davies, Quantum Fields in Curved Space, Cambridge Univ. Press, p. 173 (1982).
20. E. Brezin, J.C. Le Guillou and J. Zinn-Justin, in Phase Transitions and Critical Phenomena, Domb and Green, eds., Academic press, Vol.6, P.127 (1976); G. A. Baker, Jr., Vol. 9, p.234 (1984).
21. M. Jacob (ed.), Dual Theory, North-Holland, Amsterdam (1974).
22. M. A. Virasoro, Phys. Rev. D1, 2933 (1970).
23. A. M. Polyakov, Zh. Eksp. Teor. Fiz. Pis. Red. 12, 538 (1970), [Sov. Phys. JETP Lett. 12, 381 (1970)].
24. V.G. Kac., in Group Theoretical Methods in Physics, edited by W. Beiglbock, A. Bohm, Lecture Notes in Phys. Vol. 94 (springer-Verlag, New York, 1979), P.441; B. L. Feigin and D. B. Fuchs, Funct. Anal. Prilozhen, 16, 47 (1982) [Funct. Anal. Appl. 16, 114 (1982)].
25. D. Friedan, Z. Qiu and S. Shenker, Phys. Rev. Lett. 52, 1575 (1984).
26. V. S. Dotsenko and V. A. Fateev, Nucl. Phys. B240, 312 (1984).
27. D. Friedan, in Recent Advances in Field Theory and Statistical Mechanics, Proceedings of 1982 Les Houches Summer School (J-B. Zuber and R. Stora, eds.), p.839, North-Holland, Amsterdam (1984).

28. J.L. Cardy, in Phase Transitions and Critical Phenomena, Domb and Lebowitz, eds., Academic press, Vol.11, p. 55 (1987).
29. P. A. Pearce and D. Kim, J. Phys. A20, 6471 (1987).
30. J. Bagger, D. Nemeschansky and S. Yankielowicz, Phys. Rev. Lett. 60, 389 (1988).
31. A. N. Kitilov and N. Y. Reshetikhin, J. Phys. A20, 1565 (1987).
32. F. C. Alcaraz and M. J. Martins, J. Phys. A22, 1829 (1989).
33. H. M. Babujan, Phys. Lett. A90, 479 (1982).
34. I. Affleck, Phys. Rev. Lett. 56, 756 (1986).
35. H. Johannesson, J. Phys. A21, L611 (1988).

CHAPTER III

MEAN-FIELD THEORY OF QUASI-TWO DIMENSIONAL SPIN-1/2 ANISOTROPIC HEISENBERG ANTIFERROMAGNETS

Introduction

Magnetic phase diagrams of antiferromagnets have been studied both theoretically and experimentally for a long time. Experimentally, much attention has been devoted to uniaxial antiferromagnets. These systems exhibit a bicritical point at a finite magnetic field \bar{H} parallel to the easy axis. Many of the theoretical predictions, particularly from mean-field theory, renormalization group approach and high-temperature series expansions, concerning the bicritical phase diagram have been confirmed by experiment. In general, it is expected that weakly anisotropic uniaxial antiferromagnets in a magnetic field \bar{H} parallel to the easy axis should exhibit a multicritical point at some finite, nonzero value of \bar{H} . The existence of a bicritical or tetracritical point in uniaxial antiferromagnets is usually determined by the fourth-order spin anisotropy in the Hamiltonian.^[1,2] Scaling analysis, renormalization-group approaches, and ϵ -expansions techniques have proved extremely fruitful when analyzing the thermodynamic behavior in the vicinity of these points.^[3-10] However, to derive global phase diagrams for the whole temperature and field range instead of just near those multicritical points, mean-field theory seems to be uniquely successful.^[11-17]

The mean-field approximation has been applied to study phase transitions in a variety of physical systems. For many spin systems, this approximation not only gives a satisfactory qualitative description of the experimental results, but also gives a surprisingly good quantitative description of macroscopic phase formations. A typical example is the study, within mean-field theory, of the supersolid phase in the quantum lattice gas model.^[18] The supersolid phase introduced in the early 70's is a state in which both diagonal (crystalline) long-range order and off-diagonal (superfluid) long-range order coexist in the quantum crystal model.^[18-23] This phase was first found experimentally by Rudnick *et al.*^[24] and Goodstein *et al.*^[25] who showed that a thin film of ^4He undergoes a transition from superfluid phase to solid phase with no latent heat, implying that there is no first-order phase transition between superfluid and crystalline states. In the correspondence to the quantum lattice gas model, no two particles can occupy the same lattice site. Thus, the crystalline order is due to strong forces of repulsion embodied in the effective potential $V(r)$. In the low pressure region, a superfluid phase is formed with off-diagonal long-range order closely related to Bose condensation, and an off-diagonal kinetic energy, $t(R,R')$, associated with tunneling from lattice site R to lattice site R' . The latter ensures the particle motions that are necessary to have a superfluid component.^[22] This model can also be represented by the standard boson Hamiltonian in second-quantized form. In this form the Hamiltonian is fully analogous to that of an anisotropic Heisenberg spin systems.^[18,19,23] We refer here to an anisotropic (biaxial) Heisenberg spin system with two types of exchange interactions, $J(J_x, J_y, J_z)$ and $J'(J'_x, J'_y, J'_z)$. The ferromagnetic and antiferromagnetic exchange energies in the spin flop (or antiferromagnetic) phase are analogous to the attractive (or repulsive) and repulsive (or

attractive) potentials in the superfluid (or solid phase), respectively, in the quantum lattice gas. With a field along the \hat{x} axis, we refer to the \hat{y} and \hat{z} components of the spin coupling as "off-diagonal".^[18] There may exist an intermediate phase between the spin flop and antiferromagnetic phases due to a competition between the interlayer and intralayer exchange anisotropies, which would correspond to the supersolid phase in the quantum lattice gas. This intermediate phase should be characterized by a coexistence of spin flop and antiferromagnetic phases.

However, the spin system corresponding to the quantum crystal has many aspects which are different from the usual uniaxial antiferromagnets mentioned at the beginning: (a) the system is of biaxial anisotropic form (anisotropic Heisenberg or XYZ-like); (b) the system contains two types of exchange interactions (J and J'); and (c) the spin Hamiltonian contains only linear (Zeeman) and quadratic (exchange) terms. Thus, several important questions may remain unresolved. (1) What kind of real spin systems can exhibit an intermediate phase? (2) If they do exist, what should the global phase diagrams be? (3) Is there a tetracritical point, without cubic and fourth-order terms in the Hamiltonian? (4) Is it possible to confirm this intermediate phase experimentally? With an emphasis on these questions we will study the phase transitions and phase diagrams of quasi-two dimensional spin-1/2 anisotropic Heisenberg antiferromagnets, within mean-field theory. In the next section a generalized form of the mean-field approximation for a bilinear interaction system is outlined with a special attention to the spin systems. Following the work of Van Wier *et al.*,^[26] the complete solutions of the quasi-2D anisotropic Heisenberg antiferromagnets at $T=0$ are discussed. The finite temperature phase diagrams are also derived in this chapter. Liu and Fisher's^[18]

analysis of a supersolid phase in the quantum lattice gas is directly applied to study of an intermediate phase in the quasi-2D spin-1/2 anisotropic Heisenberg systems. In the last section, we discuss the effect of spin-canting at the transition between the spin-flop and the antiferromagnetic phase. The necessary formulae for carrying out a numerical calculation are given.

Generalized Formalism of the Mean Field Approximation
for a Spin Bilinear Interaction System

Mean field approximation can be made in a variety of equivalent ways.^[12,15,17] For a quantum system consisting of many-body interactions an exact calculation of partition function, Z , may be difficult or impossible. Consider a quantum spin system for which \hat{H} includes a single-spin part and a bilinear interaction part

$$\hat{H} = - \sum_{\langle ij \rangle} \sum_{\lambda=1}^n \sum_{\sigma=1}^n J_{\lambda\sigma}^{ij} \hat{S}_i^\lambda \hat{S}_j^\sigma - \sum_{i=1}^N \left(\sum_{\lambda=1}^n h_\lambda \hat{S}_i^\lambda \right) \quad (1)$$

where \hat{S}_i^λ denotes a spin operator on the lattice site i with component λ and $J_{\lambda\sigma}^{ij}$ is interaction energy between the sites i and j corresponding to components λ and σ ($\sigma = x, y$ and z). $J_{ij}^{\lambda\sigma}$ are the anti- and symmetric exchange energies, and h_λ are the components of the external field.

By considering the inequalities of Gibbs, Falk^[27] has shown that for any approximate density matrix ρ' , such that $Tr \rho' = 1$, the free energy F satisfies the inequality

$$F \leq \Phi = Tr(\rho'H) + \beta^{-1} Tr(\rho' \ln \rho') \quad (2)$$

where $\beta^{-1} = k_B T$. Thus the best way to obtain the free energy associated with the Hamiltonian (1) is to minimize the function Φ with respect to the approximate density matrix ρ' .

Although there is a variety of equivalent approaches in the mean field approximation, all methods have in common the approximation wherein the average of a product of variables is replaced by the product of the averages. That is

$$\hat{\rho}_{MF} = \prod_i^N \hat{\rho}_i = \hat{\rho}_1 \otimes \hat{\rho}_2 \otimes \hat{\rho}_3 \dots \otimes \hat{\rho}_N$$

where

$$\hat{\rho}_i = \frac{e^{-\beta \hat{H}_i}}{\text{Tr} e^{-\beta \hat{H}_i}} \quad (3)$$

is a density matrix defined for the single site i . Putting ρ_{MF} into (2), we have

$$\begin{aligned} \Phi(\rho_{MF}) = & - \sum_{\langle ij \rangle}^N \sum_{\lambda=1}^n \sum_{\sigma=1}^n J_{\lambda\sigma}^{ij} m_i^\lambda m_j^\sigma \\ & + \sum_{i=1}^N \text{Tr} \left[- \sum_{\lambda=1}^n h_\lambda \prod_k^N \hat{\rho}_k \hat{S}_i^\lambda + \beta^{-1} \prod_k^N \rho_k \text{Ln} \rho_i \right], \end{aligned} \quad (4)$$

where

$$\begin{aligned} m_i^\lambda m_j^\sigma &= \langle \hat{S}_i^\lambda \rangle \langle \hat{S}_j^\sigma \rangle \\ &= \langle \hat{S}_i^\lambda \hat{S}_j^\sigma \rangle = \text{Tr} (\hat{\rho}_{MA} \hat{S}_i^\lambda \hat{S}_j^\sigma) \end{aligned}$$

To minimize $\Phi(\rho_{MF})$ under the constraints $\text{Tr} \hat{\rho}_i = 1$ and $\text{Tr} (\hat{\rho}_i \hat{S}_i^\lambda) = m_i^\lambda$, we should

introduce Lagrange parameters α_i , γ_i^λ . Thus, we write

$$\partial \left(\Phi - \alpha_i \text{Tr} \hat{\rho}_i - \sum_{\lambda} \gamma_i^{\lambda} \text{Tr} \hat{\rho}_i \hat{S}_i^{\lambda} \right) / \partial \hat{\rho}_i = 0,$$

which leads to

$$-\sum_{\lambda=1}^n h_{\lambda} \hat{S}_i^{\lambda} + \beta^{-1} \ln \rho_i + \beta^{-1} - \alpha_i - \sum_{\lambda} \gamma_i^{\lambda} \hat{S}_i^{\lambda} = 0 \quad (5)$$

where $\text{Tr} \left(\prod_k \hat{\rho}_k \hat{S}_i \right) = \text{Tr}(\hat{\rho}_i \hat{S}_i)$ was used. Eq. (5) yields

$$\rho_i = \left(e^{\beta \alpha_i - 1} \right) \exp \left[\beta \sum_{\lambda=1}^n (h_{\lambda} + \gamma_i^{\lambda}) \hat{S}_i^{\lambda} \right],$$

or

$$\rho_i = \frac{\exp \left[\beta \sum_{\lambda=1}^n (h_{\lambda} + \gamma_i^{\lambda}) \hat{S}_i^{\lambda} \right]}{\text{Tr} \exp \left[\beta \sum_{\lambda=1}^n (h_{\lambda} + \gamma_i^{\lambda}) \hat{S}_i^{\lambda} \right]} \quad (6)$$

where $\text{Tr} \exp \left[\beta \sum_{\lambda=1}^n (h_{\lambda} + \gamma_i^{\lambda}) \hat{S}_i^{\lambda} \right] = \left(e^{\beta \alpha_i - 1} \right)^{-1} = Z_i$. The average of \hat{S}_i^{λ} can be

written as

$$\begin{aligned} m_i^{\lambda} &= \langle \hat{S}_i^{\lambda} \rangle = \text{Tr}(\rho_i \hat{S}_i^{\lambda}) = \\ &= \frac{d(\ln Z_i)}{d(\beta \gamma_i^{\lambda})} = B_i(h_{\lambda} + \gamma_i^{\lambda}) \end{aligned} \quad (7)$$

This equation is single particle equation of state, with the external field h_{λ} replaced by $h_{\lambda} + \gamma_i^{\lambda}$. Now we assume we can calculate all the single particle properties. Thus one can calculate the Lagrange parameter γ_i^{λ} from the inverse $\gamma_i^{\lambda} = B_i^{-1}(m_i^{\lambda}) - h_{\lambda}$. From eq. (6) we have

$$\ln \rho_i = \left[\beta \sum_{\lambda=1}^n (h_\lambda + \gamma_i^\lambda) \hat{S}_i \right] - \ln Z_i.$$

By substituting this equation into the last terms of eq. (4), we obtain the expression for the function Φ ,

$$\begin{aligned} \Phi(\{m_i^\lambda\}, T) &= - \sum_{\langle ij \rangle}^N \sum_{\lambda=1}^n \sum_{\sigma=1}^n J_{\lambda\sigma}^{ij} m_i^\lambda m_j^\sigma \\ &\quad + \sum_{i=1}^N \left(\sum_{\lambda=1}^n \gamma_i^\lambda m_i^\lambda - \beta^{-1} \ln Z_i \right) \\ &= \sum_i^N \Phi_i - \sum_{\langle ij \rangle}^N \sum_{\lambda=1}^n \sum_{\sigma=1}^n J_{\lambda\sigma}^{ij} m_i^\lambda m_j^\sigma, \end{aligned} \quad (8)$$

where the single particle potential Φ_i for a given m_i^λ is

$$\Phi_i(m_i^\lambda, T) = \sum_{\lambda=1}^n \gamma_i^\lambda m_i^\lambda - \beta^{-1} \ln Z_i. \quad (9)$$

In order to obtain the thermodynamic equilibrium free energy, eq. (2), the value of the function Φ should be minimized with respect to the m_i^λ . Taking the derivative

$$\frac{\partial \Phi}{\partial m_i^\lambda} = \frac{\partial \Phi_i}{\partial m_i^\lambda} - \sum_{j=1}^N \sum_{\sigma=1}^n J_{\lambda\sigma}^{ij} m_j^\sigma = 0 \quad (10)$$

where

$$\frac{\partial \Phi_i}{\partial m_i^\lambda} = \gamma_i^\lambda + m_i^\lambda \frac{\partial \gamma_i^\lambda}{\partial m_i^\lambda} - \beta^{-1} \frac{\partial \ln Z_i}{\partial m_i^\lambda},$$

and using the fact that

$$\beta^{-1} \frac{\partial \ln Z_i}{\partial m_i^\lambda} = \frac{\partial \ln Z_i}{\partial (\beta \gamma_i^\lambda)} \cdot \frac{\partial \gamma_i^\lambda}{\partial m_i^\lambda} = m_i^\lambda \frac{\partial \gamma_i^\lambda}{\partial m_i^\lambda},$$

we have

$$\frac{\partial \Phi}{\partial m_i^\lambda} = \gamma_i^\lambda, \quad (11)$$

and

$$\gamma_i^\lambda = \sum_j^N \sum_\sigma^n J_{\lambda\sigma}^{ij} m_j^\sigma. \quad (12a)$$

It is clear now that at thermodynamic equilibrium the Lagrange parameters γ_i^λ in eq. (6)

have the simple interpretation of mean molecular field or effective field,

$$H_i^\lambda = \gamma_i^\lambda + h_i^\lambda. \quad (12b)$$

By substituting eq. (12) into (6), eq. (7) then yields the equation of state

$$m_i^\lambda = B_i \left(\left\{ \sum_j^N \sum_\sigma^n J_{\lambda\sigma}^{ij} m_j^\sigma + h_i^\lambda \right\}, T \right), \quad (13)$$

or

$$m_i^\lambda = B_i(H_i^\lambda, T) \quad \text{where } i = 1, 2, \dots, N, \lambda = 1, 2, \dots, n,$$

by which $\{m_i^\lambda\}$ can be solved self-consistently. To be local minima, the solutions of Eq.

(10), which are equivalent to the solutions of eq. (13), should be combined with the condition that $\partial^2 \Phi / \partial m_i^\lambda \partial m_j^\lambda$ be a positive definite matrix.

If there are several local minima, it is necessary to select the one corresponding to the smallest value of Φ . If the matrix of $\partial^2 \Phi / \partial m_i^\lambda \partial m_j^\lambda$ has a zero eigenvalue, it is necessary to consider higher derivatives to determine stability. When there is stability, the existence of a zero eigenvalue corresponds to criticality.

To describe the critical behavior and phase transition by mean field theory, without loss of generality, we refer (1) to the Hamiltonian of a N-spin system. Therefore \hat{S}_i^λ is

the λ component of a spin operator at lattice site i , where $\lambda = x, y$ and z ($n = 3$). If we consider the interaction only linking nearest neighbors $\langle ij \rangle$, $J_{\lambda\sigma}$ denotes the exchange interaction and h_λ is an external field ($\lambda = x, y, z$). The number of degree of freedom in this case is $3N$. It is convenient to denote the solution of eq. 13 (or eq. 10), magnetization, as

$$\{m(h, T)\} = \{m_1, m_2, \dots, m_{3N}\}. \quad (14)$$

The local minima and local stability of Φ are determined by $\partial\Phi/\partial m_\alpha = 0$ (eq.(10) or (13), $i=1, 2 \dots 3N$) and the condition that $\det |\partial^2 \Phi/\partial m_\alpha \partial m_\beta| > 0$. Criticality is defined by $\det |\partial^2 \Phi/\partial m_\alpha \partial m_\beta| = 0$, at an absolute minimum Φ . Therefore, the phase boundaries for second order transitions are determined by both eq. (10) (or 13) and $\det |\partial^2 \Phi/\partial m_\alpha \partial m_\beta| = 0$. In other words, one should obtain a second-order phase boundary, $h_c = h_c(T)$, by substituting (14) into $\det |\partial^2 \Phi/\partial m_\alpha \partial m_\beta| = 0$.

We introduce an expansion analogous to a Landau expansion in one order parameter. Consider deviations in the magnetization space from the equilibrium point $\{m(h, T)\} = (m_1, m_2, \dots, m_{3N})$ in a direction, say $x = (x_1, x_2, \dots, x_{3N})$, measured by the small parameter δm , i.e.,

$$\begin{aligned} \bar{m} = (\bar{m}_1, \bar{m}_2, \dots, \bar{m}_{3N}) &= (m_1, m_2, \dots, m_{3N}) \\ &+ (x_1, x_2, \dots, x_{3N})\delta m. \end{aligned} \quad (16)$$

The expansion of Φ at point $\{m\}$ is given by

$$\Phi(\bar{m}) = \Phi(m) + \sum_{n=1}^{\infty} \frac{C_n(m)}{n!} (\delta m)^n \quad (17)$$

where

$$C_n(m) = \sum_{\alpha_1, \dots, \alpha_n=1}^{3N} \left(\frac{\partial^n \Phi}{\partial m_{\alpha_1} \dots \partial m_{\alpha_n}} \right) x_{\alpha_1} \dots x_{\alpha_n}. \quad (18)$$

The extremum condition $\partial\Phi/\partial m_\alpha = 0$ (eq. 10), $\alpha = 1, 2, \dots, 3N$, implies that the term linear in δm vanishes, $C_1 = 0$. A necessary condition for a stable critical point is that C_3 vanish. Otherwise, instead of a minimum one has a saddle point. In expansion (17), $\Phi(\bar{m})$ is expanded around any thermodynamic equilibrium point $\{m_i\}$. Thus the deviation, δm , is a global order parameter to serve in all temperature and field ranges. Analogous to the Landau expansion, the critical behavior and order of the phase transitions may be classified by the signs of coefficients, C_n :

- 1) for a stable phase, $C_2 > 0$;
- 2) for a second order transition, $C_2 = 0, C_3 \neq 0, C_4 > 0$;
- 3) for a first order transition, $C_2 = 0, C_3 \neq 0, C_4 < 0$;
- 4) for a critical point, $C_2 = 0, C_3 = 0, C_4 \neq 0$;
- 5) for a tricritical point, $C_2 = 0, C_3 = 0, C_4 = 0$.

C_2 is given by eq. (18)

$$\begin{aligned} C_2(m) &= \sum_{\alpha_1, \alpha_2=1}^{3N} \left(\frac{\partial^2 \Phi}{\partial m_{\alpha_1} \partial m_{\alpha_2}} \right) x_{\alpha_1} x_{\alpha_2} \\ &= \sum_{\alpha_2}^{3N} \left(\sum_{\alpha_1}^{3N} \frac{\partial^2 \Phi}{\partial m_{\alpha_1} \partial m_{\alpha_2}} x_{\alpha_1} \right) x_{\alpha_2}. \end{aligned}$$

At criticality, $C_2 = 0$, thus we let

$$\sum_{\alpha_1}^{3N} \frac{\partial^2 \Phi(m)}{\partial m_{\alpha_1} \partial m_{\alpha_2}} x_{\alpha_1} = 0 \quad (\alpha_2 = 1, 2, \dots, 3N),$$

which means that we choose $\{x\}$ to be the eigenvector of the Jacobian matrix $\partial^2\Phi(m)/\partial m_{\alpha_1}\partial m_{\alpha_2}$ corresponding to the zero eigenvalue so that

$$\det |\partial^2\Phi/\partial m_{\alpha_1}\partial m_{\alpha_2}| = 0 \quad (19)$$

Therefore, eq. (19) together with eq. (10) (or 13) determines a phase boundary $h = h_c(T)$. The critical point (T_c, h_c) then can be determined by combining with equation $C_3 = 0$. To determine whether or not this point is a tricritical point, it is necessary to check out C_4 .

To discuss the phase diagrams by mean field theory in our case, we may define the phases by recognizing their specific symmetries from the stable solutions. For a given spectrum of $\{J_{\lambda\sigma}^{ij}, h_\lambda\}$ in the Hamiltonian (say, anti- or ferromagnetic Ising, xy , or Heisenberg ... models with a specific direction of the external field), in the different regions of h - T space if there exists a set of stable solutions in eq. (10) (or 13) whose symmetries are distinguishable (characterized by some order parameters), then the thermodynamic equilibrium states of the system corresponding to the different stable solutions are called phases. We denote by $\{m_I(T, h)\}$, $\{m_{II}(T, h)\}$... these different stable solutions. A phase transition will occur when the external physical parameters h and T are varied to cross to a phase boundary between the different phases. The thermodynamic potential Φ is continuous at a phase boundary, $\Phi_I = \Phi_{II}$. If the first derivatives of Φ with respect to the T and h_λ are discontinuous at the phase boundary,

$$\frac{\partial\Phi_I}{\partial T} \neq \frac{\partial\Phi_{II}}{\partial T}, \quad \frac{\partial\Phi_I}{\partial h_\lambda} \neq \frac{\partial\Phi_{II}}{\partial h_\lambda},$$

then this type of transition is usually called a first order transition. If the first derivatives of Φ are continuous, but the second derivatives

$$\frac{\partial^2 \Phi}{\partial T^2}, \quad \frac{\partial^2 \Phi}{\partial h_\lambda^2} \quad \text{and} \quad \frac{\partial^2 \Phi}{\partial T \partial h_\lambda}$$

have discontinuities at the phase boundary, this kind of transition is referred to as a second order (or continuous) transition.

For example, the phase diagram of a uniaxial antiferromagnet with the magnetic field along the easy axis (say, \hat{x} axis) is drawn schematically in Fig. 4. The paramagnetic phase (PM) is separated from the spin-flop (SF) phase and the antiferromagnetic (AF) phase by the two second-order phase boundaries, SF-PM and AF-PM, respectively. The symmetries of those states could be recognized from the solutions of sublattice magnetizations. The PM phase is characterized by $m_{x1} = m_{x2} \neq 0$ and $m_{z1} = m_{z2} = m_{y1} = m_{y2} = 0$, while the AF and SF phases are described by $m_{x1} \neq m_{x2}$ ($m_{x1} < 0$, $m_{x2} > 0$), $m_{z1} = m_{z2} = m_{y1} = m_{y2} = 0$ and $m_{z1} = -m_{z2} \neq 0$ (or $m_{z1} = m_{z2}$), $m_{x1} = m_{x2} \neq 0$, $m_{y1} = m_{y2} = 0$ (assuming \hat{y} is the hard axis), respectively. It is clear from the symmetries of the solutions that the magnetizations are continuous at SF-PM and AF-PM phase boundaries (second order) and discontinuous at an AF-SF boundary (first order). Because the symmetries of both phases at the second-order phase boundaries are exactly the same, the phase boundary can be given by instabilities (stability limits, eq. (19)) in either phase. However, the AF phase is separated from the SF phase by a first-order phase transition which meets the PM phase boundary in the bicritical point T_b . Thus, the stability limit of the SF phase ($\det |\partial^2 \Phi_{SF} / \partial m_i \partial m_j| = 0$) and the AF phase ($\det |\partial^2 \Phi_{AF} / \partial m_i \partial m_j| = 0$) may not be the same. The first order phase boundary is determined by the condition $H_T^C(T)$, $\Phi_{AF} = \Phi_{SF}$, and is located between the instability lines (shown as the dashed lines H_{AF}^C and H_{SF}^C in fig. 4). Whether the actual observed transition occurs at $H_T^C(T)$ without hysteresis,

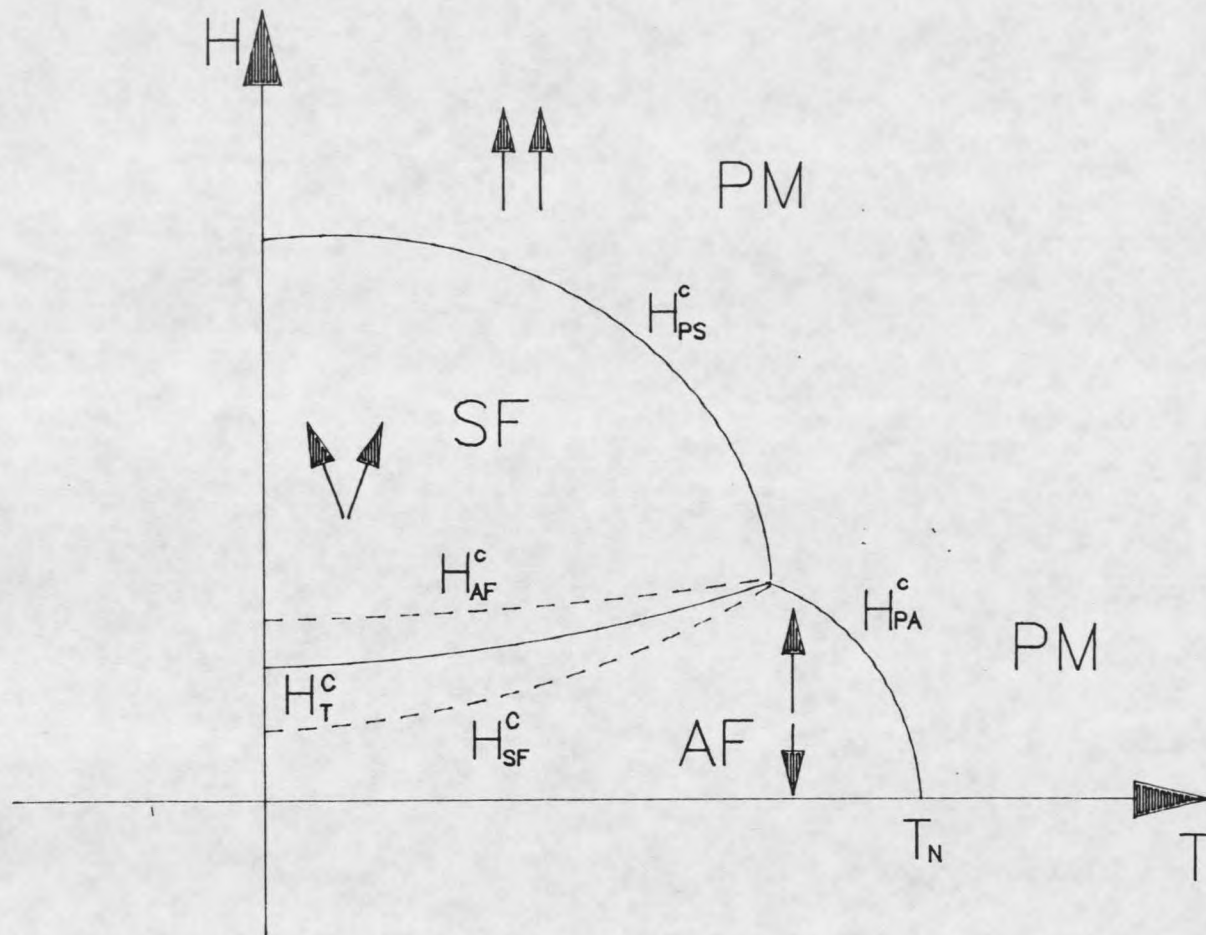


Fig. 4. Schematic phase diagram of a uniaxial antiferromagnet for the field applied along the easy axis. $H_{PS}^c(T)$ and $H_{PA}^c(T)$ phase lines represent the phase boundaries between the PM and the SF phases and between the PM and the AF phases, respectively. The first-order AF-SF transition line is indicated by $H_T^c(T)$. The stability limits of the AF and SF phases are illustrated as the dashed lines H_{AF}^c and H_{SF}^c .

or near H_{AF}^C and H_{SF}^C with hysteresis, depends upon the presence or absence of nucleating centers and local inhomogeneities.^[28] This problem is fully analogous to the super-heating and super-cooling metastability in a conventional gas-liquid first-order phase transition. Fig. 5 shows a conventional P - V isotherm for a gas-liquid transition, and the corresponding H - M isotherm for the SF - AF transition. At point A the liquid is locally stable and the value of the free energy is equal to that in the gas at point D; the pressure $P_A = P_D$ is the pressure of the true first-order transition at temperature T , which is shown in Fig. 5(c). For an antiferromagnet, if the field is quasistatically increased above H_A along the T_1 isotherm in Fig. 5(b), the local minimum of the free energy changes shape, and the quadratic terms finally turn out to be negative definite at the point B. In spin wave theory, it has also been shown that the spin-wave frequency corresponding to the antiferromagnetic eigenmode vanishes at this point. Thus the point B in Fig. 5(b) and the corresponding curve in Fig. 5(d) give the limit of local stability of the antiferromagnetic phase at T_1 . However, in a mean field calculation for the simple antiferromagnet it turns out that $H_{AF}^C = H_{SF}^C = H_T^C$ if one considers anisotropic exchange only. This may mean that there would be a first-order phase transition at this field but hysteresis. The spin-wave calculation has shown that $H_{AF}^C > H_{SF}^C$ when spin-wave interactions are taken into account due to zero-point motion of the spin waves.^[29,30,31] In this case the hysteresis is entirely due to quantum-mechanical effects, but this transition has never been observed by magnetization or magnetothermal measurements, presumably because there are always enough nucleation centers present to drive the crystal into the other phase at the thermodynamic critical field before the field reaches the instability.^[28] It should be pointed out that eq. (19) may fail to determine the instability for some quadratic interaction

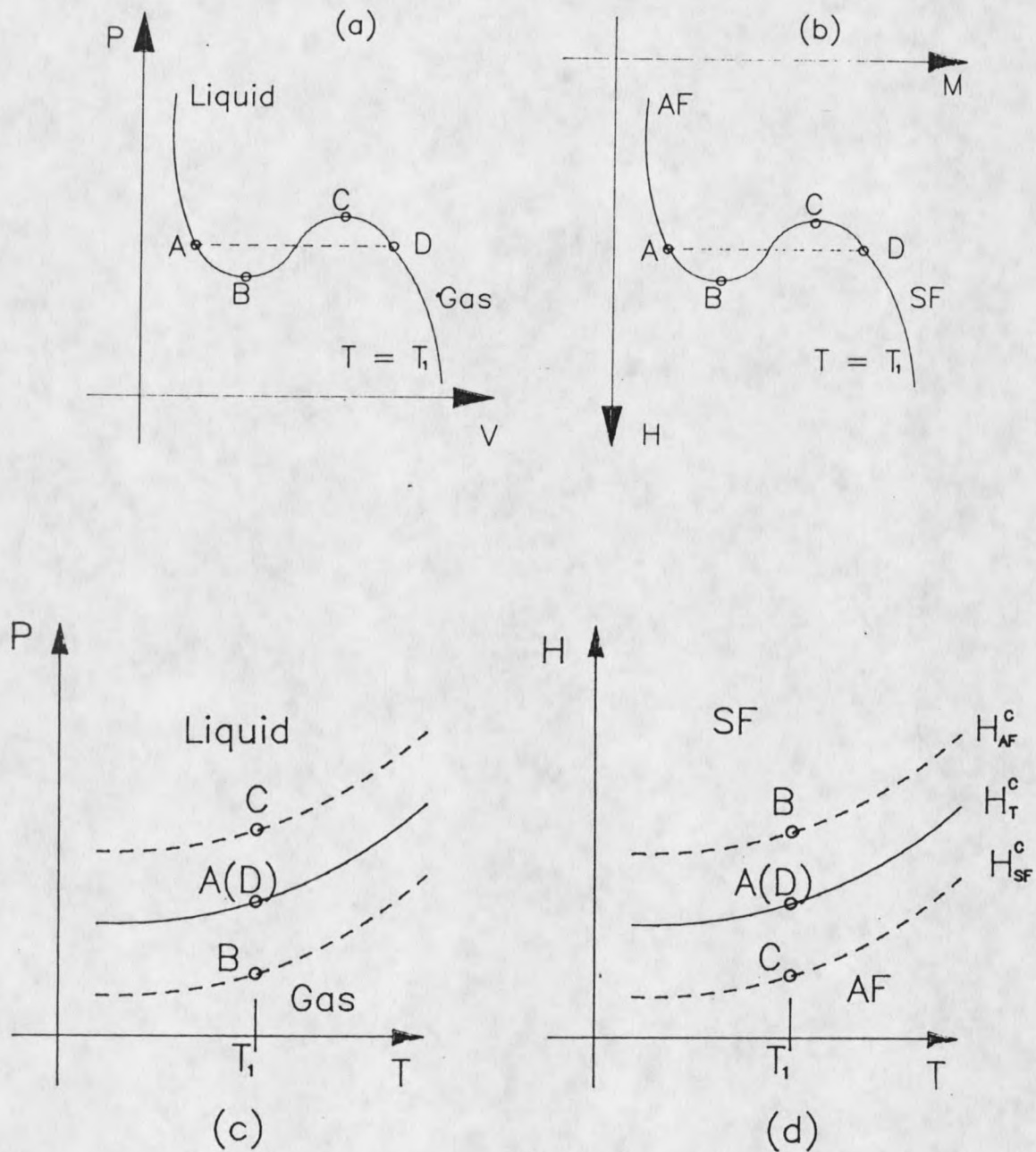


Fig. 5. (a) and (b) illustrate the fluid-magnet analogy in the isotherms. The instability points B and C correspond to $H_{AF}^c(T)$ and $H_{SF}^c(T)$ shown in the phase diagrams (c) and (d).

systems. In this case, it is necessary to make a nonlinear coordinate transformation for the solution (eq. 14) of eq. (10) (or 13), or to choose other relevant order parameters to carry out the expansion (17). The general formalism of the mean field theory presented here will be valid for a relevant order parameter in a proper representation.

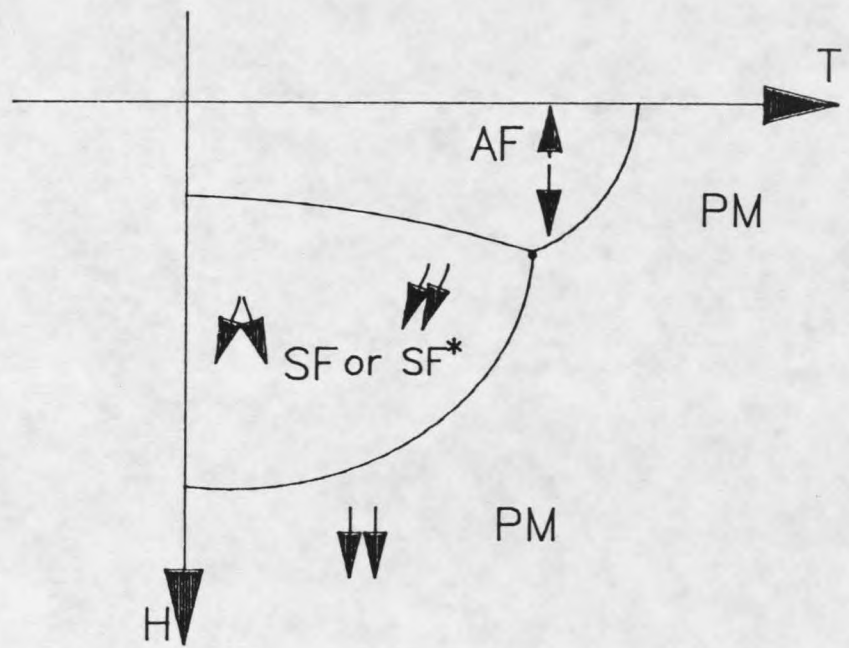
An Intermediate Phase in Antiferromagnets and a Supersolid Phase in the ^4He Film

Studies of phase transitions in magnetism have contributed to the understanding of many aspects of other physical systems through the analogy with spin models. For example, the supersolid phase in quantum crystals is fully analogous to the intermediate phase in an anisotropic Heisenberg antiferromagnet.^[18,19,23]

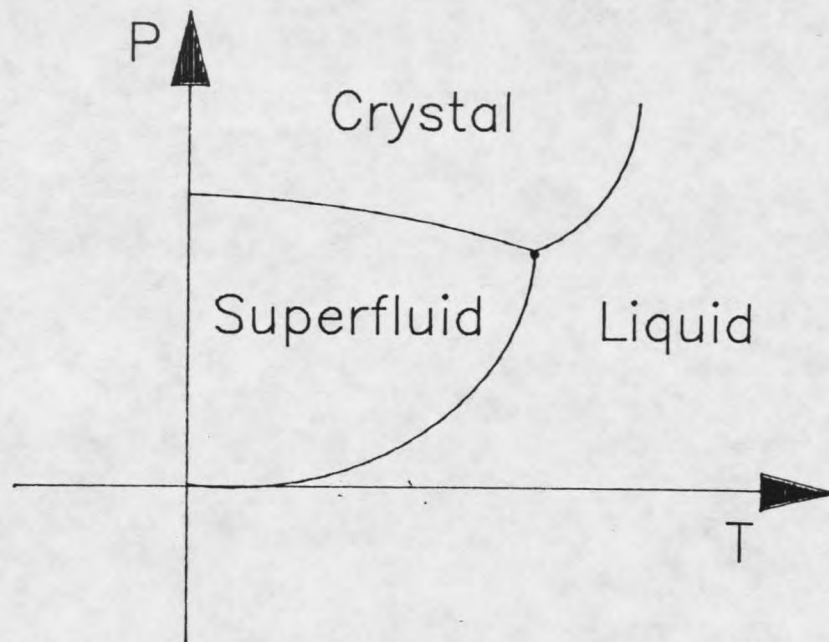
Several theoretical speculations concerning the possibility of a supersolid phase in quantum crystals were advanced in the early 70's.^[18-23] This new phase consists of two kinds of long-range order, namely off-diagonal (superfluid) and diagonal (crystalline). It has been reasonably well established that the usual superfluid phase of helium, liquid He-II, possesses off-diagonal long-range order while the normally observed solid phase of helium displays crystalline order. It has long been known that the λ -transition in liquid ^4He can be understood in terms of a Bose condensation, as occurs in the ideal Bose gas. Thus the superfluid phase in ^4He has been treated as a Bose-condensate state in a quantum lattice gas model, where one^[19-23] works with a lattice of discrete lattice points rather than a continuum. It is then assumed that no two particles can occupy the same lattice site. This constraint represents the strong forces of repulsion embodied in the potential $V(r)$, the hard-core term in the Hamiltonian, which provides a strong long-range order (diagonal order) to form the crystalline phase at high pressure. The

superfluid phase is characterized by the existence of an off-diagonal long-range order, related to the Bose condensation. The off-diagonal kinetic energy, $t(R, R')$, associated with tunneling from lattice site R to lattice site R' ensures the particle motions that are necessary to have a superfluid component in the solid.

Several models have been proposed to describe the superfluid and crystalline phases using the standard Boson Hamiltonian in second-quantized form.^[19,21-23] The form of the Hamiltonian has been found to be fully analogous to that of the anisotropic Heisenberg system.^[18,19,23] The complete equivalence between the variables in the two systems can be found in references (18) and (32). Fisher^[32] has pointed out the analogies between the magnetic and fluid phase diagrams. The phase diagrams of an antiferromagnet and the quantum lattice gas are illustrated in fig. 6. It is apparent from fig. 6 that the analogy has helped in understanding the essential features of the phase diagram of real ^4He . It is noticed that in the mean field approximation one considers essentially only the averaged effect of the potential. Thus in the low-pressure region (high field), the effective potential is attractive (ferromagnetic). While at high pressure (low field), it is repulsive (antiferromagnetic). If one considers only models with a repulsive (antiferromagnetic) interaction between the nearest-neighbors and a weakly attractive (ferromagnetic) interaction between the next-nearest-neighbors, then mean field theory will be reasonable to describe the lambda (antiferromagnetic-spin flop) and the melting (antiferromagnetic-paramagnetic) transitions, but should not represent accurately the effect of the longer range weak attractions that are important in the low-density (and low pressure) region where the liquid-gas transition occurs. Thus, in this model the liquid-gas transition line is missing in fig. 6.



(a)



(b)

Fig. 6. Phase diagrams for (a) the magnetic system, the anisotropic Heisenberg model, and (b) the quantum lattice gas model.^[18]

A significant difference between ^4He film and bulk was found in late 1969. Experiments by Rudnick *et al.*^[24] and Goodstein *et al.*^[25] showed that surface waves in the unsaturated ^4He film vanish abruptly at a critical film thickness with no latent heat which implies that the first order melting line between superfluid and solid phases could disappear when the thickness of the ^4He film is below a critical value. Thus, a new phase, so called supersolid, as characteristic of the coexistence of the superfluid and solid phases had been introduced. By analogy with the spin system, the supersolid phase in the thin film of ^4He is completely equivalent to an intermediate phase between the SF and AF phase in the anisotropic Heisenberg antiferromagnet. Fig. 7 illustrates this analogy. In general one can show by using mean-field theory that there can exist an intermediate phase characterized by coexistence of the SF and AF phases lying between the SF and AF phases and separated from these by second-order phase boundaries. Similarly, in this work we strongly suggest that an intermediate phase may exist in the quasi-two dimensional anisotropic Heisenberg systems with strongly ferromagnetic intralayer exchange and weakly antiferromagnetic interlayer. It may be possible to verify this phase in a large variety of layer-type magnetic metallate compounds since a rich variety of nonmagnetic organic cations produce large and variable separation between the magnetic metallate layers.

Mean Field results for Quasi-two Dimensional,

Anisotropic, Heisenberg Systems at $T = 0$ K

We consider a general quasi-2D system with a biaxial anisotropy in the exchange energy. The solutions at $T = 0$ for an external field applied parallel to the axis preferred

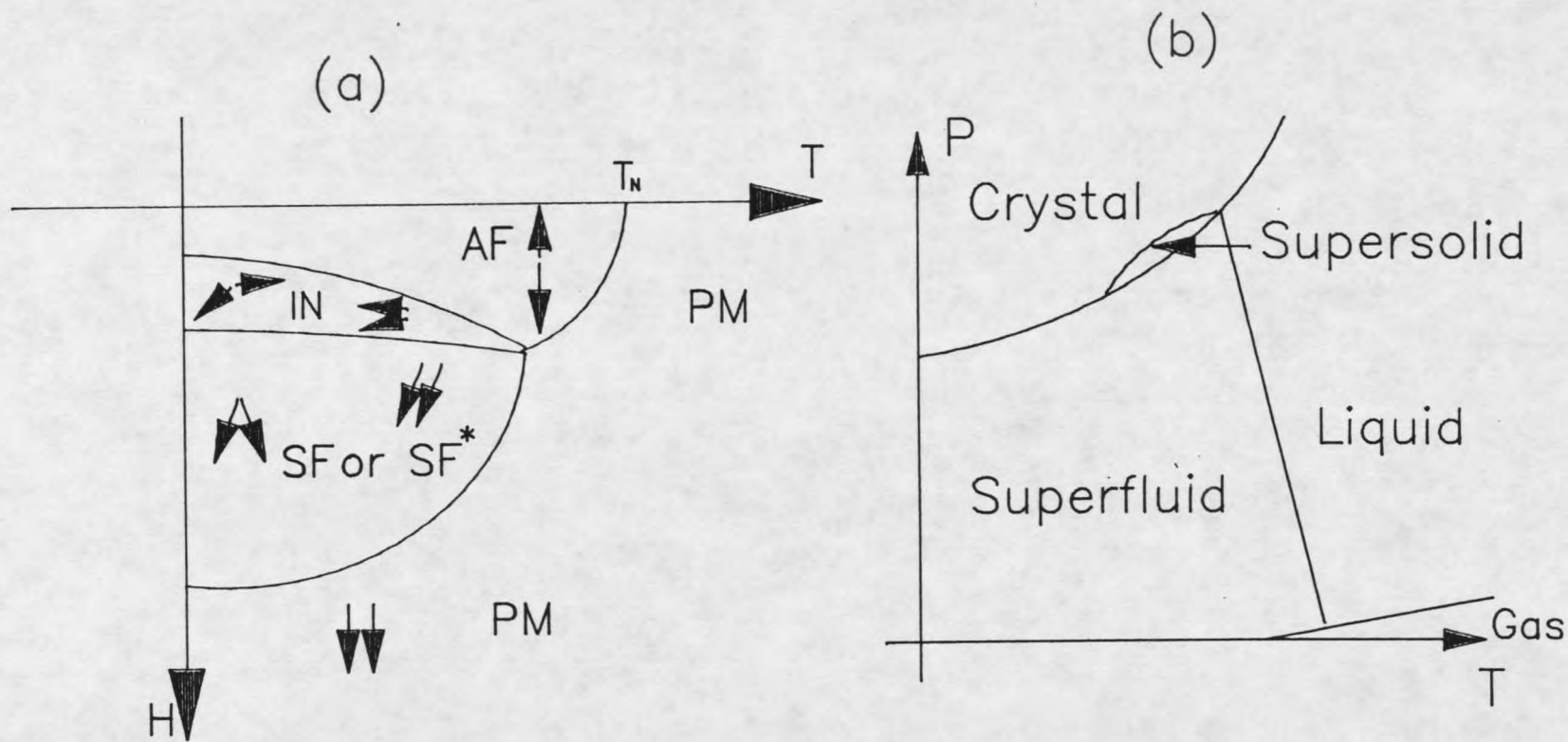


Fig. 7. (a) phase diagram of a quasi-two dimensional antiferromagnet with an intermediate phase (IN), and (b) phase diagram for the thin film of ^4He with the supersolid phase.

(easy) for antiferromagnetic-alignment or to the second next preferred (intermediate) axis can be given by mean-field theory.

The Hamiltonian of this model is written as

$$\begin{aligned}
 H = & -2 \sum_{\alpha, \alpha'} \{J_x S_\alpha^x S_{\alpha'}^x + J_y S_\alpha^y S_{\alpha'}^y + J_z S_\alpha^z S_{\alpha'}^z\} \\
 & -2 \sum_{\beta, \beta'} \{J_x S_\beta^x S_{\beta'}^x + J_y S_\beta^y S_{\beta'}^y + J_z S_\beta^z S_{\beta'}^z\} \\
 & -2 \sum_{\substack{\alpha, \beta \\ < \alpha, \beta' >}} \{J'_x S_\alpha^x S_\beta^x + J'_y S_\alpha^y S_\beta^y + J'_z S_\alpha^z S_\beta^z\} \\
 & -2 \sum_{\alpha, \beta}^N \vec{h} \cdot \{\vec{q}_\alpha \cdot \vec{S}_\alpha + \vec{q}_\beta \cdot \vec{S}_\beta\}
 \end{aligned} \tag{20}$$

where J_x, J_y and J_z are exchange constants within the layer, and J'_x, J'_y and J'_z are exchange constants between the layers. Let A and B denote the two sublattices associated with adjacent layers. α and α' denote nearest neighbor spin sites in sublattice A ($\alpha, \alpha' \in A$), and β, β' denote nearest neighbor spin sites in the sublattice B ($\beta, \beta' \in B$). We assume that the intralayer exchange (J_i) is positive (ferromagnetic interaction) and that the average of the interlayer exchange components ($J'_x + J'_y + J'_z$) is negative (effectively antiferromagnetic interaction). If $|J'| \ll |J|$, the model represents ferromagnetic planes coupled antiferromagnetically to each other. Spin anisotropies due to exchange have been taken into account both within and between layers. This microscopic Hamiltonian may be suitable for study of many copper-layer compounds. In general, the interaction terms in the Hamiltonian (20) are dependent on the specific lattice and details of the exchange paths. However, we only consider the nearest-neighbor interaction between the layers as well as within the layers in this work. Thus, in the mean-field

scheme, we assume that

$$2 \sum_{\langle \alpha, \alpha' \rangle} J_i \langle S_\alpha^i S_{\alpha'}^i \rangle = \left(\frac{NZJ_i}{4} \right) \langle S^i S^i \rangle_n$$

$$2 \sum_{\langle \alpha, \beta \rangle} J'_i \langle S_\alpha^i S_\beta^i \rangle = \left(\frac{NZ'J'_i}{4} \right) \langle S^i S^i \rangle_n$$

$$(i = x, y, z),$$

where the normalization constant N is the total number of spin sites in the systems and Z and Z' are the structure constants determined by the structure of the exchange paths within and between the layers, respectively, and $\langle S^i S^i \rangle_n$ and $\langle S^i S^i \rangle_n$ are components of the nearest-pair spin correlations due to within and between the layers, respectively.

A general method to solve Hamiltonian (20) by mean field approximation has been discussed in the second section. The solutions can be given by solving eq. (12) and (13) corresponding to (20). The number of degrees of freedom in this case is 6 ($n = 3$ (x, y and z); $N = 2$, (A, B) two-sublattice model). The six nonlinear coupled self-consistent equations (eq. 13) may give many possible solutions. All of the physical solutions can be determined by employing the thermodynamic stability conditions. To discuss general solutions of (2), we first consider the case of $T = 0$. In the next section, we will study the case of finite temperature.

For a two-sublattice model, $\hat{\rho}_A = e^{-\beta \hat{H}_A} / \text{Tr} e^{-\beta \hat{H}_A}$ and $\hat{\rho}_B = e^{-\beta \hat{H}_B} / \text{Tr} e^{-\beta \hat{H}_B}$, at $T = 0$, ($\beta \rightarrow \infty$) we have $\hat{\rho}_A = \hat{\rho}_B$. Thus, the length of the sublattice magnetization should be, $\overline{m}_A^2 = \overline{m}_B^2 = \sum_{i=x,y,z} [\text{Tr}(\hat{S}_A^i \rho_A)]^2 = S^2$, constant. Therefore, the number of degrees of freedom at $T = 0$ is reduced to 4. In biaxial anisotropic systems, however, with the field directed along the easy or intermediate axes, the hard axis component of the sublattice magnetizations can be assumed to be zero, $\langle S_A^h \rangle = \langle S_B^h \rangle = 0$. In

this work special attention is given to the case in which the external field is applied along the easy axis or intermediate axis. The number of degree of freedom in this case then turns out to be 2. We let the \hat{x} axis be the direction preferred for antiferromagnetic ($J'_x < 0$) alignment (easy direction), $|J'_x| > |J'_y|$ and $|J'_x| > |J'_z|$ and the \hat{z} axis be the intermediate axis, which implies that $|J_y| + |J'_y|$ is smaller than both $|J_x| + |J'_x|$ and $|J_z| + |J'_z|$. For the case of the applied field along the easy axis, the zero temperature Gibbs free energy G corresponding to Hamiltonian (20) can then be obtained from eq. (4)

$$\begin{aligned} \frac{G}{N} = & -\frac{ZJ_x}{4} [(m_A^x)^2 + (m_B^x)^2] - \frac{ZJ_z}{4} [(m_A^z)^2 + (m_B^z)^2] \\ & - \frac{Z'J'_x}{2} (m_A^x m_B^x) - \frac{Z'J'_z}{2} (m_A^z m_B^z) \\ & - \frac{\mu_x}{2} H_x (m_A^x + m_B^x). \end{aligned} \quad (21a)$$

At $T = 0$ the two sublattices must be completely saturated, so

$$(m_A^x)^2 + (m_A^z)^2 = S^2,$$

$$(m_B^x)^2 + (m_B^z)^2 = S^2.$$

Thus, two variable α and β are introduced by

$$m_A^x = S \cos \alpha, \quad m_A^z = S \sin \alpha,$$

$$m_B^x = S \cos \beta, \quad m_B^z = S \sin \beta.$$

The expression (21a) then can be written as

$$\begin{aligned}
\frac{G}{NS^2} = & -\frac{ZJ_z}{4} - \frac{Z}{8}(J_x - J_z)(\cos^2 \alpha + \cos^2 \beta) \\
& -\frac{ZJ_x}{4} - \frac{Z}{8}(J_x - J_z)(\sin^2 \alpha + \sin^2 \beta) \\
& -\frac{Z'J'_x}{2} \cos \alpha \cos \beta - \frac{Z'J'_z}{2} \sin \alpha \sin \beta \\
& -\frac{\mu_x}{2S} H_x (\cos \alpha + \cos \beta)
\end{aligned} \tag{21b}$$

All of the possible solutions can be found by solving eq. (10), namely $\partial G/\partial \alpha = 0$ and $\partial G/\partial \beta = 0$.

According to the symmetries of the solutions, the different phases can be defined. To determine the stable solutions, the dynamical (local) stability conditions should be considered:

$$\det \left| \frac{\partial^2 G}{\partial m_i \partial m_j} \right| = \left[\left(\frac{\partial^2 G}{\partial \alpha^2} \quad \frac{\partial^2 G}{\partial \beta^2} \right) - \left(\frac{\partial^2 G}{\partial \alpha \partial \beta} \right)^2 \right] > 0$$

and

$$\frac{\partial^2 G}{\partial \alpha^2} > 0 \quad \left(\text{so } \frac{\partial^2 G}{\partial \beta^2} > 0 \right).$$

However, there may exist several stable solutions (different phases) at an appropriate range of field H . The thermodynamically stable phase is, of course, the solution with the lowest G for a given H . Van Wier *et al.*^[26] have fully discussed this problem for the antiferromagnet in an orthorhombic crystal. Because of the similarity of the Hamiltonians, their results can be directly applied to a general quasi-2D antiferromagnetic system.

All of the phases due to the solutions of $\partial G/\partial \alpha = 0$ and $\partial G/\partial \beta = 0$ are

described as follows (also illustrated in fig. 8):

- (a) paramagnetic phase (PM): $\alpha = \beta = 0$;
- (b) antiferromagnetic phase (AF): $\alpha = 0, \beta = \pi$;
- (c) intermediate phase (IN): $|\alpha| \neq |\beta|$;
- (d) spin flop phase I (SF): $\alpha = -\beta \neq 0 (J'_z < 0)$;
- (e) spin flop phase II (SP*): $\alpha = \beta \neq 0 (J'_z > 0)$.

The intermediate phase introduced here is characterized by $m_z^\pm = m_A^z \pm m_B^z \neq 0$. In general, there is no a priori reason that the intermediate phase should be ruled out. The nature of the intermediate phase is similar to that of the supersolid phase in the quantum crystals.^[18] The non-vanishing direct or staggered magnetizations (m_z^+ or m_z^-) are relevant order parameters in the intermediate phase. They reflect gradual rotation from the \hat{x} to the \hat{z} axis or vice versa (for m_z^+) with increasing H_x . This phase should occur for certain combinations of the inter- and intralayer exchange constants. To see this, it is necessary to examine the local and global stability conditions.

Solving equations (22), the direct magnetization along the x direction is $m_x^+ = S/2 (\cos \alpha + \cos \beta)$, are^[26]

- (a) PM: $\alpha = \beta = 0, m_x^+ = S, m_x^- = 0$,
- (b) AF: $\alpha = 0, \beta = \pi, m_x^+ = 0, m_x^- = S$,
- (c) IN: $\alpha \neq -\beta \neq 0, \alpha \neq \beta \neq 0$,

$$\cos(\alpha + \beta) = + \frac{\mu H}{Z(J_x - J_z)S} \left[\frac{Z'(J'_x + J'_z) - Z(J_x - J_z)}{Z'(J'_x - J'_z) - Z(J_x - J_z)} \right]^{1/2} - \frac{Z'(J'_x + J'_z)}{Z(J_z - J_x)},$$

$$\cos(\alpha - \beta) = + \frac{\mu g H}{Z(J_x - J_z)S} \left[\frac{Z'(J'_x - J'_z) - Z(J_x - J_z)}{Z'(J'_x + J'_z) - Z(J_x - J_z)} \right]^{1/2} - \frac{Z'(J'_x - J'_z)}{Z(J_x - J_z)}$$

and so

$$\begin{aligned} m_x &= \frac{S}{2} (\cos \alpha + \cos \beta) = S \cos \frac{\alpha + \beta}{2} \cos \frac{\alpha - \beta}{2} \\ &= \frac{S}{2} [1 + \cos(\alpha + \beta)]^{1/2} \cdot [1 + \cos(\alpha - \beta)]^{1/2}; \end{aligned}$$

(d) SF: $\alpha = -\beta = \cos^{-1} \left\{ \frac{-\mu H/S}{[Z'(J'_x + J'_z) + Z(J_x - J_z)]} \right\}$, and so

$$m_x^+ = \frac{-\mu H/S}{[Z'(J'_x + J'_z) + Z(J_x - J_z)]}$$

(e) SF*:

$$\alpha = \beta = \cos^{-1} \left\{ \frac{-\mu H/S}{(-Z'J'_x + Z'J'_z - ZJ_x + ZJ_z)} \right\},$$

$$m_x^+ = \frac{\mu H/S}{Z'(J'_z - J'_x) + Z(J_z - J_x)}$$

By applying the local stability conditions $\det |\partial^2 G / \partial \alpha \partial \beta| > 0$, $\partial^2 G / \partial \alpha^2 > 0$, the limits of the field corresponding to different phases could be given. These limits (phase boundaries) present the appropriate field ranges where the respective phases are allowed.

Which phase actually occurs for particular H is determined by global stability. That is the thermodynamically stable phase must be of the lowest G . Also the free energy G should be continuous at the phase boundaries. Fig.9 shows the sequences of thermodynamically stable phases at $T = 0$ K occurring for different combinations of the exchange constants^[26] ($J_x > 0, J_z > 0$ and $J'_x < 0$) in our quasi-2D model with a field along the \hat{x} axis.

For $Z(J_x - J_z) > Z' |J'_z|$, only the AF-PM phase transition will occur. Because of strong anisotropy within the layer (large J_x or small J_z), the system is Ising-like at $T=0$. The magnetization vs. field is illustrated in fig. 10(a). The critical field H_{PA}^C due to the first order AF-PM transition is $H_{PA}^C = \frac{p+s}{2}$ where $p = Z(J_x - J_z) - Z'(J'_x + J'_z)$ and $s = Z'(J'_z - J'_x) - Z(J_x - J_z)$.

As the anisotropy of the intralayer interaction decreases to the regime $Z(J_x - J_z) < Z' |J'_z|$, $Z'(-|J'_z| - J'_x) + Z(J_x - J_z) > 0$ and $\frac{Z(J_z - J_x)}{ZJ'_x} > 0$ as shown in fig. 9, a SF (or SF*) phase occurs between the PM and AF phases. It is apparent in this case, $J_x > J_z$ and $|J'_x| > |J'_z| + (Z/Z')(J_z - J_x)$, that the system behaves as a usual anisotropic Heisenberg antiferromagnet with the easy axis along \hat{x} . Fig. 10(b) illustrates the behavior of m_x vs H_x . The critical fields H_{SA}^C due to the first-order AF-SF (or AF-SF*) transition and H_{PS}^C due to the second-order SF-PM (SF*-PM) transition are $q^{1/2} r^{1/2}$ (or $p^{1/2} s^{1/2}$) and r (or s), respectively, where $q = Z'(J'_z - J'_x) + Z(J_x - J_z)$ and $r = -Z'(J'_x + J'_z) - Z(J_x - J_z)$.

However, if $J_z > J_x$ and $Z'(-|J'_z| - J'_x) + Z(J_x - J_z) > 0$, an IN phase exists between the AF and SF (or SF*) phases, separated from these by second order phase boundaries. It is obvious that the existence of an IN phase is a result of frustrated spin-alignment

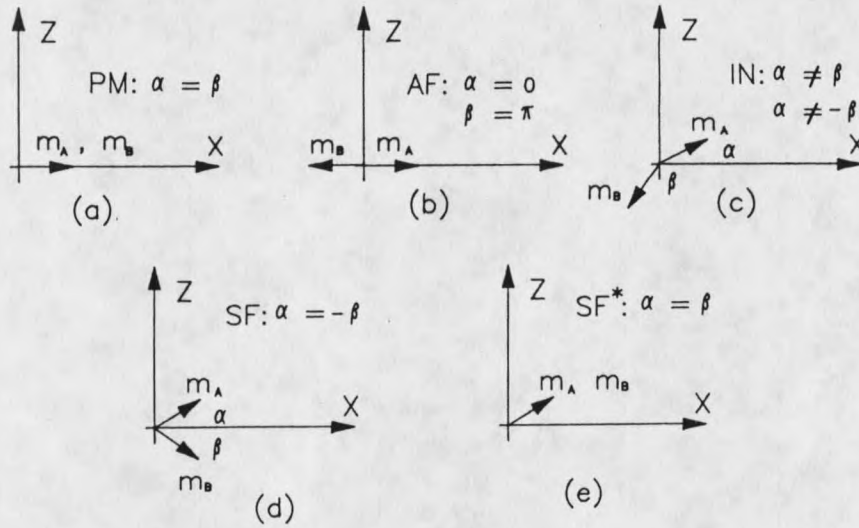


Fig. 8. Magnetization of the two sublattices according to the five different phases.

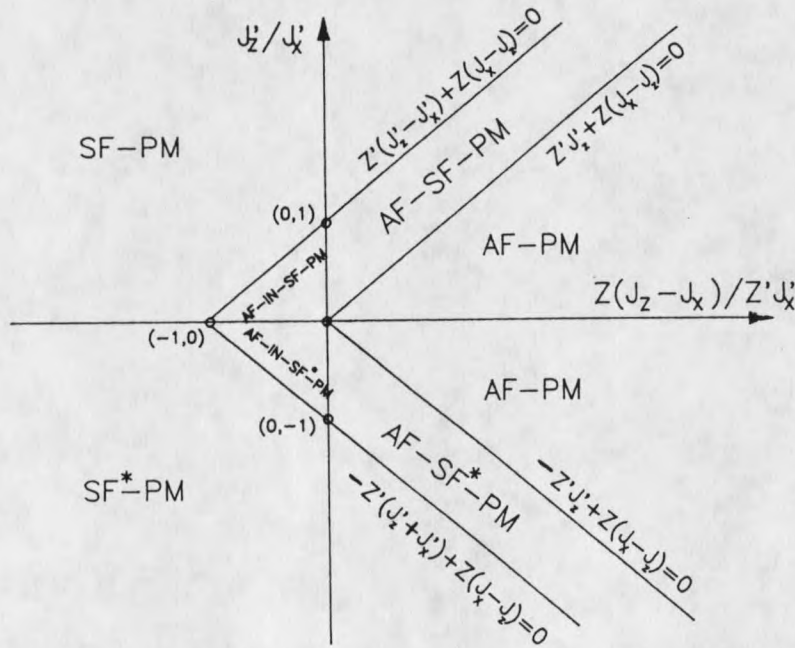


Fig. 9. Sequences of the different phase transitions for different combinations of exchange constants at $T = 0$ (taken from Ref. 26) where J_x and J_z are positive and J'_x is negative.

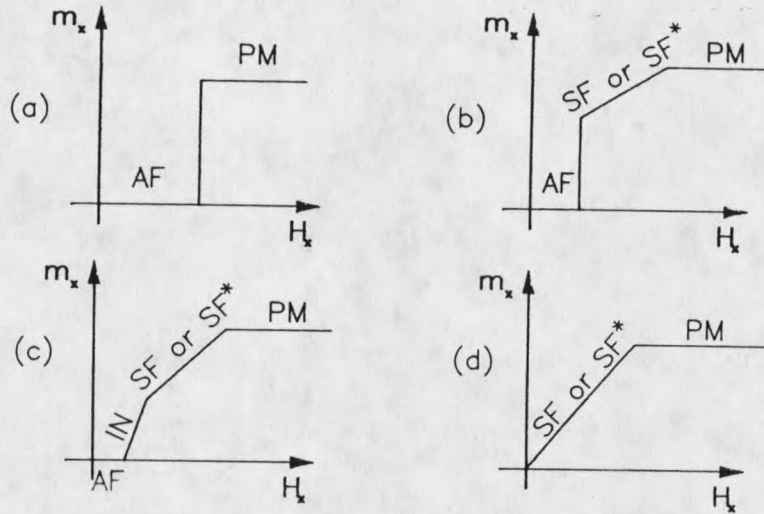


Fig. 10. Illustrating the different behavior of the magnetization at $T = 0$ corresponding to the consequences shown in fig. 9; (a) $Z'J'_z \pm Z(J_x - J_z) > 0$ (or $Z(J_x - J_z) > J' |J'_z|$), (b) $Z'J'_z \pm Z(J_x - J_z) < 0$ (or $Z(Z_x - J_z) < Z' |J'_z|$), $Z'(J'_z - J'_x) \pm Z(J_x - J_z) > 0$ and $Z(J_z - J_x) / Z'J'_x > 0$, (c) $J_z > J_x$ and $Z'(J'_z - J'_x) \pm Z(J_x - J_z) > 0$ (d) $Z'(J'_z - J'_x) \pm Z(J_x - J_z) < 0$.

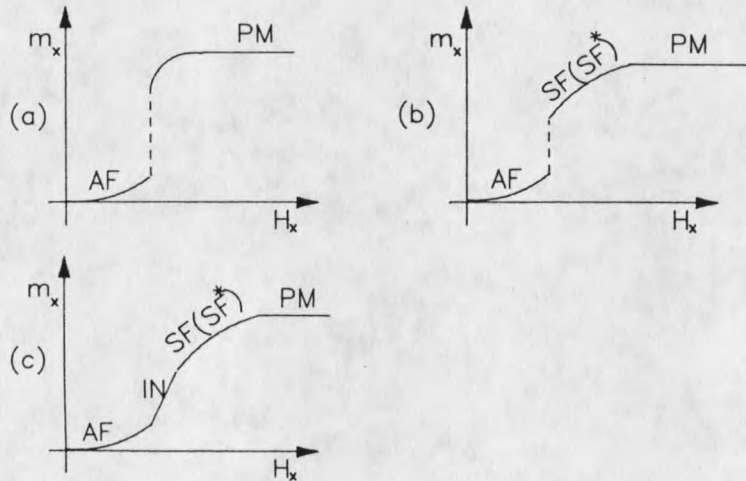


Fig. 11. Illustrating the magnetization behavior at finite temperatures for the different phases.

since $|J'_x| > |J'_z|$; $J_z > J_x$ and $\frac{|J'_x| - |J'_z|}{J_z - J_x} > \frac{z}{z'}$. The behavior of m_x vs. H_x in this case is shown in fig. 10(c). The critical fields are $H_{IA}^C = P^{1/2} q^{1/2}$, $H_{SI}^C = r q^{1/2} p^{-1/2}$ (or $sp^{1/2} q^{1/2}$) and $H_{PS}^C = r$ (or s). It is noticeable from fig. 9 that the area of the region (triangle), in the parameter space, where the IN phase can occur is comparably small. Thus, it may be difficult to verify an IN phase experimentally. In most copper-layer compounds, the ratio of the inter- to intralayer exchange, $\frac{|J'|}{|J|}$, is around $10^{-2} \sim 10^{-5}$. Even though some compounds with magnetically inequivalent layers may have the behavior $|J'_x| > |J'_z|$ and $J_z > J_x$, it may not match the confined condition $\frac{|J'_x| - |J'_z|}{J_z - J_x} > \frac{z}{z'}$.

For the case of $Z'(-|J'_z| - J'_x) + Z(J_x - J_z) < 0$, it eventually results in the easy axis being along the \hat{z} axis instead of \hat{x} axis. Thus, the antiferromagnetic-alignment between the layers along the \hat{x} axis is destroyed and only SF (or SF*) and PM phases can be seen in this direction. The behavior of m_x vs. H_x is shown in fig. 10(d) where the critical field $H_{PS}^C = r$ (or s).

Mean Field Calculation at Finite Temperatures

In this section, we discuss the details of the possibility of the existence of an intermediate phase at $T > 0$ for the quasi-2D systems phase boundaries between the SF (SF*) and IN, and between the IN and AF phases.

At finite temperature the density matrix ρ_i (eq. 6) is no longer constant. In our two-sublattice model we take ρ_A and ρ_B as

$$\begin{aligned} \rho_A &= \frac{\exp(\beta \vec{H}_A \cdot \vec{S}_A)}{\text{Tr} \exp(\beta \vec{H}_A \cdot \vec{S}_A)}, \\ \rho_B &= \frac{\exp(\beta \vec{H}_B \cdot \vec{S}_B)}{\text{Tr} \exp(\beta \vec{H}_B \cdot \vec{S}_B)}, \end{aligned} \quad (22)$$

and so $\rho = \prod_{\alpha, \beta} \rho_{\alpha} \rho_{\beta}$, where \vec{H}_A (\vec{H}_B) is an "effective" or "molecular" field at a plane of

type A (B) which is given by (11) and (12) corresponding to the Hamiltonian (20). Thus the sublattice magnetizations are $\langle \vec{S}_{A,B} \rangle = \vec{M}_{A,B} = \text{Tr}(\hat{\rho}_{A,B} \cdot \hat{S}_{A,B})$. Noting that $\vec{H}_{A,B} \parallel \vec{M}_{A,B}$ implies

$$m_{A,B}^i = \frac{H_{A,B}^i}{H_{A,B}} M_{A,B} = \frac{H_{A,B}^i}{H_{A,B}} \text{Tr}(\rho_{A,B} \cdot S_{A,B}), \quad (23)$$

for $S = 1/2$ the self-consistent eq. (13) then become

$$\frac{\langle S_{A,B}^i \rangle}{S} = \frac{m_{A,B}^i}{S} = \frac{H_{A,B}^i}{H_{A,B}} \tanh(\beta H_{A,B} S) \quad (24a)$$

where $i = x, y$ and z .

From eq. (11) and (12), we have the effective fields corresponding to (20)

$$H_{A,B}^i = ZJ_i m_{A,B}^i + Z'J'_i m_B^i + h^i \quad (24b)$$

with $i = x, y, z$, and the lengths of the effective fields

$$H_{A,B} = \left[(H_{A,B}^x)^2 + (H_{A,B}^y)^2 + (H_{A,B}^z)^2 \right]^{1/2}. \quad (24c)$$

For the case of an applied field along the easy axis (x axis) eq. (24) turns out to

be

$$\frac{\langle S_A^x \rangle}{S} = \frac{m_A^x}{S} = \frac{H_A^x}{H_A} \tanh(\beta H_A) \quad (25a)$$

$$\frac{\langle S_A^z \rangle}{S} = \frac{m_A^z}{S} = \frac{H_A^z}{H_A} \tanh(\beta H_A) \quad (25b)$$

$$\frac{\langle S_B^x \rangle}{S} = \frac{m_B^x}{S} = \frac{H_B^x}{H_B} \tanh(\beta H_B) \quad (25c)$$

$$\frac{\langle S_B^z \rangle}{S} = \frac{m_B^z}{S} = \frac{H_B^z}{H_B} \tanh(\beta H_B) \quad (25d)$$

$$H_A^x = ZJ_x m_A^x + Z'J'_x m_B^x + h^x \quad (26a)$$

$$H_A^z = ZJ_z m_A^z + Z'J'_z m_B^z \quad (26b)$$

$$H_B^x = ZJ_x m_B^x + Z'J'_x m_A^x + h^x \quad (26c)$$

$$H_B^z = ZJ_z m_B^z + Z'J'_z m_A^z \quad (26d)$$

and

$$H_{A,B}^2 = (H_{A,B}^x)^2 + (H_{A,B}^z)^2 \quad (27)$$

At a finite temperature, it is in general possible to solve the self-consistent equations (25) - (27) only by numerical methods. All the types of phases can be identified by the symmetries of the solutions of equations (25) - (27). The phase boundaries due to second-order transitions can be obtained from the criticality condition, eq. (19), with expression (8). For a first-order transition, the phase transition line between two phases is given by the boundary condition of thermodynamic stability, $\Phi_I = \Phi_{II}$, where $\Phi_{I,II}$ are of the expression (8) corresponding to two different phases at the transition line. The results discussed in the last section for $T=0$ will then follow as a special limit here.

Similarly for the case of $T=0$, the magnetization behavior at finite temperatures for the different phases are represented schematically in fig. 11. The lengths of the sublattice magnetization $\langle \vec{S}_{A,B} \rangle^2 (\vec{m}_{A,B}^2)$ are no longer constant at $T \neq 0$. They are a

function of both the temperature and the field. Since there are no analytic solutions for equations (25)-(27), $m_{A,B}^i$ ($i = x, y, z$) are not appropriate order parameters to analytically study the phase transition. It can be shown that, by choosing appropriate order parameters to replace $m_{A,B}^i$ in equations (16) - (19), the method discussed in the second section can still be applied nicely in most of the cases to yield an analytic solution for the phase boundaries.

For the AF-PM phase transition as shown in fig. 11(a) similar to fig. 10(a) at $T=0$, the appropriate order parameter for analyzing the transition is $m_-^x = m_A^x - m_B^x$. AF and PM phases are characterized by $m_-^x \neq 0$ and $m_-^x = 0$, respectively. Fig. 11(a) shows an Ising-like case ($m_{A,B}^z = 0$). However, for an anisotropic-Heisenberg antiferromagnet at a finite temperature, the thermal fluctuation always leads to $\langle S_{A,B}^z \rangle \neq 0$ so that SF (SF*) will occur before the PM phase takes place with increasing field. Thus, the appropriate formal order parameter for analyzing the PM-SF (SF*) transition is m_A^z or m_B^z ; for the SF-AF (or SF*-AF) transition it is $m_-^x = m_A^x - m_B^x$. Fig. 11(b) shows the behavior of magnetization vs. field at $T \neq 0$. The phase diagrams corresponding to this case are illustrated in figs. 4 and 6.

Once the IN phase occurs, the first-order AF-SF (or AF-SF*) transition is forbidden. The IN phase exists between the AF and SF (SF*) phases, separated from these by second-order phase boundaries. The magnetization behavior for this case are shown in fig. 11(c) corresponding to the possible phase diagrams illustrated in fig. 7(a). The appropriate order parameter for analyzing the SF-IN (or SF*-IN) transition is $m_{\pm}^z = m_A^z \pm m_B^z$; for the IN-AF phase transition it is m_A^z or m_B^z . If there exists a multicritical point, there is an AF-PM second order transition. The five phase-boundary

lines, PM-SF (or PM-SF^{*}), SF-AF (or SF^{*}-AF), SF-IN (or SF^{*}-IN), IN-AF and PM-AF, will be called the PS (PS^{*}), SA (SA^{*}), SI (SI^{*}), IA and PA lines, respectively. In this section our special attention focuses on the case of existence the IN phase.

Liu and Fisher^[18] studied the phase diagrams of a quantum lattice gas model with particular reference to the existence of a supersolid phase. Analogous to antiferromagnetism, the SF^{*} phase was considered characterized by $m_A^z = m_B^z \neq 0$ ($\vec{m}_A = \vec{m}_B$). In their model, J'_z is positive ($J'_z > 0$, in their notation). To study the IA and SI^{*} phase boundaries, they have chosen $m_-^z = m_A^z - m_B^z$ as an order parameter. However, for $J'_z < 0$ the SF phase is characterized by $m_A^z = -m_B^z$ so that the sign of m_A^z is opposed to that of m_B^z at SF phase (fig. 7(a)). Thus, we may choose $m_+^z = m_A^z + m_B^z$ as a order parameter to study SF-IN and IN-AF phase transitions. Following their work, we discuss the details of phase boundaries in the both cases of $J'_z > 0$ (SF^{*}) and $J'_z < 0$ (SF).

To obtain the IA boundary, it is convenient to start from low field where AF phase is described by $m_A^z = m_B^z = 0$. Above the IA boundary, the IN phase is assumed to occur described by $m_A^z \neq m_B^z$ and $m_A^z \neq -m_B^z$. Thus, an appropriate order parameter should be

$$m_{\pm}^z = \frac{1}{2}(m_A^z \pm m_B^z). \quad (28)$$

Introducing a small perturbation resultant field $(1/2)h_{\pm}$ in the Hamiltonian along the \hat{z} axis, $h_{\pm}/2 \sum_{\alpha,\beta} (S_{\alpha}^z + S_{\beta}^z)$, for $J'_z < 0$, and a staggered field $(1/2)h_{\pm}$, $(h_{\pm}/2) \sum_{\alpha,\beta} (S_{\alpha}^z - S_{\beta}^z)$ for $J'_z > 0$, equations (25) and (26) then become

$$m_A^z = \left(ZJ_z m_A^z \mp Z'J'_z m_B^z + \frac{1}{2} h_{\pm} \right) \frac{\tanh(\beta H_A)}{H_A} \quad (31)$$

$$m_B^z = \left(ZJ_z m_B^z + Z'J'_z m_A^z - \frac{1}{2} h_{\pm} \right) \frac{\tanh(\beta H_B)}{H_B} \quad (32)$$

with the rest of equations remaining unchanged. The Gibbs free energy, G , can be obtained from the Helmholtz free energy, $\Phi(h^x, T, h_{\pm})$, by

$$G = \Phi - \int h_{\pm} dm_{\pm}^z = \Phi - h_{\pm} \left(\frac{\partial \Phi}{\partial h_{\pm}} \right) \quad (33)$$

where

$$h_{\pm} = \frac{\partial G}{\partial m_{\pm}^z}, \quad (34)$$

and Φ is given by expression (8) corresponding to the equations (25a), (25c) (26a), (26c), (27), (31) and (32).

G can be expanded in a power series of m_{\pm}^z near criticality as

$$G = G_0 + C_2(m_{\pm}^z)^2 + C_4(m_{\pm}^z)^4 + C_6(m_{\pm}^z)^6 + \dots \quad (35)$$

From (34), we have

$$h_{\pm} = 2C_2(m_{\pm}^z) + 4C_4(m_{\pm}^z)^3 + \dots \quad (36)$$

The equilibrium condition is determined by $h_{\pm} = 0$. The stability implies $C_2 > 0$. As we discussed in the second section, the instability condition (19), $C_2(h^x, T) = 0$, will give the required IA second-order phase boundary.

By substituting eq. (36) into eq. (31) and (32), subtracting eq. (32) from (31) and adding eq. (32) to (31), one finds that m_A^z and m_B^z can be expressed in terms of m_{\pm}^z , m_{\pm}^z , H_A and H_B . Also, h_{\pm} or h_{\pm} can be expressed in terms of m_{\pm}^z , m_{\pm}^z , H_A and H_B from eq. (31) and (32). Replacing m_{\pm}^z (or m_{\pm}^z) by a power series of m_{\pm}^z , $m_{\pm}^z = \sum_{n=0}^{\infty} S_n^+(m_{\pm}^z)^n$, (or m_{\pm}^z , $m_{\pm}^z = \sum_{n=0}^{\infty} S_n^-(m_{\pm}^z)^n$), thus left sides of equations (35) and (36) can be expressed in

terms of m_+^z (or m_-^z) H_A and H_B . By equating the coefficients of equal powers of m_+^z (or m_-^z) on both sides of equations (35) and (36), Liu and Fisher^[18] have shown in zeroth order

$$H_{A0} = ZJ_x \tanh(\beta H_{A0}) + Z'J'_x \tanh(\beta H_{B0}) + h^x \quad (37)$$

$$H_{B0} = ZJ_x \tanh(\beta H_{B0}) + Z'J'_x \tanh(\beta H_{A0}) + h^x \quad (38)$$

where H_{A0} and H_{B0} are effective fields with $h_{\pm}=0$, and in first order

$$\frac{1}{2} C_2 F_1 + (J^{\pm} F_1 - 1) S_1^{\pm} = (1 - J^{\mp} F_1) \quad (39)$$

$$-\frac{1}{2} C_2 F_2 + (J^{\pm} F_2 - 1) S_1^{\pm} = -(1 - J^{\mp} F_2) \quad (40)$$

where

$$J^{\pm} = (ZJ_z \pm Z'J'_z)$$

$$J^{\mp} = (ZJ_z \mp Z'J'_z)$$

$$F_1 = H_{A0}^{-1} \tanh(\beta H_{A0}),$$

$$F_2 = H_{B0}^{-1} \tanh(\beta H_{B0}).$$

At the IA phase boundary, $C_2=0$, eliminating S_1^{\pm} in equations (39) and (40), we have

$$\begin{aligned} & [(Z'J'_z)^2 - (ZJ_z)^2] (H_{A0} \cdot H_{B0})^{-1} \\ & \cdot \tanh(\beta H_{A0}) \cdot \tanh(\beta H_{B0}) + ZJ_z [\tanh(\beta H_{A0}) \\ & + \tanh(\beta H_{B0})] - 1 = 0. \end{aligned} \quad (41)$$

Simultaneous solutions of equations (37), (38) and (41) gives the IA phase boundary, $h^x = H_{IA}(T)$.

To derive the SI (SI*) phase boundary it is convenient to start from the high field side where, throughout the SF (SF*) phase, we have $|m_A^z| = |m_B^z|$ and $m_A^x = m_B^x$. Again we consider the same perturbation field $(1/2)h_{\pm}$ along the \hat{z} axis and $m_{\pm}^z = 1/2(m_A^z \pm m_B^z)$ as the order parameter. By considering the terms of the same order in m_{\pm}^z and noting $H_{A0} = H_{B0} = H_0$, it is found in zeroth order that

$$(S_0^{\pm})^2 + (h^x)^2 / (ZJ_z + |Z'J'_z| - Z'J'_x - ZJ_x)^2 = \tanh^2(\beta H_0) \quad (42)$$

$$\tanh(\beta H_0) = H_0 / (ZJ_z + Z'|J'_z|), \quad (43)$$

and in second order

$$\begin{aligned} & (S_0^{\pm})^2 [(Z'J'_x)^2 - (ZJ_z \pm Z'J'_z - ZJ_x)^2] \cdot \\ & (ZJ_z \pm Z'J'_z - Z'J'_x - ZJ_x) \left[1 - \frac{1}{2H_0} (ZJ_z \pm Z'J'_z)\right. \\ & \left. \cdot \left(\frac{1}{2}C_2 + ZJ_z \mp Z'J'_z\right) f'(H_0)\right] = \\ & [2(ZJ_z \pm Z'J'_z) - \frac{1}{2}C_2] \left[1 - \frac{1}{2H_0} f'(H_0)\right] \cdot \end{aligned} \quad (44)$$

$$(Z'J'_x - ZJ_x) \cdot (\pm Z'J'_z + ZJ_z)]$$

where $f'(H_0) = \frac{d}{dH_0} [H_0^{-1} \tanh(\beta H_0)]$. By using the instability condition $C_2=0$ (at SI phase

boundary) and combining equations (42) and (43), the relation (44) becomes

$$h^{x2} = H_{SI^*,SI}^2 \left[\frac{1 + \beta(\pm Z'J'_z - ZJ_z) \cdot \text{sech}^2(\beta H_0)}{1 - \beta(ZJ_z \pm Z'J'_z) \cdot \text{sech}^2(\beta H_0)} \right] \tanh^2(\beta H_0) \quad (45)$$

where $H_{SI^*,SI}$ is a critical field at $T=0$,

$$H_{SI^*,SI}^2 = \frac{[ZJ_z \pm Z'J'_z - ZJ_x - Z'J'_x]}{[ZJ_x - ZJ_z \pm Z'J'_z - Z'J'_x]} \cdot [(ZJ_x - Z'J'_x - ZJ_z)^2 - (Z'J'_z)^2]^{1/2}. \quad (46)$$

The SI and SI* phase boundaries, $h^x = H_{SI^*,SI}(T)$, then can be given by a simultaneous solution of (43) and (45). The \pm sign in Eq.(43) and (45) correspond to $J'_z > 0$ (SI*) and $J'_z < 0$ (SI) cases, respectively.

The paramagnetic phase boundaries, PS (or PS*) and PA phase lines which are well known^[33-35] could be determined in the same way. The PS (or PS*) boundary, $h^x = H_{PS}(T)$ (or H_{PS^*}), is given by

$$\tanh \beta H_0 = \frac{2H_0}{ZJ_z \pm Z'J'_z} \quad (47)$$

and

$$h^x / (ZJ_z \pm Z'J'_z - Z'J'_x - ZJ_x) = \frac{H_0}{ZJ_z \pm Z'J'_z}, \quad (48)$$

where the \pm sign refers to $J'_z > 0$ for PS* and $J'_z < 0$ for PS, respectively.

The PA line, $h^x = H_{PA}(T)$, is determined by

$$1 + \beta(Z'J'_x - ZJ_x) \operatorname{sech}^2(\beta H_0) = 0 \quad (49)$$

and

$$H_0 = (Z'J'_x + ZJ_x) \tanh(\beta H_0) + h^x. \quad (50)$$

As $T \rightarrow 0$, so that $\beta \rightarrow \infty$, one finds that $H_{IA}(T)$ (eq. (37), (38) and (41)), $H_{SI^*,SI}(T)$ (eq. (43) and (45)) and $H_{PS,PS^*}(T)$ (eq. (47) and (48)) reduce to the zero-temperature results, namely, H_{IA}^C , $H_{SI^*,SI}^C$ and H_{PS,PS^*}^C given in the previous section. Also, one may show that the SF (SF*), IN and AF phases are the appropriate stable phases by demonstrating

that the coefficient C_2 of G expression have the correct sign on both sides of the phase boundary lines.

At the AF phase, the expression of C_2 could be derived through eq. (37) - (41), $C_2 = C_2(H_{IA}, h^x, \beta, H_{A0}, H_{B0})$. Since eqs. (37) - (41) are obtained from the AF phase, C_2 should be positive $h^x < H_{IA}$. Unfortunately, even though there is an exact expression for C_2 it is so complicated that one cannot easily see what relation it imposes on the various temperature, field and interaction parameters. At very low temperature, Liu and Fisher have shown

$$C_2 \approx [(h^x)^2 - (H_{IA})^2] / (ZJ_z \pm Z'J'_z + Z'J'_x - Z'J'_x) \quad (51)$$

At zero-temperature, the denominator in (51) is negative, which is the criterion for the existence of the NI phase at $T=0$ discussed in the last section. Therefore, the AP phase should be stable at low temperature ($C_2 > 0$, $h^x < H_{IA}$).

In the SF phase, it can be shown from equations (42) - (46) that $C_2 > 0$ for $h^x > H_{SI}$ (H_{SI^*}). Thus the SF (SF^{*}) phase is stable.

Before ending this section we briefly discuss the possibility of existence of a tetracritical point. We know that there may be an intermediate phase between the spin-flop and antiferromagnetic phases, at $T \geq 0$. The two phase boundaries, SI and IA, depend on the exchange constants in a rather complicated manner. Liu and Fisher^[18] have pointed out that there is a special case in which the four lambda lines (second order phase transition lines), PS (PS^{*}), PA, SI (SI^{*}) and IA, meet together at a single point. In this case the point at which the four phases coexist is referred to as a tetracritical point. At the tetracritical point, (T_T, H_T) , the effective field H_0 (a solution of (47) and (48)) for the PS boundary is also a solution of both sets of equations that determine the IA and SI

boundaries ((37), (38), (41), (43) and (45)), $H_0 = H_{\infty} = H_{\beta_0}$.

The existence of a tetracritical point is well understood for systems usually having high order interaction terms, cubic and fourth-order, with strong anisotropies in the Hamiltonian. For example, mean-field calculations for the spin-1 Ising model in ternary mixtures and for tetragonal XY-like antiferromagnets have shown the existence of a tetracritical point. But according to Gibbs' phase rule, a single-component (one order parameter expression in G) system cannot have more than three coexisting phases. Thus in general the tetracritical point exists only in the systems with high order anisotropic terms (symmetry-breaking fields) in the Hamiltonian. Indeed, Gibbs' rule applies only to phases which are sufficiently distinct which transition between them is of first order. In quadratic-interaction systems (our case), however, the four phase lines (lambda lines or second-order lines) joining together at tetracritical point correspond to continuous transitions. Thus, as Liu and Fisher pointed out, it seems to mislead to regard the distinct phases as "coexisting" at the tetracritical point. It could be understood as two distinct types of long-range order occurring simultaneously.

Since there is no completely analytic solution for this system, there is no generally sufficient criterion for the existence of an intermediate phase at a finite temperature. In fact the presence of a tetracritical point ensures the existence of the intermediate phase. Thus one may seek a sufficient criterion for its existence in this case. From (49) and (50), one finds the Néel temperature

$$T_N k_B = (ZJ_x - Z'J'_x). \quad (52)$$

If the AF-PM transition is of second order for $T_T < T < T_N$ and $h^x < H_T$, then the tetracritical point should be the common intersection point of the PA, PS (PS*) and SI (SI*) lines. Thus, it can be shown from equations (43), (45), (47), (48), (49), (50) and (52) that

$$T_T/T_N = \operatorname{sech}^2 \left\{ \left(\frac{ZJ_z \pm Z'J'_z}{k_B T_T} \right) [1 - T_T/T_N]^{1/2} \right\}. \quad (53)$$

Liu and Fisher have presented a practical criterion which states that if the IA phase line lies below the SI phase line ($H_{IA} < H_{SI}$), then at the tetracritical point (T_T, H_T) there must be

$$[dH_{SI}(T)/dT]_{T=T_T} < [dH_{IA}(T)/dT]_{T=T_T} \quad (54)$$

where T_T is given by (52) and (53). The derivative (54) could be analytically evaluated from (43), (45), (47), (48), (49) and (50), but this expression is too complicated to see what relation it imposes on the various interaction parameters. It is apparent that this criterion strongly contrasts with that at $T=0$ as given by $Z'(-J'_z | -J'_x) + Z(J_x - J_z) > 0$. Therefore, it has been suggested that an IN phase occurring at finite temperature with a tetracritical point might not extend down to zero temperature.

Since there is no general criterion for the existence of an IN phase at a finite temperature, the first-order SF-AF (SF*-AF) transition may occur below the temperature at which an IN phase terminates. To solve for the first-order SF (SF*)-AF phase transition line, it is necessary to solve the self-consistent equations (25) - (27). Putting two sets of stable solutions of eq. (25) - (27) corresponding to SF (SF*) and AF phases respectively into the expression of Helmholtz free energy Φ , eq. (8), one can obtain a SA (SA*) first order phase boundary $h^x = H_{SA,SA^*}(T)$ from thermodynamic boundary condition, $\Phi_{SF,SF^*}(h^x, T) = \Phi_{AF}(h^x, T)$. From the behavior of the metamagnets,^[36-41] it is well

known that the PA phase transition may change from second-order in low fields near T_N , to a first-order transition at high fields and low temperature. There is strong evidence from numerical calculations to support this conclusion.^[18]

Spin Canting Effect in the Transitions of Quasi-two Dimensional Systems

The spin canting effect responsible for weak ferromagnetic behavior in essentially antiferromagnetic materials is caused primarily by two types of mechanisms, *i.e.*, single-ion anisotropy and antisymmetric exchange. The antisymmetric exchange term with form $\vec{D}_{ij} \cdot (\vec{S}_i \times \vec{S}_j)$ was originally suggested by Dzyaloshinsky^[42] on purely symmetry grounds. Moriya^[43,44] showed that it was due to the effect of the spin-orbit term on the superexchange interaction. In the Brillouin-Wigner perturbation treatment, this term is a second order spin-orbit interaction in the spin Hamiltonian.^[43] The constant vector, \vec{D}_{ij} , is due to the difference of matrix elements of orbital angular momentum between the two ions. Thus, the direction of \vec{D}_{ij} is dependent on a difference of the local crystal field axes between the two ions. The magnitude of \vec{D} is around the order of $\frac{\Delta g}{g} J$, estimated by Moriya.^[43,44]

Studies of the phase transitions of the simple uniaxial antiferromagnet with Dzyaloshinsky-Moriya (DM) interaction have been made in the mean-field approximation at $T=0$. For a uniaxial anisotropic antiferromagnet (anisotropic exchange) with a \vec{D} vector perpendicular to the easy axis and an applied field along the easy axis, it was found that there is a gradual rotation of the antiferromagnetic axis, with increasing field, from a position parallel to one perpendicular to the easy direction. Thus there is no first order SF-AF transition as would occur in the case of an antiferromagnet.^[45] With an

additional single-ion uniaxial anisotropy, Fairall and Cowen^[46] have shown that a first-order SF-AF transition will occur even with an applied field away from the easy axis by an angle $\alpha < \alpha_c$ where α_c is a critical angle which is strongly dependent on $|\vec{D}|$, exchange and single-ion anisotropies. Although there is no analytical expression for α_c , numerical calculations showed that for angles larger than this critical angle the sublattice magnetizations turn continuously from an antiferromagnetic configuration into a spin-flop configuration.^[46] For $\vec{D} = 0$, this critical angle is of the order^[47-48] anisotropy/exchange. With DM vector, \vec{D} , perpendicular to the direction of applied field, the paramagnetic transition is destroyed.^[45,46] For \vec{H} not parallel to \vec{D} , a quasi-paramagnetic^[46] transition is observed which manifests itself as an inflection point in the susceptibility.

In this section, we study an effect of DM interaction in the anisotropic Heisenberg (biaxial anisotropy) quasi-2D system with applied field along the spin axes at $T > 0$. Several configurations of sublattice magnetizations and phase transitions are proposed. Due to a complexity, a general formalism at finite temperatures is presented in order to carry out a numerical calculation.

For the quasi-2D systems, by means of $|J'|/|J| \ll 1$ it is still possible that the DM interaction presents both within and between the layers. In this work, we discuss a case that DM interaction only presents within the layer processing in the next-neighbor since $|\vec{D}| \sim |\frac{\Delta g}{g} J|$ and $|\vec{D}'| \sim |\frac{\Delta g'}{g} J'|$ (for the most of copper-layer compounds, $|J'/J| \sim 10^{-2} - 10^{-5}$). Also, we assume that \vec{D} is perpendicular to the x - y plane (parallel to \hat{y} axis). Thus at ground state with a zero field ($T=0, \vec{H} = 0$) spins in the layers will be canted each other within the x - y plane (easy plane) as shown in fig. 12(a). In this case weak antiferromagnetic behavior occurs along \hat{z} axis. There is no weak antiferromagnetic

behavior along \hat{y} axis unless \vec{D} vector rotates away from \hat{y} axis.

For the case of an applied field along \hat{x} axis ($\vec{h} = h\hat{x}$), the three configurations of sublattice magnetizations with the simplest (highest) symmetry, x - y plane as a mirror symmetry plane, are identified. Fig. 12(b) shows an AF phase with the canting angle $\beta > \alpha$ where $\vec{S}_\alpha, \vec{S}_\alpha'$ belong to one layer (layer 1) and $\vec{S}_\beta, \vec{S}_\beta'$ belong to another layer (layer 2). With increasing field, a first-order transition between the AF and SF phases will occur. The SF phase are illustrated in fig. 12(c) in which $\vec{S}_\alpha, \vec{S}_\beta$ belong to layer 1 and $\vec{S}_\alpha', \vec{S}_\beta'$ belong to layer 2. A quasi-paramagnetic phase (QP), is defined as shown in fig. 12(d) ($\vec{S}_\alpha, \vec{S}_\beta \in$ layer 1, and $\vec{S}_\alpha', \vec{S}_\beta' \in$ layer 2). The magnetization behavior is schematically shown in fig. 12(e).

Due to the symmetry, a two-sublattice model is adequate here. Thus the effective fields can be denoted as follows,

AF phase (fig. 12(b)):

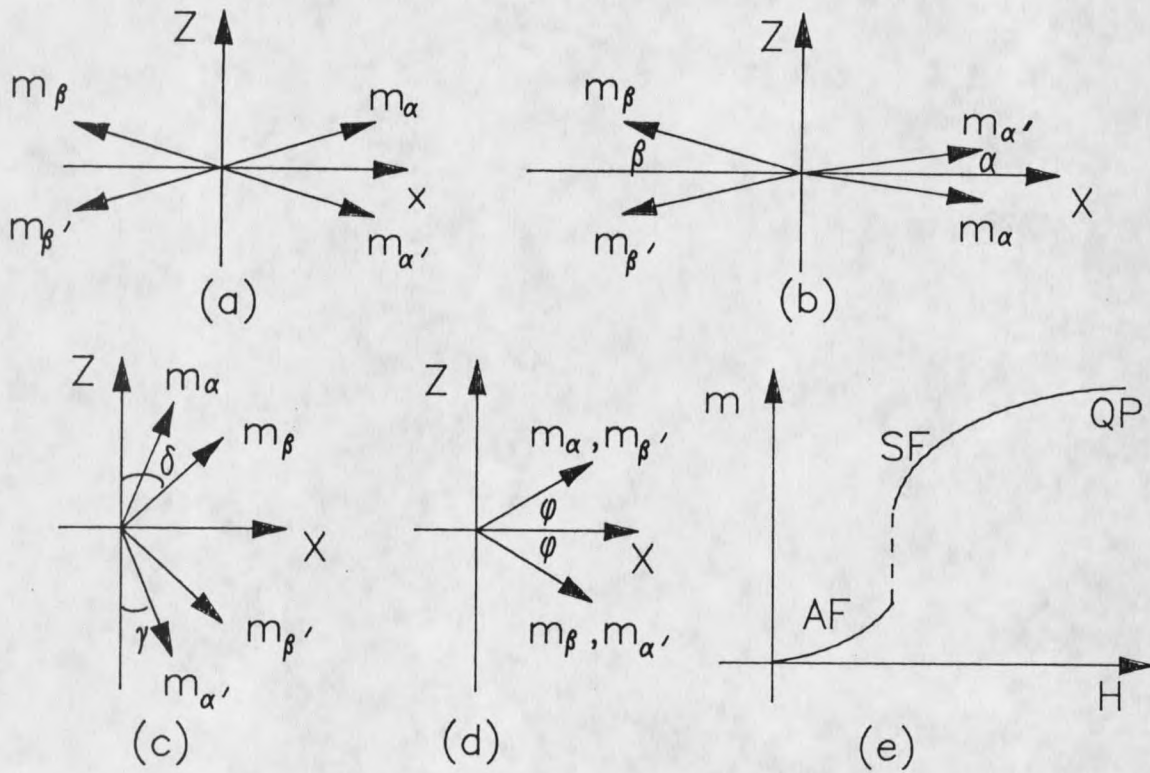


Fig. 12. Magnetization of the two sublattice corresponds to the Hamiltonian (20) adding the Dzyaloshinsky-Moriya interaction. (a) AF phase for the $\vec{H} = 0$, (b) AF phase for $0 < H_x < H_{SA}^C$ (c) SF phase for the $H_x > H_{SA}^C$, and (d) QP phase for the $H_x > H_{QS}^C$.

$$H_{\alpha'}^x = H_{\alpha}^x = H_A \cos \alpha,$$

$$H_{\alpha'}^z = -H_{\alpha}^z = -H_A \sin \alpha,$$

$$H_{\beta'}^x = H_{\beta}^x = H_B \cos \beta,$$

$$\text{and } H_{\beta'}^z = -H_{\beta}^z = -H_B \sin \beta$$

where $\alpha, \alpha' \in$ layer 1 and also belong to magnetic sublattice A, β and $\beta' \in$ layer 2 and

also belong to magnetic sublattice B;

SF phase (fig. 12(c)):

$$\tilde{H}_{\alpha'}^x = \tilde{H}_{\alpha}^x = \tilde{H}_A \sin \gamma,$$

$$\tilde{H}_{\alpha'}^z = -\tilde{H}_{\alpha}^z = -\tilde{H}_A \cos \gamma,$$

$$\text{and } \tilde{H}_{\beta'}^x = \tilde{H}_{\beta}^x = \tilde{H}_B \sin \delta,$$

$$\tilde{H}_{\beta'}^z = -\tilde{H}_{\beta}^z = -\tilde{H}_B \cos \delta,$$

where $\alpha, \beta \in$ layer 1, $\alpha' \wedge \beta' \in$ layer 2, α and $\alpha' \in$ sublattice A and $\beta, \beta' \in$ magnetic

sublattice B;

QP phase (fig. 12(d)):

$$\bar{H}_{\alpha'}^x = \bar{H}_{\beta}^x = \bar{H}_{\alpha}^x = \bar{H}_{\beta'}^x = \bar{H} \cos \phi$$

$$\bar{H}_{\alpha'}^z = \bar{H}_{\beta}^z = -\bar{H}_{\alpha}^z = -\bar{H}_{\beta'}^z = -\bar{H} \sin \phi$$

where $\alpha, \beta \in$ layer 1 and $\alpha', \beta' \in$ layer 2, one sublattice model is reduced here.

For the AF phase, we take ρ of the form in eq. (2)

$$\rho = \prod_{i,j} \frac{\exp(\beta \vec{H}_A \cdot \vec{S}_i)}{\text{Tr} \exp(\beta \vec{H}_A \cdot \vec{S}_i)} \frac{\exp(\beta \vec{H}_B \cdot \vec{S}_j)}{\text{Tr} \exp(\beta \vec{H}_B \cdot \vec{S}_j)}$$

where $i \in A$, and $j \in B$. One has, for $S = 1/2$,

$$\text{Tr} \exp(\beta \vec{H}_{A,B} \cdot \vec{S}_{i,j}) = 2 \cosh(\beta H_{A,B} \cdot S) (\vec{H}_{A,B} / S_{i,j}), \text{ and thus}$$

$$\frac{1}{\beta N} \text{Tr}(\rho \ln \rho) = \frac{1}{2} \sum_{l=A,B} \left\{ \vec{H}_l \cdot \vec{m}_l - \frac{1}{\beta} \ln[2 \cos(\beta H_l S)] \right\}$$

where the lengths of sublattice magnetization are

$$m_{A,B} = S \cdot \tanh(\beta H_{A,B} S). \quad (55)$$

Now we add *DM* interaction term, $\sum_{\langle ij \rangle} \vec{D} \cdot (\vec{S}_i \times \vec{S}_j)$, into Hamiltonian (20) and consider

the expression (2). We have expression of Φ for the AF phase

$$\begin{aligned} \frac{\Phi}{N} = & -\frac{ZJ_x}{4} [-k m_A^2 \sin^2 \alpha + m_A^2 \cos^2 \alpha] \\ & -\frac{ZJ_x}{4} [-k m_B^2 \sin^2 \beta + m_B^2 \cos^2 \beta] \\ & -\frac{ZD}{4} [m_A^2 \sin 2\alpha] - \frac{ZD}{4} [m_B^2 \sin^2 2\beta] \\ & -\frac{Z'J'_x}{2} m_A m_B (-\sin \alpha \sin \beta - \cos \alpha \cos \beta) \\ & -\frac{Z'J'_x}{2} m_A m_B (1 - k') \sin \alpha \sin \beta \\ & -\frac{h^x}{2} (m_A \cos \alpha - m_B \cos \beta) \\ & +\frac{1}{2} (H_A m_A + H_B m_B) - \frac{1}{2\beta} \ln [2 \cosh(\beta H_A S)] \\ & -\frac{1}{2\beta} \ln [2 \cosh(\beta H_B S)], \end{aligned} \quad (56)$$

where $k = J_z/J_x$, $k' = J'_z/J'_x$, and $m_{A,B}$ is given by eq. (55). Free energy in the AF phase

is obtained by minimizing (56) with respect to m_A , m_B , α and β :

$$\begin{aligned}
\frac{\partial \Phi}{\partial m_A} &= \frac{ZJ_x}{2} m_A [k \sin^2 \alpha - \cos^2 \alpha] \\
&- \frac{ZD}{2} m_A \sin 2\alpha + \frac{Z'J'_x}{2} m_B \cos(\alpha - \beta) \\
&- \frac{Z'J'_x}{2} m_B (1 - k') \sin \alpha \sin \beta \\
&- \frac{h}{2} \cos \alpha + \frac{H_A}{2} = 0
\end{aligned} \tag{57a}$$

$$\begin{aligned}
\frac{\partial \Phi}{\partial m_B} &= \frac{ZJ_x}{2} m_B [k \sin^2 \beta - \cos^2 \beta] \\
&- \frac{ZD}{2} m_B \sin 2\beta + \frac{Z'Z'_x}{2} m_A \cos(\alpha - \beta) \\
&- \frac{Z'J'_x}{2} m_A (1 - k') \sin \alpha \sin \beta \\
&+ \frac{h}{2} \cos \beta + \frac{H_B}{2} = 0
\end{aligned} \tag{57b}$$

$$\begin{aligned}
\frac{\partial \Phi}{\partial \alpha} &= \frac{ZJ_x}{4} m_A^2 (k + 1) \sin 2\alpha - \frac{ZD}{2} m_A^2 \cos 2\alpha \\
&+ \frac{Z'J'_x}{2} m_A m_B \sin(\beta - \alpha) \\
&- \frac{Z'J'_x}{2} m_A m_B (1 - k') \cos \alpha \cdot \sin \beta \\
&+ \frac{h}{2} m_A \sin \alpha = 0
\end{aligned} \tag{57c}$$

$$\begin{aligned}
\frac{\partial \Phi}{\partial \alpha} &= \frac{ZJ_x}{4} m_B^2 (k+1) \sin 2\beta - \frac{ZD}{2} m_B^2 \cos 2\beta \\
&- \frac{Z'J'_x}{2} m_A m_B \sin(\beta - \alpha) \\
&- \frac{Z'J'_x}{2} m_A m_B (1 - k') \sin \alpha \cos \beta \\
&- \frac{h}{2} m_B \sin \beta = 0
\end{aligned} \tag{57d}$$

The equilibrium variables, $m_A(T, h)$, $m_B(T, h)$, $\alpha(T, h)$, $\beta(T, h)$, $H_A(T, h)$ and $H_B(T, h)$, are the simultaneous solutions of (55) and (57). By substituting these solutions into (56) we have free energy in terms of T and h for the AF phase,

$$\Phi_{AF} = F_{AF}(T, h). \tag{58}$$

For the SF phase, the expression of Φ is given as

$$\begin{aligned}
\frac{\Phi}{N} &= \frac{-ZJ_x}{2} \bar{m}_A \bar{m}_B (\sin \gamma \sin \delta + k \cos \gamma \cos \delta) \\
&- \frac{Z'J'_x}{2} \bar{m}_A \bar{m}_B (\sin \gamma \sin \delta - k' \cos \gamma \cos \delta) \\
&- \frac{ZD}{2} \bar{m}_A \bar{m}_B \sin(\delta - \gamma) \\
&- \frac{h}{2} (\bar{m}_A \sin \gamma + \bar{m}_B \sin \delta) + \frac{1}{2} (\bar{H}_A \bar{m}_A + \bar{H}_B \bar{m}_B) \\
&- \frac{1}{2\beta} \ln[2 \cos(\beta H_A S)] - \frac{1}{2\beta} \ln[2 \cos(\beta H_B S)].
\end{aligned} \tag{59}$$

where

$$\bar{m}_{A,B} = S \cdot \tanh(\beta \bar{H}_{A,B} S) \tag{60}$$

Similarly, the free energy of SF phase is given by minimizing (59) with respect to \bar{m}_A , \bar{m}_B , γ and δ :

$$\frac{\partial \Phi}{\partial \bar{m}_A} = 0 \quad (61a)$$

$$\frac{\partial \Phi}{\partial \bar{m}_B} = 0 \quad (61b)$$

$$\frac{\partial \Phi}{\partial \gamma} = 0 \quad (61c)$$

$$\frac{\partial \Phi}{\partial \delta} = 0 \quad (61d)$$

Simultaneous solutions of (60) - (61) give us the equilibrium variables, $\bar{m}_A(T, h)$, $\bar{m}_B(T, h)$, $\gamma(T, h)$, $\delta(T, h)$, $\bar{H}_A(T, h)$, and $\bar{H}_B(T, h)$. Thus free energy for the SF phase can be obtained from (59),

$$\Phi_{SF} = F_{SF}(T, h). \quad (62)$$

The phase boundary, $h = H_{AS}(T)$, between AF and SF phases (first order) then can be given by matching eq. (62) to (58), $F_{SF}(T, h) = F_{AF}(T, h)$.

To obtain a second-order phase boundary between SF and QP phases, it is necessary to employ the instability condition, eq. (19). We list all of the elements of Jacobian matrix corresponding to free energy expression (59) in the polar coordinate for SF phase:

$$\frac{\partial^2 \Phi}{\partial \bar{m}_A^2} = 0, \quad \frac{\partial^2 \Phi}{\partial \bar{m}_B^2} = 0,$$

$$\begin{aligned} b &= \frac{\partial^2 \Phi}{\partial \bar{m}_A \partial \bar{m}_B} = -\frac{ZJ_x}{2} (\sin \gamma \sin \delta + k \cos \gamma \cos \delta) \\ &+ \frac{Z'J'_x}{2} \cos(\gamma + \delta) - \frac{Z'J'_x}{2} (k' - 1) \sin \gamma \sin \delta \\ &- \frac{ZD}{2} \sin(\delta - \gamma), \end{aligned}$$

$$\begin{aligned} c &= \frac{\partial^2 \Phi}{\partial \bar{m}_A \partial \gamma} = -\frac{ZJ_x}{2} \bar{m}_B (\cos \gamma \sin \delta - k \sin \gamma \cos \delta) \\ &- \frac{Z'J'_x}{2} \bar{m}_B \sin(\gamma + \delta) - \frac{Z'J'_x}{2} \bar{m}_B (k' - 1) \cos \gamma \sin \delta \\ &+ \frac{ZD}{2} \bar{m}_B \cos(\delta - \gamma) - \frac{h}{2} \cos \gamma, \end{aligned}$$

$$\begin{aligned} d &= \frac{\partial^2 \Phi}{\partial \bar{m}_A \partial \delta} = -\frac{ZJ_x}{2} \bar{m}_B (\sin \gamma \cos \delta - k \cos \gamma \sin \delta) \\ &- \frac{Z'J'_x}{2} \bar{m}_B \sin(\gamma + \delta) - \frac{Z'J'_x}{2} \bar{m}_B (k' - 1) \sin \gamma \cos \delta \\ &- \frac{ZD}{2} \bar{m}_B \cos(\delta - \gamma), \end{aligned}$$

$$\begin{aligned} f &= \frac{\partial^2 \Phi}{\partial \bar{m}_B \partial \gamma} = -\frac{ZJ_x}{2} \bar{m}_A (\cos \gamma \sin \delta - k \sin \gamma \cos \delta) \\ &- \frac{Z'J'_x}{2} \bar{m}_B \sin(\delta + \gamma) - \frac{Z'Z'_x}{2} \bar{m}_A (k' - 1) \\ &\cos \gamma \sin \delta + \frac{ZD}{2} \bar{m}_A \cos(\delta - \gamma), \end{aligned}$$

$$\begin{aligned}
g &= \frac{\partial^2 \Phi}{\partial \bar{m}_B \partial \delta} = -\frac{ZJ_x}{2} \bar{m}_A (\sin \gamma \sin \delta - k \cos \gamma \sin \delta) \\
&\quad - \frac{Z'J'_x}{2} \bar{m}_A \sin(\gamma + \delta) - \frac{Z'J'_x}{2} \bar{m}_A (k' - 1) \\
&\quad \sin \gamma \cos \delta - \frac{ZD}{2} \bar{m}_A \cos(\delta - \gamma) - \frac{h}{2} \cos \delta, \\
h &= \frac{\partial^2 \Phi}{\partial \gamma^2} = \frac{ZJ_x}{2} \bar{m}_A \bar{m}_B (\sin \gamma \sin \delta + k \cos \gamma \cos \delta) \\
&\quad - \frac{Z'J'_x}{2} \bar{m}_A \bar{m}_B \cos(\delta + \gamma) \\
&\quad + \frac{Z'J'_x}{2} \bar{m}_A \bar{m}_B (k' - 1) \sin \gamma \sin \delta \\
&\quad + \frac{ZD}{2} \bar{m}_A \bar{m}_B \sin(\delta - \gamma) + \frac{h}{2} \bar{m}_A \sin \gamma, \\
i &= \frac{\partial^2 \Phi}{\partial \gamma \partial \delta} = -\frac{ZJ_x}{2} \bar{m}_A \bar{m}_B (\cos \gamma \cos \delta + k \sin \gamma \sin \beta) \\
&\quad - \frac{Z'J'_x}{2} \bar{m}_A \bar{m}_B \cos(\gamma + \delta) - \frac{Z'J'_x}{2} \bar{m}_A \bar{m}_B \\
&\quad (k' - 1) \cos \gamma \cos \beta - \frac{ZD}{2} \bar{m}_A \bar{m}_B \sin(\delta - \gamma),
\end{aligned}$$

$$\begin{aligned}
j &= \frac{\partial^2 \Phi}{\partial \delta^2} = \frac{ZJ_x}{2} \bar{m}_A \bar{m}_B (\sin \gamma \sin \delta + k \cos \gamma \cos \delta) \\
&- \frac{Z'J'_x}{2} \bar{m}_A \bar{m}_B \cos(\gamma + \delta) \\
&+ \frac{Z'J'_x}{2} \bar{m}_A \bar{m}_B (k' - 1) \sin \gamma \sin \delta \\
&+ \frac{ZD}{2} \bar{m}_A \bar{m}_B \sin(\delta - \gamma) + \frac{h}{2} \bar{m}_B \sin \delta,
\end{aligned}$$

where \bar{m}_A , \bar{m}_B , γ and δ are given by the simultaneous solutions of equations (60)

- (61). The critical line for the SF phase can be obtained from eq. (19), which is

$$\begin{aligned}
&- b^2 h j + 2 b c f i + b^2 i^2 - 2 b c g i \\
&- 2 b d f i + 2 b d g h + c^2 g^2 - 2 c d f g \\
&+ d^2 f^2 = 0.
\end{aligned} \tag{63}$$

Eq. (63) gives us an instability line

$$h = H_{QS}(T) \tag{64}$$

at which the SF phase terminates. Above this line, $h > H_{QS}(T)$, the QP phase occurs. Since the transition between SF and QP phase is of the second order which means the free energy and magnetization are continuous at the phase boundary, the equation (63) is a necessary and sufficient condition to determine the phase boundary.

In the QP phase, which configuration of sublattice magnetization is shown in fig. 10(d), the expression Φ simply is of

$$\begin{aligned}
\frac{\Phi}{N} &= -\frac{ZJ_x}{2} \bar{m}^2 [-k \sin^2 \phi + \cos^2 \phi] \\
&\quad -\frac{ZD}{2} \bar{m}^2 \sin 2\phi - \frac{Z'J'_x}{2} \bar{m}^2 \cos 2\phi \\
&\quad -\frac{Z'J'_x}{2} \bar{m}^2 (1 - k') \sin^2 \phi - h\bar{m} \cos \phi \\
&\quad -\bar{H}\bar{m} - \frac{1}{\beta} \ln [2 \cosh (\beta \bar{H}S)]
\end{aligned} \tag{65}$$

where

$$\bar{m} = S \cdot \tanh(\beta \bar{H}S). \tag{66}$$

Free energy is then given by minimizing Φ with respect to \bar{m} and ϕ :

$$\begin{aligned}
\frac{\partial \Phi}{\partial \bar{m}} &= ZJ_x \bar{m} [k \sin^2 \phi - \cos^2 \phi] \\
&\quad - ZD \bar{m} \sin 2\phi \\
&\quad - Z'J'_x \bar{m} \cos 2\phi - Z'J'_x (1 - k') \bar{m} \sin^2 \phi \\
&\quad - h \cos \phi + \bar{H} = 0
\end{aligned} \tag{67a}$$

and

$$\begin{aligned}
\frac{\partial \Phi}{\partial \phi} &= \frac{ZJ_x}{2} \bar{m}^2 (k + 1) \sin 2\phi \\
&\quad - ZD \bar{m}^2 \cos 2\phi + Z'J'_x \bar{m} \sin 2\phi \\
&\quad - \frac{Z'J'_x}{2} (1 - k') \bar{m}^2 \sin 2\phi + h\bar{m} \sin \phi = 0.
\end{aligned} \tag{67b}$$

Thus solutions of equations (66), (67a) and (67b) give the equilibrium variables in terms of T and h , $\bar{m}(T, h)$, $\phi(T, h) \wedge \bar{H}(T, h)$, which leads to free energy (65) in terms of T and h , $\Phi_{QP} = F_{QP}(T, h)$. It is clear from eq. (67b) that a pure paramagnetic phase ($\phi = 0$) is prohibited as long as $D \neq 0$. The term "quasi-paramagnetic" phase (QP) used here is referred to this meaning.

At the second order SF-QP transition ($h=H_{QS}$ given by (64)), the free energy is continuous which implies

$$F_{QP}(T, H_{QS}(T)) = F_{SF}(T, H_{QS}(T)). \quad (68)$$

It should be pointed out that an instability field, $h=H_C(T)$, in which the QP phase determined by

$$\det | \text{Jacobian matrix} |_{QP} = \frac{\partial^2 \Phi}{\partial \bar{m}^2} \cdot \frac{\partial^2 \Phi}{\partial \phi^2} - \left(\frac{\partial^2 \Phi}{\partial \bar{m} \partial \phi} \right)^2 = 0 \quad (69)$$

should be identical to the phase boundary, $H_C(T) = H_{QP}(T)$, since the transition is of second order. Otherwise, either first order transition will occur or a third phase exists between SF and QP phases.

So far we have considered the case which an applied field is along \hat{x} (easy) axis analogous to an uniaxial anisotropic antiferromagnet with AF, SF and QP phases. In general, there may exist an intermediate phase between the SF and AF phases for the biaxial anisotropic systems with DM interaction. Because of the off-diagonal exchange coupling (referred to DM interaction) in the self-consistent eq. (25) - (26), it is nontrivial to derive analytic solutions for the phase transformation lines. However, it may be possible to verify some consequences by carrying out numerical calculation. Even though a numerical analysis is a straightforward task, we have not carried out a complete survey.

In the limited range of parameter values numerical calculation has been carried out to compare to the results of experiments.

For the case which an applied field is along \hat{z} (intermediate) axis, the analysis is fully identical to that of an applied field along \hat{x} axis in the SF and QP phases. By simply switching the spin components \hat{S}_x with \hat{S}_z in the Hamiltonian, all of the equations given for the SF and QP phase are valid to this case. Since \hat{x} axis is assumed to be easy axis, there is no SF-AF phase transition along \hat{z} axis, and so critical field is expected to be higher than that of along \hat{x} axis.

For an applied field along \hat{y} (hard) axis, a paramagnetic phase will occur since \bar{D} is a constant vector and along \hat{y} axis. A SF phase in this case is more complex than that in the previous cases. However, it is apparent that the canting angle between the two spins approaches to zero as field approaches to paramagnetic critical field. Thus, for $|\bar{D}| \ll |J'|$, paramagnetic phase boundary $h = H_{PS}(T)$ can be approximately obtained from eq. (47) and (48). For $|\bar{D}| \sim |J'|$, due to a complexity, we do not discuss the details here.

A canting angle in the ground state with zero field ($T=0, h=0$) can be obtained from eq. (57c) or (57d). Letting $\alpha = \beta$ and $m_A = m_B$, eq. (57c) or (57d) then leads to

$$2\alpha = \tan^{-1} \left[\frac{2ZD}{ZJ_x(k+1) + Z'J'_x(k'-1)} \right],$$

Of course, the effective field then can be given by solving eq. (57a) and (57b).

References of Chapter III

1. M.E. Fisher, AIP Conf. Proc 24, 273 (1975); A. Aharony and A.D. Bruce, Phys. Rev. Lett. 33, 427 (1974).

2. A.D. Bruce and A. Aharony, Phys. Rev. B11, 478 (1975).
3. J.R. Nelson, J.M. Kosterlitz and M.E. Fisher, Phys. Rev. Lett. 33, 813 (1974).
4. M.E. Fisher and D.R. Nelson, Phys. Rev. Lett. 32, 1350 (1974).
5. M.E. Fisher, Phys. Rev. Lett. 34, 1638 (1975).
6. H. Rohrer, Phys. Rev. Lett. 34, 1638 (1975).
7. G.F. Tuthill, J. Phys. C14, 2483 (1981).
8. M. Kerszberg and D. Mukamel, Phys. Rev. Lett. 43, 293 (1979).
9. M. Kerszberg and D. Mukamel, Phys. Rev. B23, 3943 (1981).
10. M. Kerszberg and D. Mukamel, Phys. Rev. B23, 3953 (1981).
11. M. Blume, V.J. Emery and B. Griffiths, Phys. Rev. A4, 1071 (1971).
12. K.W. Blazey, H. Rohrer and R. Webster, Phys. Rev. B4, 2287 (1971).
13. D. Mukamel and M. Blume, Phys. Rev. A10, 610 (1974).
14. D. Mukamel, Phys. Rev. B14, 1303 (1976).
15. M. Kerszberg and D. Mukamel, Phys. Rev. B18, 6283 (1978).
16. S. Krinsky and D. Mukamel, Phys. Rev. B12, 211 (1975).
17. S. Krinsky and D. Mukamel, Phys. Rev. B11, 399 (1975).
18. Kao-Shien Liu and M.E. Fisher, J. Low Temp. Phys. 10, 655 (1973).
19. H. Matsuda and T. Tsuneto, Progr. Theoret. Phys., Suppl. 46, 411 (1970).
20. G.V. Chester, Phys. Rev. A2, 256 (1970).
21. A.J. Leggett, Phys. Rev. Lett. 25, 1543 (1970).
22. R.A. Guyer, Phys. Rev. Lett. 26, 174 (1971).
23. W.J. Mullin, Phys. Rev. Lett. 26, 611 (1971).
24. R.S. Kagiwoda, J.S. Fraser, I. Rudnick and D. Bergman, Phys. Rev. Lett. 22, 338 (1969).

25. D.L. Goodstein and R.L. Elgin, Phys. Rev. Lett. 22, 383 (1969).
26. O.P. van Wier, T. van Peski-Tinbergen and C.J. Gorter, Physica 25, 116 (1959).
27. H. Falk, Am. J. Phys. 38, 858 (1970).
28. K.W. Blazey, K.A. Müller, M. Ondris and H. Rohrer, Phys. Rev. Lett. 24, 105 (1970).
29. Y.L. Wang and H.B. Callen, J. Phys. Chem. Solids 25, 1459 (1964).
30. F.B. Anderson and H.B. Callen, Phys. Rev. 4A, A1068 (1964).
31. J. Feder and E. Pytte, Phys. Rev. 168, 640 (1968).
32. M.E. Fisher, Reports Prog. in Phys. 30, 615 (1967).
33. C.J. Gorter and Tineke van Peski-Tinbergen, Physica 22, 273 (1956).
34. K. Motizuki, J. Phys. Soc. Japan, 14, 759 (1959).
35. R. Bidaux, P. Carrea and B. Vivet, J. Phys. Chem. Solids, 28, 2453 (1967).
36. R.P. Kenan, R.E. Mills and C.E. Campbell, J. Appl. Phys. 40, 1027 (1969).
37. V.A. Schmidt and S.A. Friedberg, Phys. Rev. B1, 2250 (1970).
38. D.B. Lossee, J.N. McElearny, G.E. Shankle, R.L. Carlin, P.J. Cresswell and W.T. Robinson, Phys. Rev. B8, 2185 (1973).
39. R.D. Spence and A.C. Botterman, Phys. Rev. B9, 2993 (1974).
40. D. Bruce Losee, William E. Hatfield and I. Bernal, Phys. Rev. Lett. 35, 1665 (1975).
41. E. Stryjewski and N. Giordano, Adv. Phys., 26, 487 (1977).
42. I. Dzialoshinski, J. Phys. Chem. Solids 4, 241 (1958).
43. T. Moriya, Phys. Rev. Lett. 4, 228 (1960).
44. T. Moriya, Phys. Rev. 120, 91 (1960).
45. G. Cinader, Phys. Rev. 155, 453 (1967).
46. C.W. Fairall and J.A. Cowen, Phys. Rev. B2, 4636 (1970).
47. H. Rohrer and H. Thomas, J. Appl. Phys. 40, 1025 (1969).

48. G.K. Chepurnykh. Sov. Phys. Solid 10, 1517 (1968); M.I. Kaganov and G.K. Chepurnykh, Sov. Phys. Solid 11, 745 (1969).

CHAPTER IV

EXPERIMENTAL STUDIES ON MAGNETIC PROPERTIES, PHASE TRANSITIONS AND CRITICAL BEHAVIOR OF QUASI TWO DIMENSIONAL SYSTEMS $[\text{C}_6\text{H}_5(\text{CH}_2)_n\text{NH}_3]_2\text{CuBr}_4$ ($n = 1, 2$ and 3)**Introduction**

The magnetic properties, phase transitions and critical behavior in layer perovskite-type transition metal salts with the general formula $(\text{RNH}_3)_2\text{MX}_4$ (R = organic group, M = divalent metal ion: $\text{X} = \text{F}^-$, Cl^- , or Br^-) have been of particular interest for a long time.^[1-10] Many of these compounds have been studied in attempts to verify theoretical predictions regarding two-dimensional (2D) and quasi-2D magnetic systems since a rich variety of nonmagnetic organic cations produce large and various separations between the magnetic metallate layers.

It is now firmly established that the phase transition for the ideal 2D Heisenberg system at nonzero temperature is not related to long-range order, even though it is characterized by an infinite initial susceptibility.^[11-14] In contrast, quasi-2D ferromagnets, which are systems that deviate from ideal isotropic 2D systems by the introduction of spatial and spin anisotropies, are well known to have a finite transition temperature related to the onset of long-range order.^[15-20] Thus, the behavior of low field magnetization and the degree of divergence of the initial susceptibility at the transition temperature play an important role in indicating the difference in the critical behavior between the real quasi-2D system and ideal isotropic 2D system.

Although a complete theoretical study of quasi-2D magnetic systems has been

not carried out yet, mean-field theory still can provide a considerable task to study phase diagrams of quasi-2D systems. One of the striking questions which remains unresolved is whether or not the intermediate phase actually exists in the real quasi-2D magnetic systems. It may be possible to verify this phase experimentally in a large variety of layer-type magnetic metallate compounds which contain strong ferromagnetic intralayer and weakly antiferromagnetic interlayer exchanges. Over the past years,^[1-3] phase diagrams of a large number of copper layer-type compounds have been studied experimentally. Much attention has been focused on the spin-flop phase. In the many cases, the anisotropy is introduced only via interlayer exchange. Within the layer it is usually assumed that exchange coupling is isotropic (Heisenberg). Thus the first-order AF-SF transition along the easy axis (antiferromagnetically aligned interaction between the layers) is expected. The isothermal magnetization is then expected to be discontinuous at the critical field in this context. However, once intralayer anisotropy is considered, the first-order AF-SF transition may be forbidden. As we have discussed in the Chapter II , within mean-field theory, an intermediate phase can exist between the AF and the SF phase while the exchange constants satisfy the conditions: $|J'_x| > |J'_z|$, $J_z > J_x > 0$ and $\frac{|J'_x| - |J'_z|}{J_z - J_x} > \frac{Z}{Z'}$. In this case the isothermal magnetization is continuous through all the phases. Even though most of the copper layer-type compounds behave as an anisotropic Heisenberg system due to both inter- and intralayer coupling, the confined conditions mentioned above may not be satisfied in many of the cases.

The magnetic susceptibilities of the series of $(RNH_3)_2CuX_4$ compounds with $X = Cl^-$ or Br^- have been studied extensively.^[1] They are characterized by nearly Heisenberg ferromagnetic intralayer coupling, with a small 1 - 5% XY (Cl) or Ising (Br) exchange anisotropy. The interlayer coupling is generally very weak, especially for

large R groups, and both ferromagnetic and antiferromagnetic interlayer coupling are observed. The class of compounds $[\text{C}_6\text{H}_5(\text{CH}_2)_n\text{NH}_3]_2\text{CuCl}_4$ have been reported to belong to the rare group of insulating 3D ferromagnets.^[21,22] A detailed EPR study of these compounds has been recently undertaken to probe their local anisotropies. One feature of this study was the observation of effects due to magnetically inequivalent layers which implied that the interlayer coupling was less than 10^{-3} K.^[23]

For the case of very small interlayer coupling, the systems may exhibit near-2D behavior even close to a critical point. It seems to be important to study the critical behavior of these systems experimentally in attempts to compare with 2D critical theories, which have been extensively developed recently.^[24-25] In particular, the principle of conformal invariance has led to remarkable progress in the theory of 2D critical phenomena.^[36-41] The classification 2D critical theories may be universally characterized by the conformal anomaly (as we have briefly introduced in Chapter I). Such applications of conformal invariance in 2D critical theories require that a system of short-range interactions at the critical point be not only translationally and rotationally invariant but also scale invariant. Although no experimental work has been reported to verify the 2D conformal critical theory so far, it is possible to verify the applicability of such "universal" 2D critical theory for a realistic 2D system by testing the scaling invariance from the critical point data. Therefore, it should be very interesting to apply the scaling law to analyze the results of isothermal magnetization measurements near the critical point for a 2D ferromagnet.

In this chapter, we report the magnetic studies of new quasi-2D systems $[\text{C}_6\text{H}_5(\text{CH}_2)_n\text{NH}_3]_2\text{CuBr}_4$ with $n = 1, 2$ and 3 . The single crystals of these compounds were supplied by the chemistry department of Washington State University. The structure determination has been made by X-ray analysis on a Nicolet RM3 diffrac-

tometer at Washington State University. All three salts contain antiferro-distortive layers of planer CuBr_4^{2-} anions separated by the double layers of the $\text{C}_6\text{H}_5(\text{CH}_2)_n\text{NH}_3^+$ cations. The arrangement for each Cu^{2+} ion is a tetragonally elongated octahedral arrangement. The structure of the $n = 2$ compound^[42] is similar to that of $(\text{C}_2\text{H}_5\text{NH}_3)_2\text{CuCl}_4$.^[43] The layer arrangement is shown in fig. 13 . The details of structures of the $n = 1$ and $n = 3$ salts are not known yet, but some features need to be noted. The lattice constants (A) are $a : b : c = 10.558 : 10.486 : 63.473, 7.654 : 7.756 : 38.042$ and $7.774 : 7.804 : 39.350$ for $n = 1, 2$ and 3 , respectively.^[44] The in-plane crystallographic axes for $n = 1$ are rotated by 45° with respect to those for the $n = 2$ structure, doubling the size of the repeat unit within the layer. The length of the c axis is also doubled leading to a four layer repeat in that direction, so that adjacent layers will not be structurally or magnetically equivalent. In all cases, the large interlayer separation ensures the presence of weakly magnetic dipolar coupling between layers.

Magnetizations and susceptibilities of these compounds are studied in this work. Isothermal and rotational measurements on the single crystals are carried out. Initial susceptibility of powder samples is also measured. Magnetization phase diagrams along spin axes are obtained. It is shown that there is strong ferromagnetic ordering within the layer and very weak antiferromagnetic coupling between the layers in these compounds. Strong spin anisotropy and complicated spin ordering are found. Along the spin easy axis due to the antiferromagnetic ordering between the layer, the experimental evidence for a possible existence of intermediate phase is given for the $n = 1$ and 2 compounds. Mean-field theory results are compared with the experimental results. It is found that the exchange anisotropy of interlayer is quite different from that of intralayer. It is suggested, due to the resolution of experiments, that there is D-M interaction within the layer. Thermodynamic analyses of the experimental results are

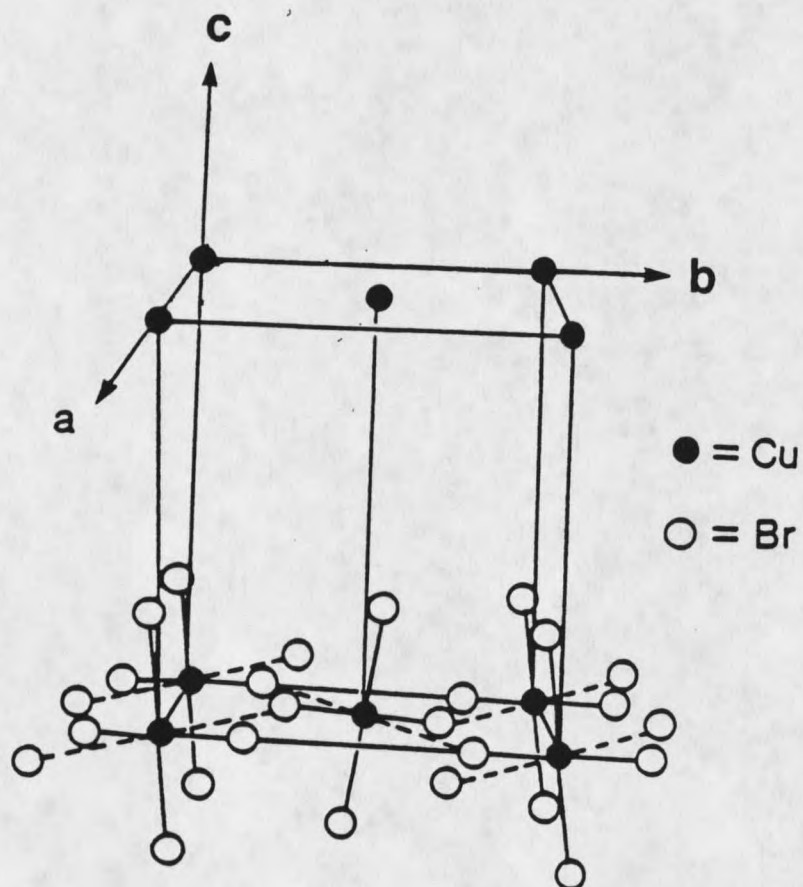


Fig. 13. Illustration of the layer structure in $[\text{C}_6\text{H}_5\text{C}_2\text{H}_4\text{NH}_3]_2\text{CuBr}_4$. The d axis is coming out of the plane of the illustration.

also presented. Scaling analyses are employed to study critical behavior of these powdered compounds. It is seen from isothermal data near the transition temperature that scaling hypothesis does not hold. Transition temperature, exchange constants, exchange anisotropies and critical exponent γ for these compounds are given in this work.

Experiments and Results

Magnetizations and susceptibilities of single crystal $[\text{C}_6\text{H}_5\text{CH}_2\text{NH}_3]_2\text{CuBr}_4$

The single crystals of $[\text{C}_6\text{H}_5(\text{CH}_2)_n\text{NH}_3]_2\text{CuBr}_4$ with $n = 1, 2$ and 3 in the form of dark shiny non-hygroscopic plates were measured by a EG&G Model 155 Vibrating Sample Magnetometer (VSM) with a Janis Variable-Temperature helium Cryostat system. The approximate dimensions of the crystals are about $4.0 \times 3.5 \times 0.45 \text{ mm}^3$, $3.0 \times 3.0 \times 0.35 \text{ mm}^3$ and $3.5 \times 2.0 \times 0.35 \text{ mm}^3$ for $n = 1, 2$ and 3 , respectively. The temperature was measured with a Lakeshore carbon-glass resistor mounted above the sample and the temperature of the sample was controlled by regulating the rate of helium gas flow and the heater current. By pumping on the sample chamber, the temperature of the helium gas in this cryostat can reach down to about 1.7 K. The Bell model 625 gaussmeter and Model XOQ4-0025 transverse flexible probe were used to measure the applied field. The set-up was calibrated via the known saturation moment of nickel obtained from the National Bureau of Standards. The systematical error of the magnetization measurement from VSM was estimated to be less than 5%. In the measurements of the isothermal magnetization, the system was given 8 seconds to come to equilibrium while the interval of swept field, ΔH , was chosen to be less than 100 Oe. In the low temperature and low field regions, the wait-time between the data points had to be set at least 10 seconds when ΔH is chosen from 100 to 300 Oe.

Because of the relatively large magnitude of the magnetization for these

compounds, the correction of demagnetization effect for the field is necessary. The demagnetization factor, \vec{d} , along the \hat{c} axis (perpendicular to the plane of plate) and in the plane of plate are estimated to be $d_c = 0.85, 0.84$ and 0.82 and $d_{ab} = 0.075, 0.075$ and 0.09 for $n = 1, 2$ and 3 , respectively. These values have been calculated for a thin oblate spheroid^[45] with the areas of cross sections approximately equal to that of the samples. Although the correction is relatively insignificant in the plane of the plate (less than 1%), the correction made perpendicular to the platelet (i.e. the \hat{c} axis) amounts to 20% for the field at the transition region.

For the $n = 1$ compound, the isothermal magnetization was first measured with an applied field perpendicular to the plate (along the \hat{c} axis). The field was swept from 250 Oe to 0 Oe. The results are shown in fig 14. No hysteresis was found. For temperatures $T > 2.6$ K, the isotherms were found to be completely reversible. It is clear from fig. 14 that there is a second order transition in the \hat{c} direction. At temperatures below about 6 K, the slopes of the isothermal magnetization vs. applied field slightly increase until the field reaches to a critical field where the magnetization starts to be saturate. At this point, the isothermal susceptibility has a discontinuity. At temperatures above 6 K, in contrast, the isotherms exhibit slight rounding near the critical field. This is indicative of a continuous transition in which the critical field is determined in principle by a point of inflection in the dM/dH vs. H curve. Full linear dependence was found at temperatures above approximately 15 K. It is noticeable that the departure portions from linearity to saturation set in at very low field region, $H_c < 100$ Oe. Thus, one may conclude that if this second order transition would be mainly thought to be a transition from spin-flop to paramagnetic phase, the spin preferred axis within the layer (due to a strongly ferromagnetic coupling) is then along the \hat{c} axis. For convenience, we may denote \hat{z} as one spin axis, along the \hat{c} axis. At temperatures below

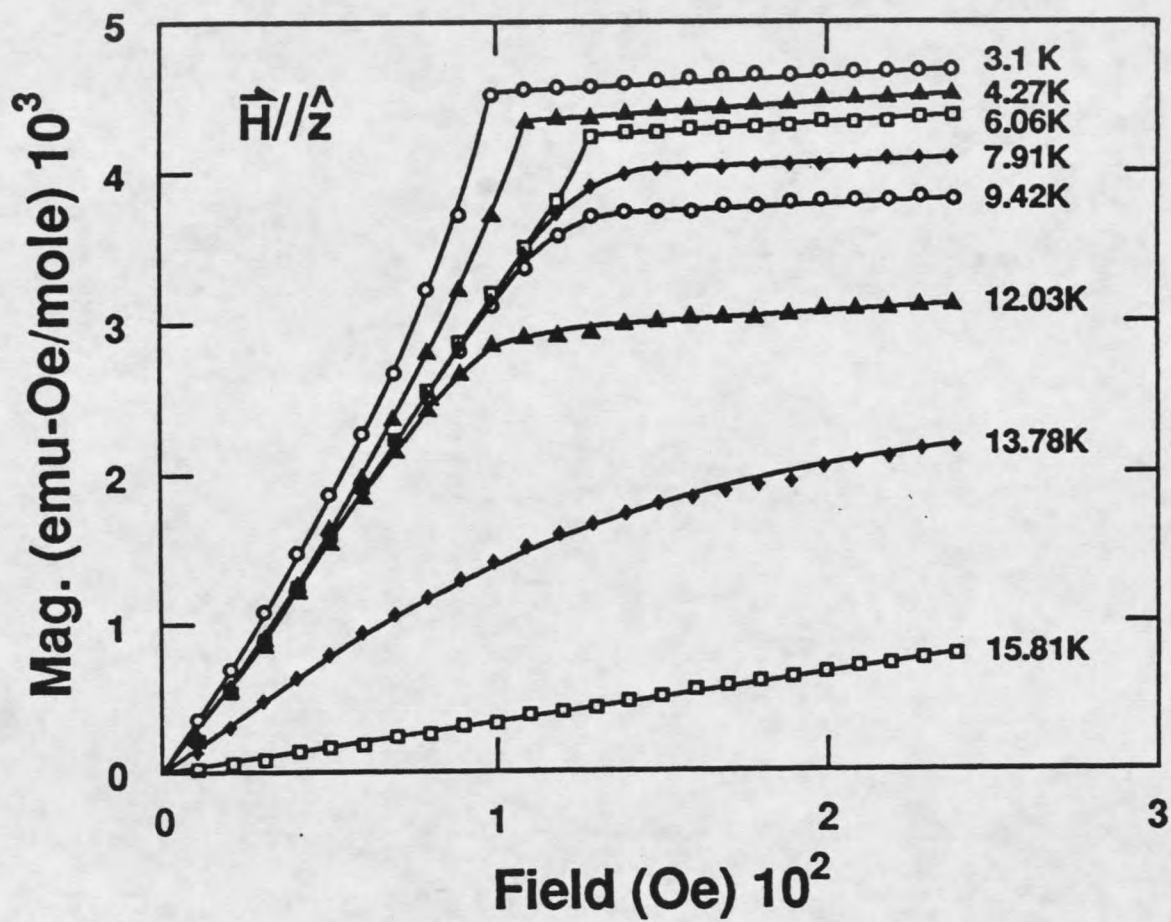


Fig. 14. Isothermal magnetization vs. internal field along the \hat{z} axis (c axis) for the $n = 1$ compound.

around 6 K, however, the magnetization before the saturation is reached increases more steeply with applied field than expected from the molecular field theory, and this deviation from linearity has a natural explanation herein. Many antiferromagnets offer this kind of nonlinearity of the perpendicular magnetization.^[46-50] and various interpretations have been suggested to explain this phenomena. De Jongh has given a review of the possible origins of this deviation^[48] and concluded that it is caused by instabilities in the magnetic system near the thermodynamic critical field.^[51] A zero-point spin-wave deviation,^[52] a biquadratic exchange term in the Hamiltonian^[53,55], a crystal-field approximation (strong cubic potential and weak trigonal distortion)^[47] and an effect of spin canting^[46,50] also cause this behavior.

With a field parallel to the surface of the plate (the ab plane) a rotational measurement of isothermal magnetization at $T = 4.5$ K was performed. By rotating the crystal along the \hat{c} (\hat{z}) axis with each step of 5° , two distinct directions in the plane of plate have been seen. Fig. 15 shows the result of this measurement for the $n = 1$ crystal. The magnetization along a direction away from one of the crystal axes with an angle of about 30° (denoted as the \hat{y} axis in fig. 15) is found to be linearly dependent on H up to about 1000 Oe. Along the direction perpendicular to \hat{y} axis in the plane (denoted the \hat{x} axis) the magnetization increases linearly up to about 200 Oe then increases rapidly where the slope exhibits a "near" divergence. As the field rotates toward the \hat{y} direction in the plane, the slope of the isothermal magnetization gradually decreases as shown in fig. 15. There is no hysteresis to be found in these orientation measurements. Fig. 16 shows the results of isothermal measurements along the \hat{x} axis at several different temperatures. It is apparent from fig. 16 that there is a critical field where the magnetization starts to rapidly and non-linearly increase (S-form). This threshold field gradually decreases as temperature rises and it disappears as T reaches around 12.6 K.

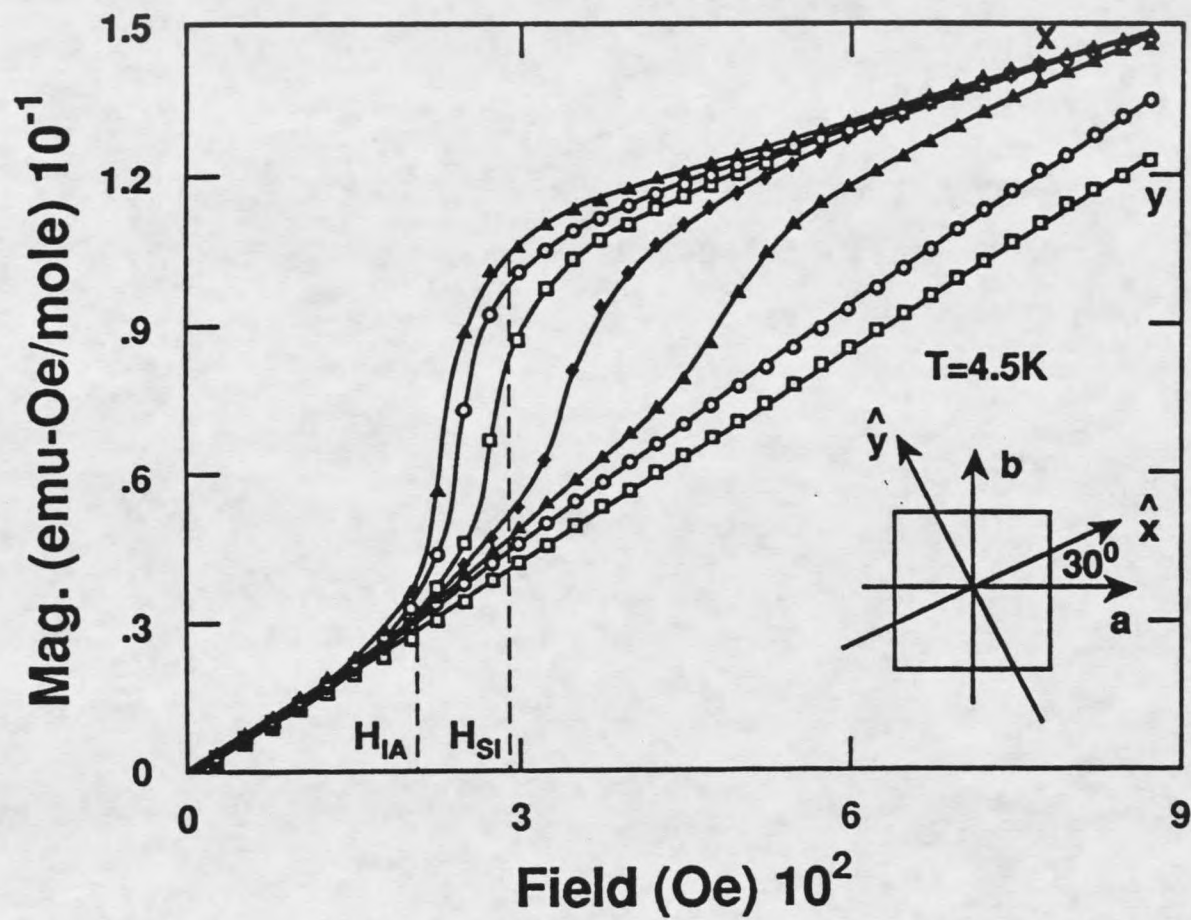


Fig. 15. The results of rotational measurements (15° apart) of isothermal magnetization at $T = 4.5\text{K}$ with field parallel to the surface of the plate (ab plane) for the $n = 1$ single crystal.

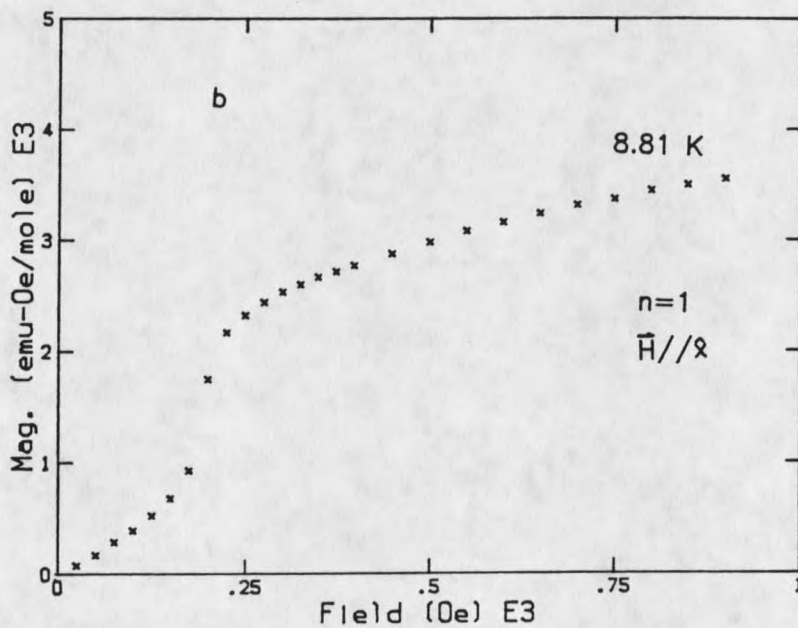
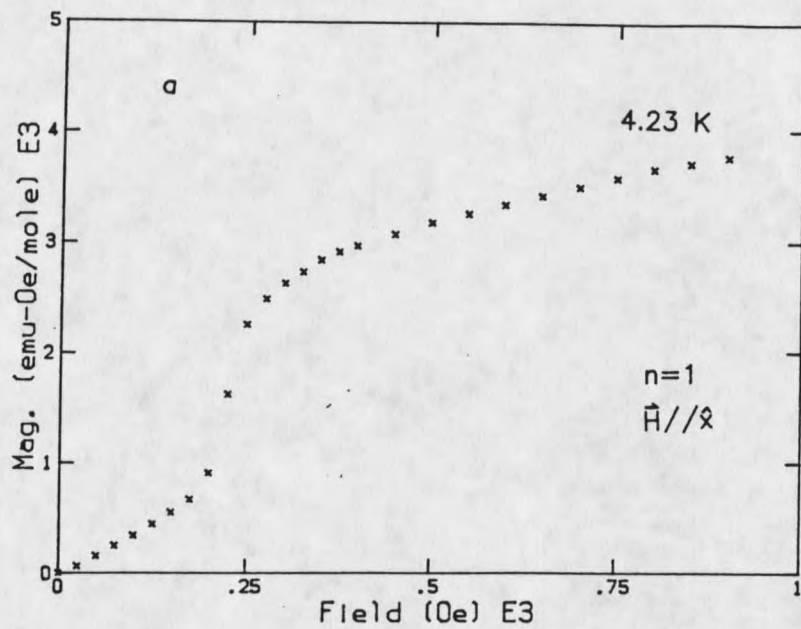
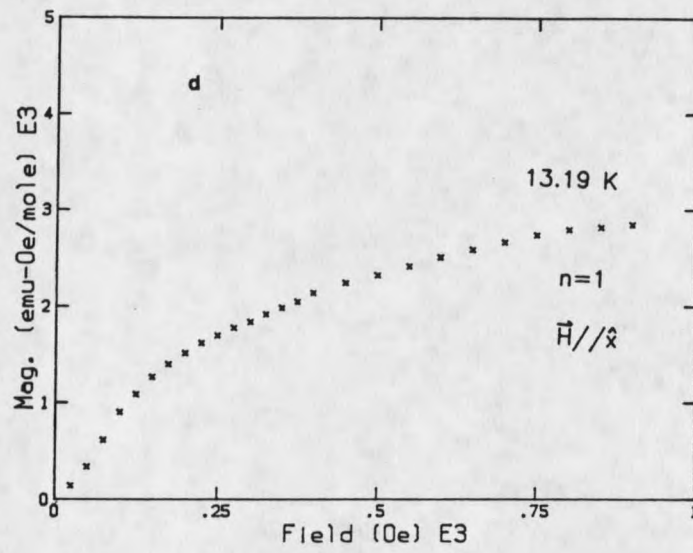
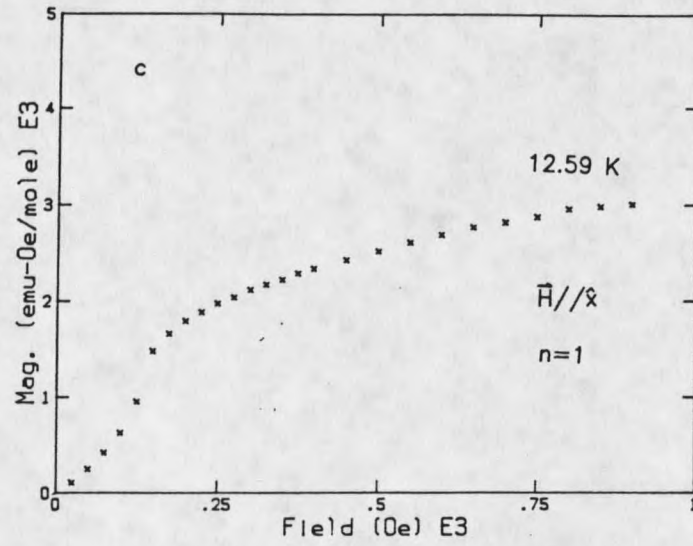


Fig. 16. Isothermal magnetization data at several different temperatures with the field along the x axis.

Figure 16 - Continued

Although the slope of the magnetization at critical field seems to be nearly divergent, there is neither a discontinuity in the magnetization nor a discontinuity in the slope of the magnetization. If the x axis actually is the easy axis, a second order transition may be occurring in this direction. An intermediate phase, therefore, may exist in this case since this phase does not produce a sharp transition as in a first order AF-SF transition. It should be pointed out, according to this measurement result alone, that this transition still can be argued to be a first order AF-SF transition for the following reason. If one assumes that there is a weak antiferromagnetic exchange between the layers with the spin preferred (easy) axis slightly out the xy (ab) plane, the transition (S-form portion of M vs. H) is expected to be a first order AF-SF transition. The small critical field, $H_c \sim 200$ Oe, is mainly due to the small antiferromagnetic interlayer exchange. The discontinuity in the isothermal magnetization exactly along the easy axis will be indeed observed with taking into demagnetizing effect account.

Along the y axis, the result of the isothermal magnetization measurement for the $n = 1$ compound is shown in fig. 17. The measurement was carried out with the field swept from 5000 Oe to 0 Oe. This result reveals ferromagnetic behavior. In the high field region, the magnetization slowly increases to reach the full saturation. It falls down linearly as the field decreases in the low temperature and low field regions.

Upon closer inspection of the M vs. H curves (fig. 18), it seems that there is no apparent SF-PM phase transition in the x direction. It can be suggested that a Dzyaloshinsky-Moriya (D-M) interaction is present within the layer. This high order anisotropy is due to the antisymmetric part of the super-exchange tensor, which describes the quadratic part of the interaction between two spins, and is of the form: $\vec{D}_{ij} \cdot (\vec{S}_i \times \vec{S}_j)$. The D-M constant vector \vec{D} may be (nearly) perpendicular to the x direction and (nearly), aligned in yz plane (rather close to y axis). In this case, the

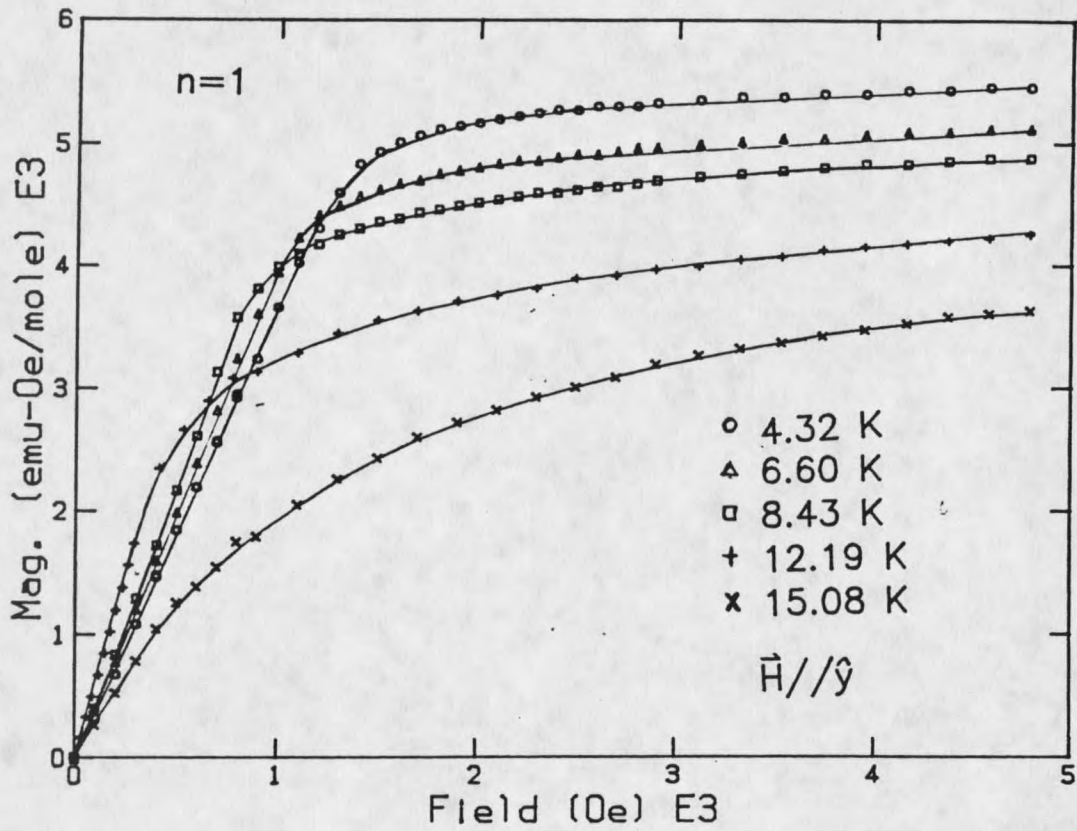


Fig. 17. Isothermal magnetization data with the field along the y axis at several different temperatures.

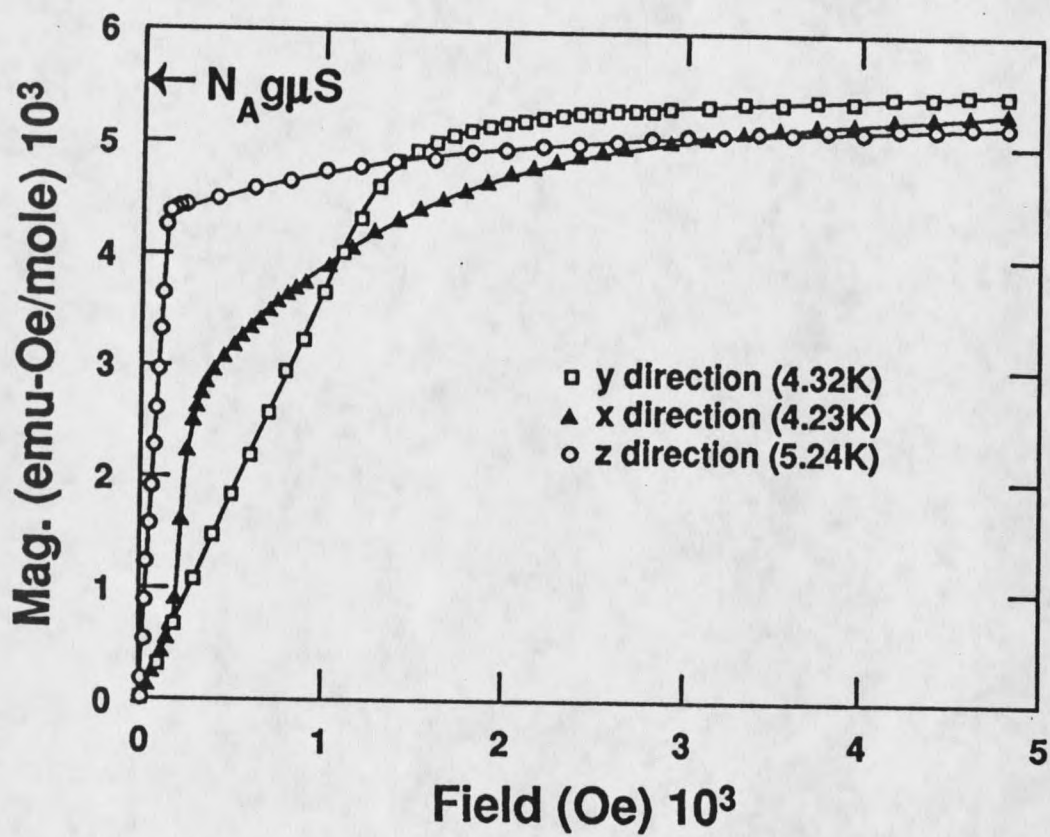


Fig. 18. Isothermal magnetization with the field along the spin principle (x, y and z) axes for the $n = 1$ single crystal.

SF-PM transition along \hat{x} axis is destroyed. Because of this effect of spin canting, only a SF-quasiparamagnetic phase transition would be expected which manifests itself as an inflection point in the susceptibility.^[56]

Measurements of the low field susceptibility as a function of temperature were carried out on the VSM with an applied field $H = 50$ Oe for a single crystal with $n = 1$. The results along the \hat{x} , \hat{y} and \hat{z} directions are shown in fig. 19. The very large susceptibility observed along \hat{z} axis is clearly indicative of a very substantial ferromagnetic interaction and predicts eventual ferromagnetic ordering along this direction. Along the \hat{x} and \hat{y} directions, the data reflect weak antiferromagnetic behavior. It is clear that this compound contains strong exchange anisotropies. The weak antiferromagnetic moment along \hat{x} axis is the result of a weak antiferromagnetic interlayer exchange. This agrees with the results of the isothermal measurements (fig. 16). Because the antisymmetric exchange vector \overline{D} may not be perfectly aligned along the \hat{y} axis and because the exchange anisotropy within the layer leads to the \hat{y} axis being hard axis, as shown in fig. 18, weak antiferromagnetic behavior in this direction is expected to be seen in the susceptibility measurement. The large magnetic moment obtained along \hat{z} axis, which remains essentially constant up to the transition temperature, indicates that the anisotropy field due to the ferromagnetic intralayer exchange along this direction is much bigger than that along \hat{y} direction. The data of χ_z shown in fig. 19 also reflects the usual behavior of perpendicular susceptibility for an antiferromagnet.

Magnetizations and susceptibilities of single crystals $[\text{C}_6\text{H}_3(\text{CH}_2)_n\text{NH}_3]_2\text{CuBr}_4$ with $n = 2$ and 3

The results of isothermal magnetization measurements show that the $n = 2$ compound has essentially the same magnetic behavior as that of the $n = 1$ compound.

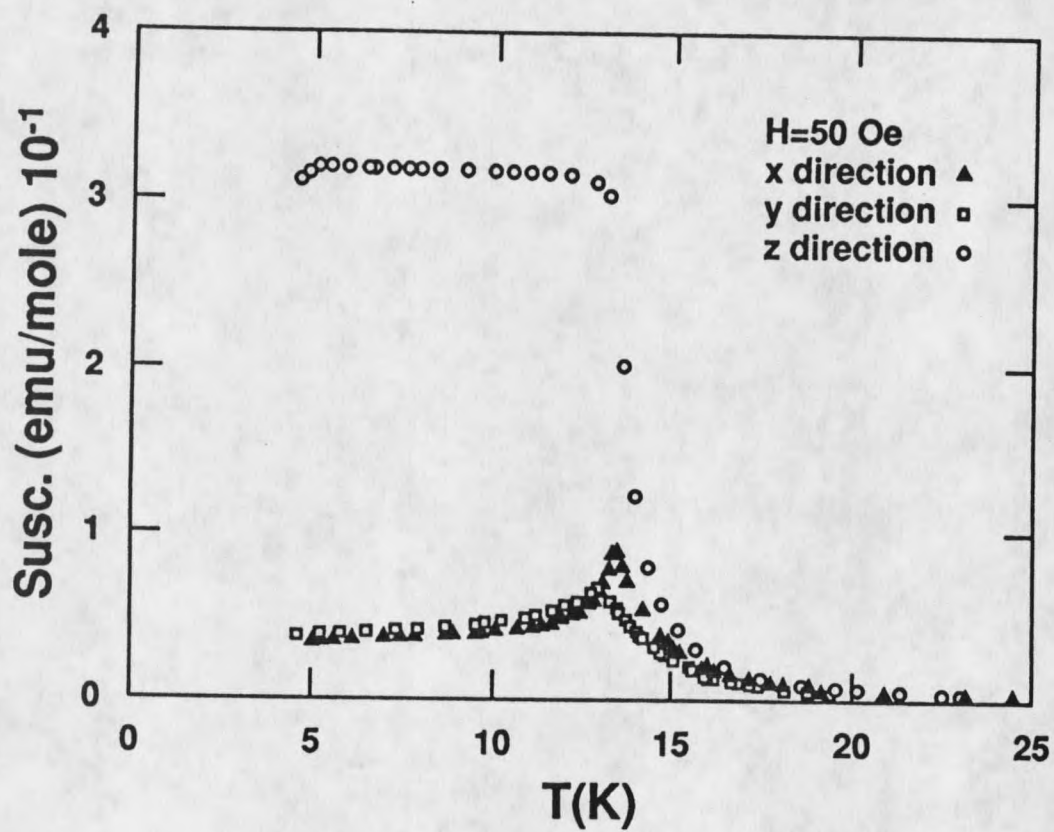


Fig. 19. Low-field d.c. Susceptibility vs. temperature along the spin principle axes ($n = 1$).

Fig 20 shows the results of isothermal measurements along the three axes. There is a small remnant magnetization at $H = 0$ for the $n = 2$ compound, and a small kink occurs at about 300-Oe along \hat{y} axis. For the $n = 3$ compound, the magnetization behaves quite differently from that of the $n = 1$ and 2 compounds in the plane of the plate. Fig. 21 shows the results of the rotational isothermal measurements in the ab (xy) plane for $n = 3$. There is no sharp first order or S-form transition to be found in the plane. However, along \hat{z} axis the magnetization behaves similarly to that of the $n = 1$ and 2 compounds. These results are shown in fig. 22. Furthermore, the low field susceptibilities along the three axes also show that the magnetic structure of this compound is similar to that of $n = 1$ and 2 compounds, as shown in fig. 23.

The fact that there is no sharp first order or S-form transition to be observed in the plane for the $n = 3$ compound may be explained by assuming that the easy axis due to the antiferromagnetic-alignment between the layers lies out of the plane of plate for this compound. Unlike the $n = 1$, and 2 compounds, the angle between the easy axis and \hat{x} axis for $n = 3$ compound may be expected to be relatively large so that the AF-SF transition eventually can not be seen within the plane. Thus, only a second order SF-PM or SF-QP phase transition can be observed in the x - y plane. It is interesting that there may exist a critical angle between the easy axis and \hat{x} axis. This critical angle characterizes a maximum angle at which the AF-SF transition can occur. The values of the critical angle for several uniaxial antiferromagnets have been calculated by using mean-field theory.^[56-58] For a simple uniaxial antiferromagnet, the critical angle α_c at $T = 0$ K was found to be around K/J , where K and J are anisotropy and exchange constants, respectively. In our case, it is nontrivial to estimate the value of α_c since the systems are constructed by inter- and intralayer exchanges. The existence of strong anisotropies due to both exchange and antisymmetric exchange results in the systems

